สำนักวิทยบริการและเทคโนโลยีสารสนเทศ
มหาวิทยาลัยราชภัฏบ้านสมเด็จเจ้าพระยา

DESIGN OF NOVEL COMPOUNDS AS POTENTIAL DPP-4 INHIBITORS

วิทยานิพนธ์

CHAIYUN TAOMALI

**A thesis submitted in partial fulfillment of the requirements
for Master of Science in Chemistry
Academic Year 2014
Copyright of Bansomdejchaopraya Rajabhat University**

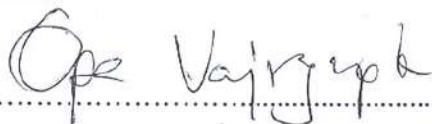| Title	Design of Novel Compound as Potential DPP-4 Inhibitors
Author	Chaiyun Taomali
Program	Chemistry
Major Advisor	Dr. Atchara Keawnoi
Co- Advisor	Dr. Phansuang Udomputtimekakul
Co- Advisor	Supot Jankun

Bansomdejchaopraya Rajabhat University approved this thesis in partial fulfillment of the requirements for the degree Masters of Science Degree in Chemistry
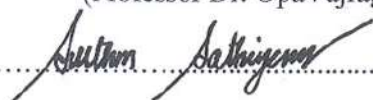
.... Dean of Graduate School

(Assistant Professor Dr. Areewan Iamsaard)

Committees:
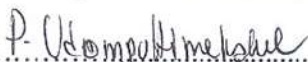
.... Chairman

(Professor Dr. OpaVajragupta)
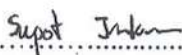
.... Committee

(Associate Professor Suthon Sathienyanon)

.... Committee

(Dr. Atchara Keawnoi)

.... Committee

(Dr. Phansuang Udomputtimekakul)

.... Committee

(Mr. Supot Jankun)

Title	Design of Novel Compound as Potential DPP-4 Inhibitors
Author	Chaiyun Taomali
Program	Chemistry
Major Advisor	Dr. Atchara Keawnoi
Co- Advisor	Dr. Phansuang Udomputtimekakul
Co- Advisor	Supot Jankun
Academic Year	2014

ABSTRACT

In searching for antidiabetic drugs, dipeptidyl peptidase IV (DPP-4) was selected as a drug target in the design of new potent DPP-4 inhibitors in this study. Novel DPP-4 inhibitors were developed based on the information of medicinal herbs and structure based drug design. The DPP-4 template was prepared from DPP-4 crystal structure derived from human DPP-4 (PDB: 1X70) and validated (RMSD 0.56 Å). The validated DPP-4 template was used as a target macromolecule. The combinatory library of 356 structures containing three main fragments (S1 and S2) linked with imine and amide functions was prepared. The S1 fragments are cysteine, L(-)-tryptophan and chromone while the S2 fragments are the varied side chains. Molecular docking of the structures in the library against DPP-4 template was conducted to identify the hit structures of increased binding capacity and consequently leading to potent inhibitory action. AutoDock 4.1 program was used in the docking study to identify the hit structures of good binding. The selected twenty top ranking compounds or hit compounds were identified which were 6 chromone imine, 10 cysteine amides and 4 L(-)-tryptophan amides. The best binding free energies of compounds in each series were -11.95 kcal/mol in series C, -11.59 kcal/mol in series B and -9.01 kcal/mol in series A. The identified hit compounds were synthesized and evaluated for the DPP-4 inhibitory action *in vitro*. Among sulfur containing compounds, compounds **24** and **26** in the series B were most active with IC_{50} of 100.0 µM and the activity of all compounds in series A and series C were weak. cysteine amides **24, 26** was the most potent in this study with IC_{50} of 95.19 µM and 96.80 µM respectively. The uniformity of interaction across the structure and percent membership in the highest cluster from docking study appeared to have significant contribution on the activity. The binding mode of cysteine amides **24, 26** showed two hydrogen bond interactions, with Glu205 and Glu206. The designed structure **24, 26** accommodates the hydrophobic cysteine nucleus to occupy in the S-1 pocket of the enzyme and interacts with the amino acid residue in this pocket (Glu205 and Glu206) resulting in the highest potency. However, compounds **24, 26** was found to be less potent than sitagliptin. Compounds **24** and **26** are the leads for further design and modification.

Keywords: DPP-4 Inhibitors / Novel Antidiabetic Agents / Type 2 Antidiabetic

ACKNOWLEDGEMENTS

CONTENTS

CONTENTS (cont.)

LIST OF TABLES

LIST OF FIGURES

LIST OF FIGURES (cont.)

LIST OF FIGURES (cont.)

LIST OF FIGURES (cont.)

CHAPTER I

INTRODUCTION

Diabetes mellitus (DM) is a life-threatening and build damage cost immensely, both of medical damage and the economy. DM is a group of metabolic diseases characterized by high blood sugar (glucose) levels, that result from defects in insulin secretion, or action, or both. Diabetes mellitus, commonly referred to as diabetes (as it will be in this article) was first identified as a disease associated with "sweet urine," and excessive muscle loss in the ancient world. Elevated levels of blood glucose (hyperglycemia) lead to spillage of glucose into the urine, hence the term sweet urine. Normally, blood glucose levels are tightly controlled by insulin, a hormone produced by the pancreas. Insulin lowers the blood glucose level. When the blood glucose elevates (for example, after eating food), insulin is released from the pancreas to normalize the glucose level. In patients with diabetes, the absence or insufficient production of insulin causes hyperglycemia. Diabetes is a chronic medical condition, meaning that although it can be controlled, it lasts a lifetime.[1,2]

The World Health Organization (WHO) has estimated that the global prevalence (for all age groups) would rise from 2.8% in 2000 to 4.4% in 2030, more than doubling the number of persons affected, from 171 million to 366 million worldwide.[3,4] Furthermore, this increased number of diabetes patients will be found in the 65-year-old age group and in developed countries, and in the 45-65 year-old age group in developing countries. DM represents a greater danger than AIDS because 3.2 million people die of this disease every year. There are two types of DM classified according to the cause feature Type 1 diabetes mellitus (T1DM) and Type 2 diabetes mellitus (T2DM). T1DM is caused by autoimmune destruction of pancreatic β-cells, leading to the reduction of insulin secretion. T2DM is becoming increasingly prevalent and globally has reached epidemic proportions.[5,6] It is currently estimated that more than 180 million people worldwide have the disease with an estimated 1.1 million deaths in 2005. Even more disturbing are the projections that the number of affected people will double by 2030. T2DM is characterized by the emergenceof postprandial (post-meal) and, subsequently, fasting hyperglycemia (fasting plasma glucose >125 mg/dl).

T2DM are unable to maintain adequate control of blood sugar through the action of endogenously generated insulin, even though they generally have functioning pancreatic islet β-cells.[7-11]

During 1929s to 1982s, researcher's discoverer two incretin hormones, glucose-dependent insulinotropic polypeptide (GIP) and glucagons-like peptide-1 (GLP-1). Both hormones are released from the small intestine into the vasculature. GLP-1 and GIP are important roles in Glucose-dependent insulin secretion.[6,11] However, GLP-1 is shown to retain insulinotropic action in diabetic patients. These

incretin hormones are very attractive targets in the development of new antidiabatic drugs because GLP-1 stimulates insulin secretion, increases islet neogenesis and differentiation, and slows apoptosis of pancreatic β-cells.[12] Besides, Gui-BaiLiangetal.Both[13] hormones are deactivated rapidly in vivo through the action of dipeptidyl peptidase IV (DPP-4). That discoverer GLP-1 have an effect on dipeptidyl peptidase IV (DPP-4) also and must be administered via continuous infusion in order to have sustained efficacy.[14] For this reason, DPP-4 inhibitors are emerging as new potential drugs of T2DM, with Sitagliptin already in the market.[13] The new antidiabetic treatment focused on the incretin hormone glucose-like peptide-1 (GLP-1) was first approved in 2005 as adjunctive therapy in diabetic patients in which sulfonylurea, metformin or both had failed. Gastrointestinal glucagons-like peptide-1 (GLP-1) and glucose-dependent insulinotropic polypeptide (GIP) are incretin hormones which are released from the small intestine into the vasculature. GLP-1 stimulates insulin secretion from β-cells, suppresses glucagon secretion, and regulates food intake and gastric emptying. In humans, GLP-1 and GIP are rapidly N-terminally degraded by the ubiquitous enzyme dipeptidyl peptidase IV (DPP-4) and this is the major, if not sole, factor leading to short half-lives of GLP-1 after the secretion. The enzyme DPP-4 activity is found ubiquitously in almost all organs and tissues with the highest local concentrations found really in the proximal tubuli and luminally on the epithelial cells of the small intestine. DPP-4 preferentially hydrolyzes N-terminal dipeptide from protein having proline or alanine in penultimate position.[14-18]

The objective of this research is to design and synthesize the novel DPP-4 inhibitors which were modified from the structure of the active compounds of medicinal plant. Cysteine, L(-)-tryptophan or chromone naturally occurring the compounds in nature especially in plants and interesting structure was found to be the important component or pharmacophores of many biologically active molecules such as antimycobacterial, antifungal, anticonvulsant, antimicrobial and anticancer agents.[19-25] Hence, Cysteine, L(-)-tryptophan or chromone was selected to be and core structure for the designed compounds. The program AutoDock version 4.1 (The Scripps Research, USA) was used for designing new compounds and for searching the active components. The docking flexible ligands into protein binding sites to explore the full range of ligand conformational rigid protein. Molecular docking was carried out to investigate the docking energy and binding mode of a crystallographic structure of human dipeptidyl peptidase IV (DPP-IV, PDB entry code: 1X70) was used to investigate and validate the docking protocol. Molecular docking of the hit structures with DPP-4 were conducted to identify with increasing binding capacity which leads to potent inhibitory action. The identified hit compounds were synthesized and tested for its inhibition action against DPP-4.The Cysteine, L(-)-tryptophan or chromone function (S1) was modified by different side chains (S2) to fit DPP-4 was active binding site. There two main fragments (S1 and S2) were linked by two functions: imine and amide leading to a combinatorial library of 356 structures

containing were designed and docked against DPP-4 template. The docked poses and the docking energies are collected and evaluated. The compounds that have good docking and lowest binding energy of biding to DPP-4 were cluster. The obtained nergies from docking were ranked. The docked pose and binding energy of the conformers in the cluster of highest number and analyzed. The selected twenty top ranking compounds or hit compounds were identified which are 6 chromone imines, 10 Cysteine amides and 4 $L(-)$-tryptophan amides for synthesis as shown in Figure 1.The inhibitory action on DPP-4 enzyme of these compounds and the standard drug, sitagliptin, were determined.

$R_1 = OCH_3$ or CH_3

Series A

$R_2 =$

$R_1 = OCH_3$ or CH_3

Series B

$R_2 =$

Series C

$R_1 =$
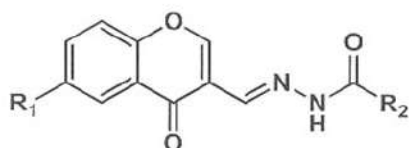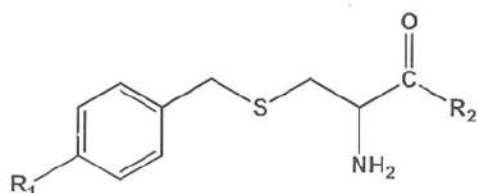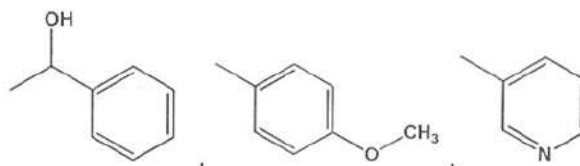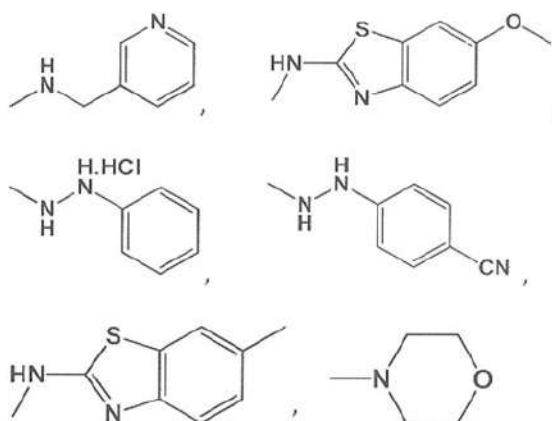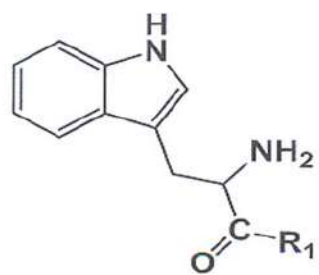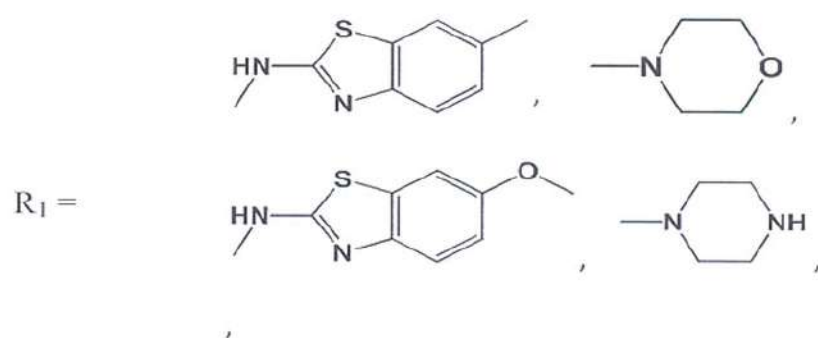
Figure 1 The selected structure for synthesis

CHAPTER II

LITERATURE REVIEW

1. The cause of Diabetes

Diabetes mellitus (DM) has a chronic disease, is a group of metabolic diseases characterized by hyperglycemia arising as a result of a relative or absolute deficiency of Insulin secretion, resistance to insulin action, or both. Diabetes is an ailment in which the body does not produce or properly use insulin. Insulin is a regulatory hormone required for energy management. The cause of diabetes continues to be a anonymity, although both genetics and environmental factors such as obesity and lack of exercise appear to play roles.[21, 26, 27] Symptoms include frequent urination, lethargy, excessive thirst, and hunger. The treatment includes changes in diet, oral medications, and in some cases, daily injections of insulin. The DM has been classified into two major types, primary and secondary type DM.[4, 5] The primary type DM is the majority of DM, including type 1 and type 2DM. The secondary type DM is the other medical conditions or rare genetic disorder such as gestational diabetes, pre-diabetes.

Type 1diabetes mellitus (T1DM) is usually due to an immune mediated destruction of pancreatic islet β-cells with consequent insulin deficiency and the need to replace insulin. Although usually having an abrupt clinical onset, the disease process unfolds slowly, with progressive loss of β-cells. T1DM is a consequence of significant loss of β-cells mass and/or function and invariably requires therapeutic replacement of insulin. T1DM is usually diagnosed in children and young adults or before age 25 year, and was previously known as juvenile diabetes. In T1DM the body stops making insulin and the blood glucose level goes very high.[21, 28-30] Treatment to control the blood glucose level is with insulin injections and a healthy diet. Conditions associated with T1DM include hyperglycemia, hypoglycemia and ketoacidosis. T1DM increases risk for many serious complications. Some complications of T1DM include: heart disease (cardiovascular disease), blindness (retinopathy), nerve damage (neuropathy), and kidney damage (nephropathy), foot and skin complications and depression.[2]

Type 2 diabetes mellitus (T2DM), the more common type, is usually due to resistance to insulin (a condition in which the body fails to properly use insulin) action in the setting of inadequate compensatory insulin secretory response), combined with relative insulin deficiency. This is depicted in **Figure 2.** Insulin resistance is actually quite common because it arises as a consequence of obesity, a sedentary lifestyle, and aging (**Figure 3**), with resulting hyperglycemia and diabetes, blood pressure elevation, and dyslipidemia. In fact, collectively these abnormalities, which often occur together, have been designated the "metabolic syndrome" or more

properly the "dysmetabolic syndrome". T2DM does not emerge in all persons with insulin resistance but rather only in those with a defect in insulin secretory capacity (presumably genetic) such that pancreatic insulin secretion fails to compensate for the insulin resistance. T2DM is the most common form of diabetes (90-95% of diabetes patients). T2DM can be found usually develops after the age of 40 year (but sometimes occurs in younger people), and is treated by diet alone, or by diet and oral medications.[4, 21, 30]

Insulin resistance

Normal β -cell function

Abnormal β -cell function

↓

↓

Compensatory Hyperinsulin....

Relative Insulin deficiency

↓

↓

Homoglycemia

Hyperglycemia.

↓
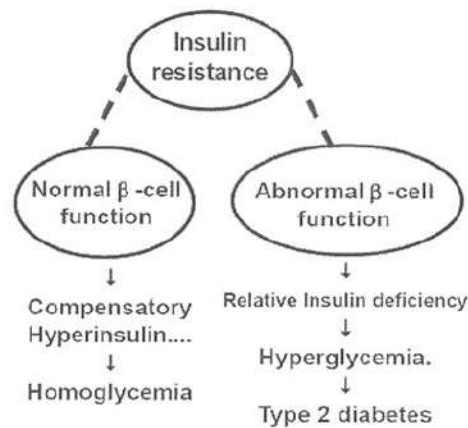
Type 2 diabetes

Figure 2 Schematic depiction of the dual defect that is necessary for Type II diabetes to be manifest: insulin resistance in the setting of impaired β-cells function inadequate to compensate for the insulin resistance. [2]

Dyslipidemia High TG, Low HDL Small Dense LDL

Glucose Intolerance Type 2 Diabetes

Hypertension

Insulin resistance

Aging →

Geneitcs

Obesity High W/H Ratio Gluttony

Sedentary Lifestyle Slothfulness

Figure 3 Causes and consequences of insulin resistance. [2]

Gestational diabetes mellitus (GDM) is means that the body has a problem with insulin during pregnancy. When women are pregnant, the body needs more insulin to keep blood sugar at the right level. Women's bodies make more insulin during pregnancy. When the extra insulin is not enough to keep blood sugar normal, women get high blood sugar. This is called GDM. Blood sugar usually returns to

normal after delivery.[31] GDM means diabetes that develops for the first time during pregnancy, and affects between 2% and 14% of all pregnancies women.[32] However, this type of diabetes is temporary but there is the opportunity of converting to T2DM.

Pre-diabetes is a new term for impaired fasting glucose or impaired glucose tolerance. It is characterized by glucose levels that are higher than normal, but not high enough to be diagnosis of T2DM. There are many people with Pre-diabetes but they don't perceive. Other secondary type DM is the result from several reasons such as disease of exocrine, infection, drug-induced genetic defects of β-cells function (maturity onset diabetes of the young) and other genetic syndromes.[33]

2. Insulin

Insulin is an important hormone for glucose metabolism. It is a peptide hormone composed of 51 amino acid residues and secreted by the pancreas within β-cell of the islets of langerhans in response the increase in blood sugars. It is initially synthesized as a single-chain 86-amino-acid precursor polypeptide called preproinsulin. Subsequently, preproinsulin is converted by the removal of the amino terminal signal peptide. Proinsulin in structurally related to insulin-like growth factors I and II, which bind weakly to the insulin receptor. Cleavage of on internal 31-reidue fragment from proinsulin generates intervening C peptide chain and the mature insulin molecule. Mature insulin composes of the A chain (21 amino acid) and B chain (30 amino acid) of biologically active insulin, which are linked by two disulfide bonds.[34]

The secretory granules in the β-cell store and secrete the mature insulin molecule (50-amino acid) and C peptide together. Since the C peptide is cleared more slowly than insulin, it is a beneficial marker of insulin secretion and allows recognition of endogenous and exogenous sources of insulin in the evaluation of hypoglycemia.[35] Although both genetics and environmental factors such as obesity and lack of exercise appear to be risk factors, the cause of diabetes skill to be obscure eventually.

In the first stage of insulin resistance, the compensate system of body is able to maintain normal glucose level by increasing the pancreatic insulin secretion. However, as the disease progresses, insulin production gradually diminish, leading to progressive stages of hyperglycemia, Hyperglycemia is first shown in the postprandial state because uptake by skeletal muscle is the metabolic fate of the majority of ingested carbohydrate energy, and the during fasting. Hepatic glucose production increases whereas insulin secretion decreases. This increases is primarily cause of the elevation of fasting glucose level in patients with T2DM.[36] Insulin resistance is also influenced at the adipocyte level, leading to unrestrained lipolysis and increment of circulating free fatty acid. Increased free fatty acid also future obstruct the insulin

response in skeletal muscle.[37, 38] Hence, T2DM arises from coexisting defect at multiple organ sites: resistance to insulin action in muscle, defective pancreatic insulin secretion and unrestrained hepatic glucose production, all of which are aggravated by defective insulin action in fat. There pathological lesions of blame for the development and progression of hyperglycemia. They are also the primary targets for pharmacological therapy.[39, 40]
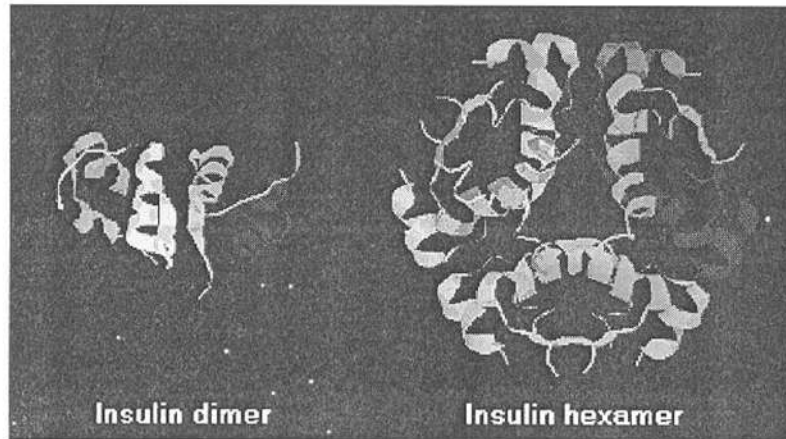
Figure 4 The Structure of Insulin. [41]

3. Insulin Secretion

The major function of insulin is to counter the concerted action of a number of hyperglycemia-generating hormones and to maintain low blood glucose levels. Because there are numerous hyperglycemic hormones, untreated disorders associated with insulin generally lead to severe hyperglycemia and shortened life span. In addition to its role in regulating glucose metabolism, insulin stimulates lipogenesis, diminishes lipolysis, and increases amino acid transport into cells. Insulin also modulates transcription, altering the cell content of numerous mRNAs. It stimulates growth, DNA synthesis, and cell replication, effects that it holds in common with the insulin-like growth factors and relaxin.

Insulin is synthesized as a preprohormone in the β-cells of the islets of Langerhans. Its signal peptide is removed in the cisternae of the endoplasmic reticulum and it is packaged into secretory vesicles in the Golgi, folded to its native structure, and locked in this conformation by the formation of 2 disulfide bonds. Specific protease activity cleaves the center third of the molecule, which dissociates as C peptide, leaving the amino terminal B peptide disulfide bonded to the carboxy terminal A peptide. Insulin secretion from β-cells is principally regulated by plasma glucose levels. Increased uptake of glucose by pancreatic β-cells leads to a concomitant increase in metabolism. The increase in metabolism leads to an

elevation in the ATP/ADP ratio. This in turn leads to the inhibition of an ATP-sensitive potassium channel (K_{ATP} channel). The net result is a depolarization of the cell leading to Ca^{2+} influx and insulin secretion.

The K_{ATP} channel is a complex of 8 polypeptides comprising four copies of the protein encoded by the ABCC8 (ATP-binding cassette, sub-family C, member 8) gene and four copies of the protein encoded by the KCNJ11 (potassium inwardly-rectifying channel, subfamily J, member 11) gene. The ABCC8 encoded protein is also known as the sulfonylurea receptor (SUR). The KCNJ11 encoded protein forms the core of the K_{ATP} channel and is called Kir6.2. As might be expected, the role of K_{ATP} channels in insulin secretion presents a viable therapeutic target for treating hyperglycemia due to insulin insufficiency as is typical in T2DM. Chronic increases in numerous other hormones, such as growth hormone, placental lactogen, estrogens, and progestins, up-regulate insulin secretion, probably by increasing the preproinsulin mRNA and enzymes involved in processing the increased preprohormone.[42-44]
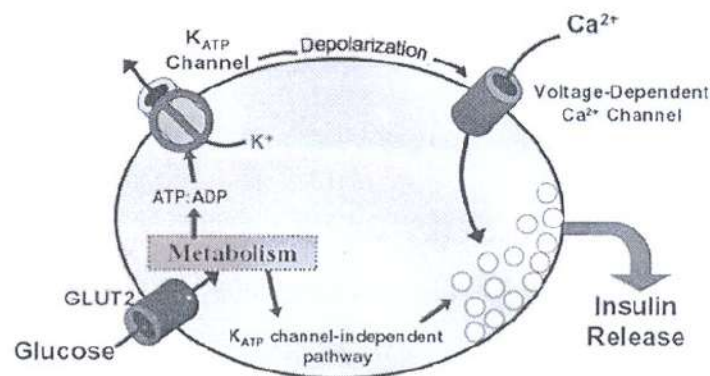
Figure 5 Pancreatic β-cell glucose-stimulated insulin secretion. Glucose enters the cell through the glucose transporter 2 (GLUT2 transporter) and is metabolized to produce ATP, which increases the cytosolic ATP/ADP ratio. This closes the K_{ATP} channel leading to membrane depolarization and activation of the voltage-dependent Ca^{2+} channel leading to an increase in cytosolic Ca^{2+} concentrations and activation of Ca^{2+}-dependent mechanisms controlling insulin secretion. In addition to the K_{ATP}-channel dependent pathway, there is also a K_{ATP} independent pathway. This pathway involves modulation of insulin secretion by some metabolite of glucose metabolism that does not involve the K_{ATP} channel.[45]

4. Action of Insulin

Insulin's actions are summarized in figure 6. The active receptor speeds uptake of amino acids and glucose, activates protein synthesis from amino acids and glycogen and triglyceride synthesis from glucose. Insulin inhibits breakdown of triglycerides in adipose tissue and gluconeogenesis in the liver. A whole series of intracellular signal substances seemed to be responsible for the many actions of insulin.[46-48]
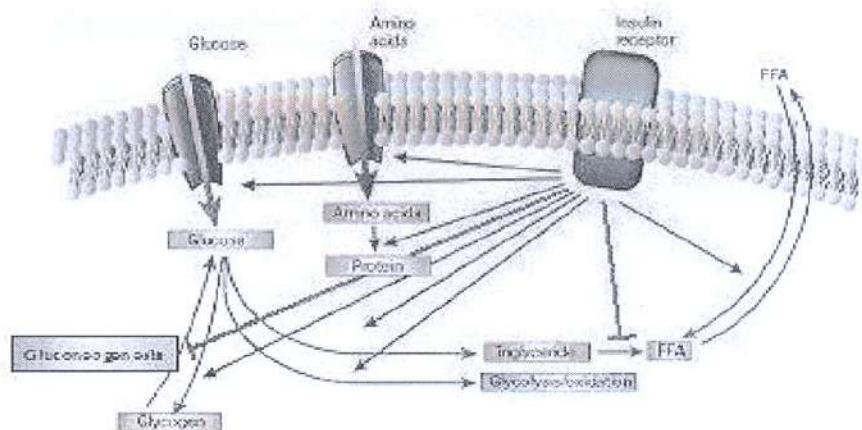
Figure 6 The regulation of metabolism by insulin.[49]

These are shown in the **Figure 7** from the work of Saltiel and Kahn. Here we can see that the phosphorylate on of the insulin receptor starts up serine-threonine phosphorylate on of a series of proteins, the so-called insulin-receptor substrates (IRS1-4). These are coupled to several additional protein kinase signal systems.

1. Pathways signaling through PI 3-kinase and phosphatidylinositol (3,4,5)P3 (PI-3 kinase and protein kinase B/Akt).

2. Mitogen-activated protein kinases (MAPKinases). NB: Both group 1 and 2 signals also activate protein kinase Cγ and Prokinase Cζ.

3. Possible interaction via kinases not coupled to IRS proteins.

It has been suggested that the most dominant is the first group (PI 3-kinase) which converts phosphatidylinositol 3,4 bisphosphate (PIP2) or [PI(3,4)P2] to phosphatidylinositol 3,4,5 triphosphate PIP3 or (PI 3,4,5)P3. These nucleotides act as anchors, binding down-line protein kinases to the plasma membrane and activating

them. These nucleotides seem to be responsible for the alterations in carbohydrate, protein and lipid metabolism that are initiated by insulin.
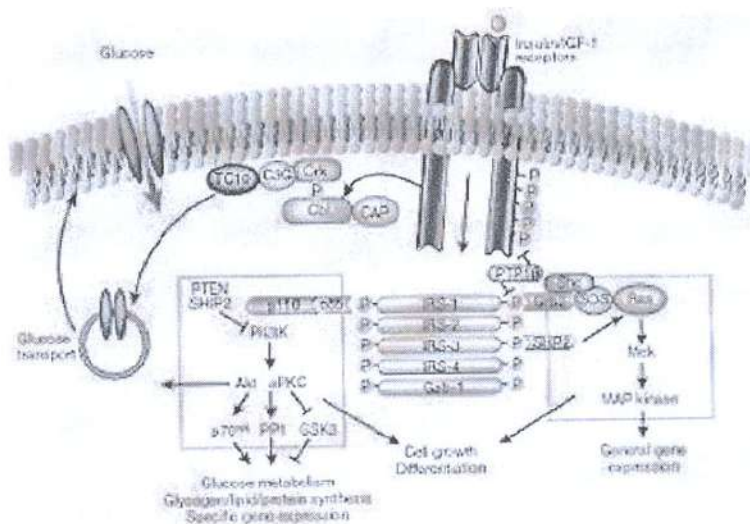
Figure 7 The mechanisms of insulin action.[49]

5. Incretin system

Incretins are gut peptides that potentiate nutrient-dependent insulin secretion following meal ingestion. The two dominant incretins glucose-dependent insulinotropic peptide (GIP) and glucagon-like peptide-1 (GLP-1) stimulate insulin secretion and promote expansion of β-cell mass in preclinical models via control of cell proliferation and inhibition of apoptosis. GLP-1, but not GIP, decreases the rate of gastric emptying, inhibits glucagon secretion, and diminishes appetite and food intake. GIP is a 42 amino acid peptide derived from a larger protein (ProGIP) and is secreted by endocrine K cells mainly present in the proximal gastrointestinal (GI) tract (duodenum and proximal jejunum). GLP-1 is a 30 amino acid or 31 amino acid peptide derived from a larger protein (proglucagon) and is secreted by L cells located predominantly in the distal GI tract (ileum and colon).[50-52]
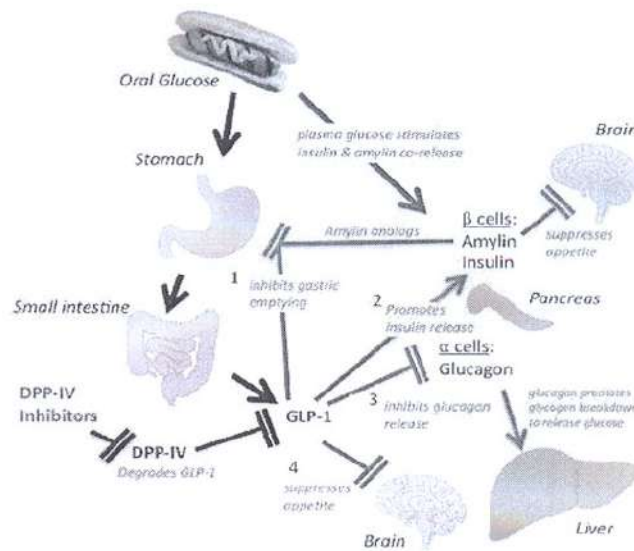
Figure 8 The Incretin System.[52]

In healthy patients the ingestion of food results in the release of gastrointestinal peptides, including GLP-1 (Glucagon Like Peptide 1), GIP (Gastric Inhibitory Peptide), as well as the pancreatic β-cell hormones insulin and amylin. GLP-1 is released from "L cells" located in the small bowel & colon. Following themabsorption of food, GLP-1 promotes insulin secretion, otherwise known as the incretin effect. In diabetes, these steps are disrupted (Figure 8). As illustrated, GLP-1 (and its mimetics, such as exenatide) have at least 4 mechanisms by which they can reduce plasma glucose levels. Both GLP-1 and amylin mimetics have inhibitory effects on gastric emptying, and appetite. (Amylin mediates its effects by different receptors than GLP-1).

After secretion, GLP-1 is rapidly metabolized by the enzyme DPP-4 (dipeptidyl peptidase-4) in the liver. The plasma half-life of GLP-1 is ~2 minutes. DPP-IV inhibitors such as sitagliptin inhibit the breakdown of GLP-1 by DPP-4. Note that DPP-IV inhibitors will only produce an effect when blood sugar is elevated, causing the release of GLP-1 from the small intestine.[52-53]
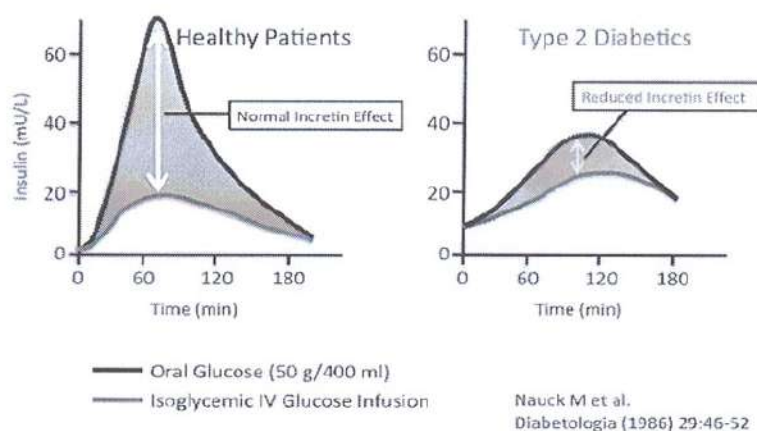
Figure 9 Diabetes & the Incretin Effect.[52]

6. Diagnostic Criteria for Diabetes Mellitus

The oral glucose tolerance test previously recommended by the National Diabetes Data Group has been replaced with the recommendation that the diagnosis of diabetes mellitus be based on two fasting plasma glucose levels of 126 mg/dL (7.0 mmol/L) or higher. Other options for diagnosis include two two-hour postprandial plasma glucose (2hrPPG) readings of 200 mg/dL (11.1 mmol/L) or higher after a glucose load of 75 g (essentially, the criterion recommended by WHO) or two casual glucose readings of 200 mg/dL (11.1 mmol/L) or higher. Measurement of the fasting plasma glucose level is the preferred diagnostic test, but any combination of two abnormal test results can be used. Fasting plasma glucose was selected as the primary diagnostic test because it predicts adverse outcomes (e.g., retinopathy) as well as the 2hr PPG test but is much more reproducible than the oral glucose tolerance test or the 2hrPPG test and easier to perform in a clinical setting.[54, 55]

Glycated hemoglobin measurement is parameter commonly used to monitor the glycemic control of patients already who are diagnosed with diabetes mellitus. Measurement of this hemoglobin, also called glycosylated hemoglobin, glycohemoglobin, hemoglobin A or hemoglobin A1c (HbA1c), hdlp the evaluation of the stable linkage of glucose to minor hemoglobin components. The normal HbA1c criterion is not more than 7.0% This parameter is related to adverse clinical outcomes.

Table 1   **Diagnostic criteria for Impaired Glucose Tolerance (IGT), Impaired Fasting Glucose (IFG) and diabetes mellitus according to WHO.**[56]

		2 hour post glucose load (mmol/L plasma)		
		< 7.8	≥ 7.8 and < 11.1	≥ 11.1
	< 6.1	Normal	IGT	Diabetes
Fasting glucose	≥ 6.1 and < 7.0	IFG	IGT	Diabetes
(mmol/L plasma)	≥ 7.0	Diabetes	Diabetes	Diabetes

7. Strategies for Diabetes Treatment

7.1 Nonpharmacological Therapy

Diet and lifestyle strategy remains significant in both T1DM and T2DM. The patients with T2DM are mostly overweight and have impaired metabolism. Weight diminution will ameliorate many of the frequently cardiovascular risk factor and decrease insulin resistance. The increment of physical activity can enhance glycemic control. Normally, implementation of optimum exercise regimens can help weight reduction and is associated with a decrease of blood pressure, total cholesterol and triglyceride levels [57]. Therefore, a controlled-energy diet and regular aerobic exercise are recommended for most of the T2DM patients with overweight.[58, 59]

7.2 Pharmacological Therapy

Insulin injection is the classical diabetes therapy. Many diabetes patients use human insulin or an insulin analog. With the creative of the novel insulin analogs, more patients begin to use physiologic insulin replacement or continuous subcutaneous insulin pumps for DM treatment. Normally, T1DM patients have to use exogenous insulin because they can not produce insulin sufficiently by themselves in contrast to T2DM patients who do not require exogenous insulin at least initially.[60-62] Insulin therapy is not used as insulin regimen complexity, misconceptions on the cost of therapy, the risk of insulin treatments, patient's fear of injection, weight gain, hypoglycemia and lack of practice guidelines for the use of insulin. There are several different types of insulin injections for optimizing the blood glucose (Table 2).[60, 63]

Table 2   **Main types of inject able insulin based on pharmacological effect of insulin.** [60, 64]

Type	Onset (hr)	Peak (hr)	Duration (hr)	Drug	
				Generic name	Trade name
Rapid - acting insulin	5 - 20 min	0.75 - 3	3 - 5	Aspart Lispro Glulisine	Novorapid Humalog Apidra
Short - acting insulin	½ - 1	2 - 5	5 - 8	Regular insulin	Humulin R Novolin R
Intermediate - acting insulin	1 - 2	6 - 12	16 – 24	NPH* (Isophane) insuiln Insulin zinc suspension	Insulatard HM or Humulin N Lente
Long - acting insulin	4 - 6 1 (glargine)	8 -20 None (glargine)	24 – 28	Protamin zinc insulin Insulin Insulin analong (glargine)	Uliralente(U) Lente
Insulin mixture	Depend on mixture type (most: < 60 min)	Depend on mixture type	15 - 24	NPH-70/Regular-30 75-NPH/25-Humanlog	Humulin 70/30, Mixtrad Humalog mix

NPH* = neutral protamine hagedorn[1] insulin.

Oral hypoglycemic drugs are used only in the treatment of type 2 diabetes which is a disorder involving resistance to secreted insulin. Type 1 diabetes involves a lack of insulin and requires insulin for treatment. There are now four classes of hypoglycemic drugs. Diabetes pills are grouped in categories based on type. There are several categories of diabetes pills each works differently.

Sulfonylurea: These medications are the oldest of the oral meds. Tolinase (tolazamide) has been around since the 1950's. It's still prescribed today. Newer drugs in this class include Glucotrol (glipizide), Glucotrol XL (glipizide extended release), Amaryl (glimepiride), Diabeta (glyburide), and Micronase (glyburide). They're hypoglycemic agents because they allow the pancreas to release more insulin into the blood which lowers the glucose level. Hypoglycemia is a common side effect. Many of these drugs are only effective for a few years and then may stop working.[65, 66]

Biguanides: These diabetes pills improve insulin's ability to move sugar into cells especially into the muscle cells. They also prevent the liver from releasing stored sugar. Biguanides should not be used in people who have kidney damage or heart failure because of the risk of precipitating a severe build up of acid (called lactic acidosis) in these patients. Biguanides can decrease the HbA1c 1%-2%. An example includes metformin (Glucophage, Glucophage XR, Riomet, Fortamet, and Glumetza). [65, 66]

Thiazolidinediones (TZD): These diabetes pills improve insulin's effectiveness (improving insulin resistance) in muscle and in fat tissue. They lower the amount of sugar released by the liver and make fat cells more sensitive to the effects of insulin. Actos (pioglitazone) and Avandia (rosiglitazone) are the two drugs of this class. A decrease in the HbA1c of 1%-2% can be seen with this class of oral diabetes medications. These drugs may take a few weeks before they have an effect in lowering blood sugar. They should be used with caution in people with heart failure. In fact, the FDA has restricted Avandia for use in new patients only if they can't control their blood sugar on other medications and are unable to take Actos. Current users can continue Avandia if they choose to do so. All patients using Avandia must review and fully understand the cardiovascular risks.[67]

Alpha-glucosidase inhibitors (AIGs) e.g. acerbose and miglitol have distinctive mechanism of action, not target at a specific pathophysiological defect of T2DM. This drug acts as competitive inhibitor of enzyme needed to digest carbohydrates. The alpha-glucosidase, an enzyme in the brush border of the proximal small intestinal epithelium, serves to break down disaccharides and more complex carbohydrates. By the competitive inhibition of this enzyme, the AGIs delay intestinal carbohydrate absorption and alleviate postpradial glucose excursion.[68, 69]

Meglitinides, including Prandin (repaglinide) and Starlix (nateglinide). These diabetes medicines lower blood sugar by stimulating the pancreas to release more insulin. The effects of these diabetes pills depend on the level of glucose. They are said to be glucose dependent. High sugars make this class of diabetes medicines release insulin. This is unlike the sulfonylureas that cause an increase in insulin release, regardless of glucose levels, and can lead to hypoglycemia.[65, 66]

8. Novel approaches for T2DMT Treatment

Although combination therapies of traditional oral hypoglycemia agent are available, these drug combinations have some limitations in practical application to late stage T2DM and require exogenous insulin therapy. To overcome these limitations, new strategies are being developed. At present, there are several recent approaches. For example, islet cell transplantation and glucagons-like peptide-1 (GLP-1) or GLP-1 analogues are used to replace and proliferate islet cells. Islet cell transplantation is suitable for T1DM, whereas GLP-1 or GLP-1 analogues are more proper for T2DM.

Dipeptidyl peptidase IV inhibitors, acetyl-coA carboxylase 2 and I kappa kinase beta (IKKB) are new targets which have the potential of increasing insulin action at target tissues, stimulate carbohydrate and fat catabolism, decrease endogenous glucose production, increase pancreatic β-cell neogenesis and glucose-dependent insulin secretion.

In order to develop more effective treatments for T2DM, it is essential to have beneficial tools to find novel targets quickly. Gene expression profiling is a tool to help researchers to identify M cell specific transporters for small particles. The gene expression profiling technique can also be used to monitor the effects of different therapeutic agents for T2DM. Additionally, information collected from this approach can potentially be used to guide the development of gene related therapies.[70]

Insulin is consistently used as a last resource for the treatment for T2DM because of the inconvenience of route of administration, the difference in disease stage and the lifestyle of these patients. So, a non–injectable drug delivery system with variable release capability for insulin could address these issues.[71] Implantable polymeric systems that have been developed to control drug delivery profiles. In other developments, there are various available treatment approaches for T2DM such as CSII (insulin pump therapy), nuclear receptors as drug targets, modulators of peroxisome proliferators activated receptors (PPAR), glucagon receptor antagonists, insulin receptor activators and protein tyrosine phosphatase inhibitors. Combination therapies together with latest findings aimed at identifying new antidiabetic agents with novel mechanisms.[72]

"Incretin therapy" was recently T2DM treatment. Incretin is a collective term for some gastrointestinal hormones and the concept of incretins is stem from the ability of incretin hormones to enhance insulin responses induced by food intake. The key hormone involving diabetes therapy is glucagon-like peptide-1 (7-36) (GLP-1). GLP-1 and its analogs are a new class of T2DM drug that potentiate glucose-dependent insulin secretion, suppress glucagon release, slow gastric emptying and reduce food intake. GLP-1 is a peptide hormone secreted by intestinal L-cells in

response to food intake (Figure 7).[72, 73] The GLP-1 is rapidly inactivated by dipeptidyl peptidase IV (DPP-4). There is a recent increase in the development of GLP-1 analogues and DPP-4 inhibitors.[74, 75]
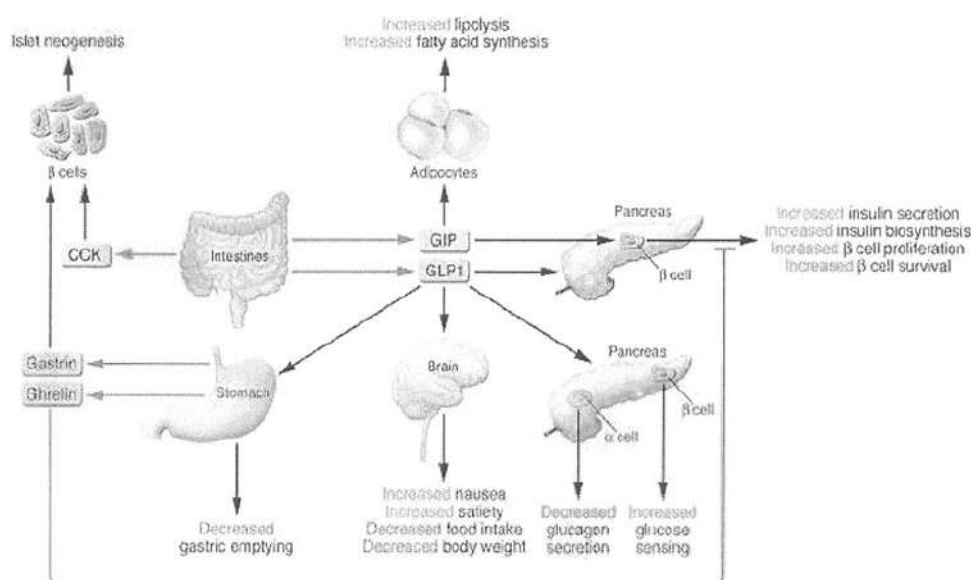
Figure 10   Actions of selected peptides on key tissues important for the control of glucose homeostasis.[76]

Both GLP1 and GIP promote insulin biosynthesis, insulin secretion, and islet β-cell survival. GLP1 exerts additional actions important for regulation of glucose homeostasis, including inhibition of glucagon secretion and gastric emptying, and induction of satiety. GIP, but not GLP1, directly engages receptors on adipocytes coupled to energy storage. In contrast, CCK and gastrin do not seem to acutely regulate levels of plasma glucose but might be important for stimulating the formation of new β-cells by stimulating islet neogenesis.

8.1 Dipeptidyl peptidase IV (DPP-4).

Serine protease, DPP-4 has been an interesting subject of research since 1967 and the first inhibitor were characterized in the late 1980s and 1990s. In early research the scientists were interested in structure and established an early structure activity relationship (SAR) for subsequent investigation. The inhibitors can be classified into two main classes, those interact covalently with DPP-4 and those that do not.[77, 78] DPP-4 selectively binds substrates that contain praline at the P1-position, therefore several DPP-4 inhibitors contain 5-membered heterocyclic rings that mimic praline structure such as pyrroridine, cyanopyrroridine, thiazoridine and cyanothiazolidine.[79] These inhibitors generally form covalent bonds to the catalytic residue Ser 630.[80] In

1994, the research form Zeria pharmaceuticals disclosed the cyanopyrrolidines and the nitrile group was assumed to form an imidate with the catalytic serine. Simultaneously, other DPP-4 inhibitors without a nitrile group were reported, they contained other serine-interacting motifs, e.g boronic acid, phosphonates. These compounds were not potent due to the similarity of DPP-4 and prolyl oligopeptidase and also suffered from chemical instability. Many attempts have been tried to improve the potency and chemical stability.

In 1995, Edwin B. Villhauer at Novartis developed the group of N-substituted glycinyl-cyanopyrrolidines based on the concept that DPP-4 recognize N-methylglycine as an N-terminal amino acid. This cyanopyrrolidine group became research in the following years. Some trials with non cyanopynolidine series of DPP-4 inhibitors have been researched.[81]

The enzyme DPP-4 activity is found ubiquitously in almost all organs and tissues with the highest local concentrations found renally in the proximal tubuli and luminally on the epithelial cells of the small intestine. DPP-4 preferentially hydrolyzes N-terminal dipeptide from protein having proline or alanine in penultimate position. [82, 83]
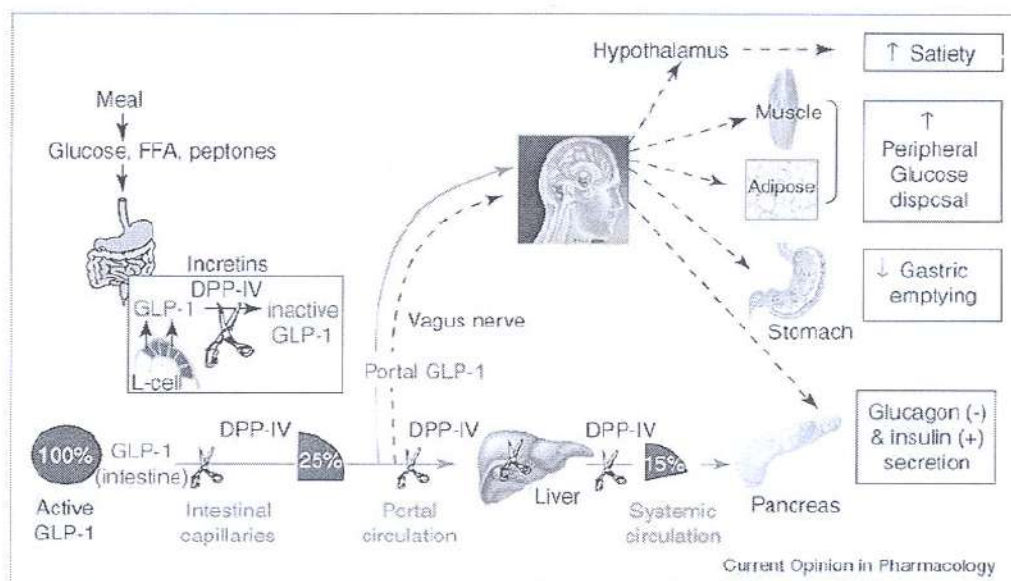

Figure 11 The effect of dipeptidyl peptidase IV (DPP-4) on GLP-1. [84]

Receptors that mediate the effects of GLP-1 and GIP have been found in widespread of body including pancreatic islets, lung, stomach and many locations in brain. The cerebral GLP-1 receptors are likely to be targets for GLP-1 stimulated after

food intake; these neurons are most likely connected to meal-induced satiety. [85, 86] The effects of GLP-1 are mediated via specific G-protein-linked transmembrane receptors. Epitopes in the C- and N-terminal regions of the peptides are involved in receptor binding, the N-terminus is crucial for receptor activation. [84, 87] (**Figure 12 b**)

12a   12b
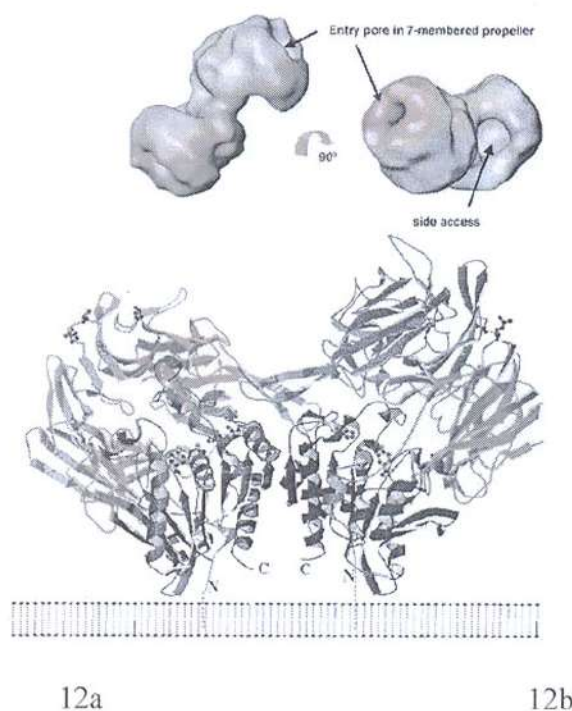
Figure 12   a) Surface representation of DPP-4 shows two entry pores at side access and bottom access.

b) Ribbon diagram of DPP-4: The domains are dark green and light green for the α/β hydrolase and β-propeller domains, respectively, of subunit A and dark blue and light blue for the other subunit.

For recent years, many attempts have been made to override the problem of rapid short half-life of GLP-1. There are two principles in the therapeutic treatment of hypoglycemia. The first approach is incretin analog and the other is DPP-4 inhibitors. [84, 88] DPP-4 is a membrane-bound, homodimeric class II serine peptidase in the prolyl oligopeptidase (POP) family and has a molecular 110-150 kD per subunit. [82, 89] (Figure 11) Each subunit represents an independent activity entity, consisting of two domains: an α/β-hydrolase domain and an N-terminal β-propeller domain. The α/β hydrolase locates closest to the membrane protein and this domain contains active triad Ser 630, Asp708 and His740 (Figure13) The eight-bladed β propeller fold is unique in the POP family proteins [82, 89-95]

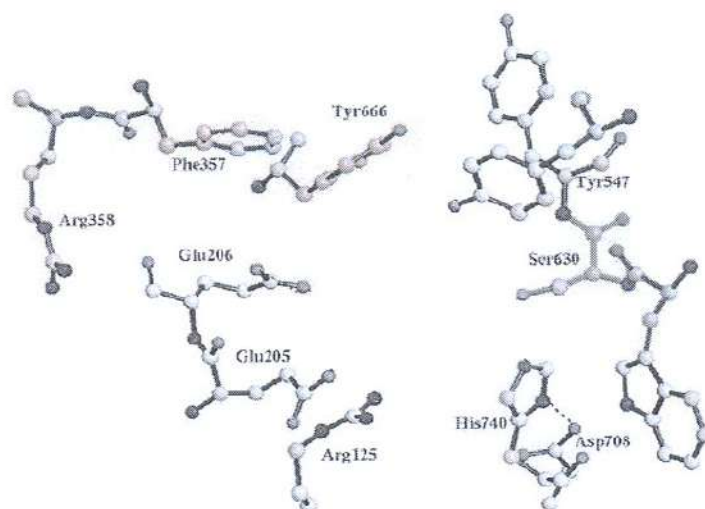**Figure 13** Surface representation of DPP-4 shows two entry pores at side access and bottom access. [92]
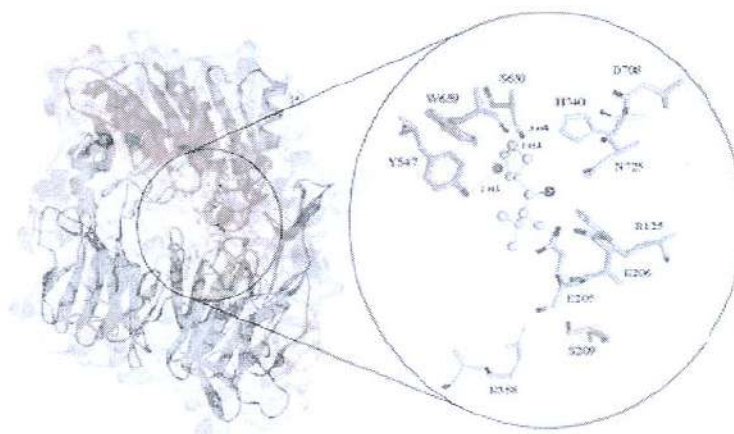

Figure 14 The structure of one monomer of DPP-4 in complex with ValPyr and close-up of the active site. The β-propeller and the α/β hydrolase domains are shown in purple and brown, respectively. Residues in close proximity of the ValPyr inhibitor are shown with interatomic distances. See text for details. [96-98]

8.2 Dipeptidyl peptidase IV (DPP-4) inhibitors.

DPP-4 inhibitor is a novel and promising therapy for T2DM. From the previous information, DPP-4 inhibitor works through preventimg the inactivation of the incretin hormone GLP-1 resulting in stimulation of insulin secretion, reduction in glucagon secretion with a poten

In the process of molecular design, the crystal structure of DPP-4 protein is essentially fundamental information. Several DPP-4 crystal structures, in both human and porcine, have been published recently, which allows structure-based drug design to be used in the search for new and different series of DPP-4 inhibitors.[99] In earlier research, DPP-4 inhibitors resemble the S2-S1 dipeptidyl substrate cleavage product, where the S1 sites contains proline mimic. [100-101] (**Figure.15** a) Consequently, many known DPP-4 inhibitors possess substituted pyrrolidines ring.[102-105] The (S)-2-cyanopyrrolidine derivatives are the earlier series that contains two parts i.e. a proline mimic to occupy S1 site and an aliphatic amino acid to occupy the S2 site. The compounds in this series have long duration of plasma DPP-4 inhibitory activity. NVP-DPP728 (Figure 15b) and NVP-LAF237 vildaglipin (Figure 15c) are the representative of (S)-2-cyanopyrrolidine that are potent inhibitor and the latter is under clinical trial as antidiuretic agent [106].
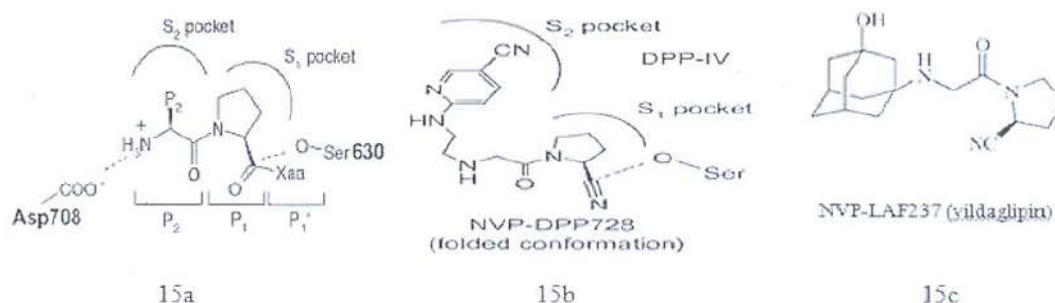

15a   15b   15c

Figure 15 (a) The concept of structure of drug design (b) The assumption of the NVP-DPP728 folded conformation (c) The structure of NVP-LAF237 (Vildaglipin)

However, the (S)-2-cyanopyrrolidine class suffers from chemical instability whereby the N-terminal amine intramolecularly cyclizes onto the nitrile, forming inactive cyclic products (**Figure 16**).
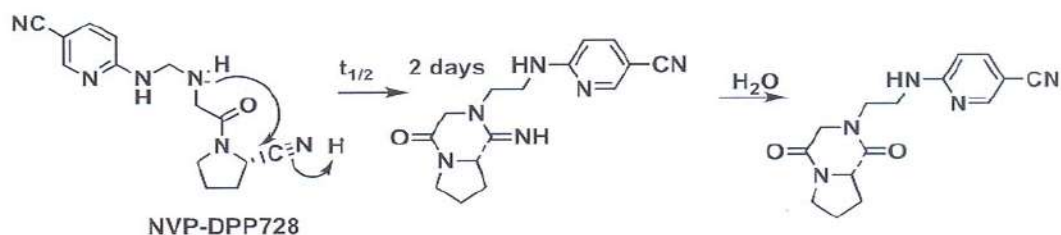
Figure 16 Inactivation of cyanopyrrolidine inhibitors such as NVP-DPP728 via internal cyclization. [107]

In order to avoid this cyclization, the most widesparead technique is the incorporation of a steric bulk. K579 (Figure 16a) is a DPP-4 hihibitor from Kyowa Hakko Kyogo. It did not only have the improved chemical stability but also a longer-lasting action. That long-lasting action was most likely due to slow dissociation of the enzyme-inhibitor complex and an active metabolite that underoes enterohepatic circulation. The discovery of this compound led to the development of vildaglipin and saxagliptin (Figure 17b). [108]

Vildagliptin is an oral medication used to improve glycaemic control in patients with T2DM. It works as a dipeptidyl peptidase-4 (DPP-4) inhibitor. This means that the DPP-4 enzyme cannot degrade the incretin hormones, glucagon-like polypeptide-1 (GLP-1) and glucose-dependent insulinotropic peptide (GIP), which are produced in response to oral food intake. An increase in GLP-1 levels produces a glucosedependent increase of insulin secretion and reduces glucagon secretion from pancreatic β- and α-cells, respectively. Vildagliptin reduces blood glucose levels and is most beneficial in reducing postprandial blood glucose elevations in patients with T2DM. [109]

Saxagliptin With increased steric bulk of the N-terminal amino acid side chain led to increased stability. To increase stability the trans-rotamer with a *cis*-4,5-methano substitution of the pyrrolidine ring, results in intermolecular van-der-Waals interaction, thus preventing intermolecular cyclisation. Because of this increased stability, the researchers continued their investigation on *cis*-4,5-methano cyanopyrrolidines and came across with a new adamantly derivative which showed extraordinary *ex vivo* DPP-4 inhibition in rat plasma. After hydroxylation on the adamantyl group they had a product with better microsomal stability and improved chemical stability. That product was named saxagliptin. [109]

The compound P32/98 (Figure 16c) from Merck is one of the earlier devoloped inhibitors. It is also designed by using the substrate-like concept by using thiazolidine as the P1-substitued group. [110] It was the first DPP-4 inhibitor that showed effective in both animals and humans but it was not further developed to market due to its side effect. Thus, there are many developments in DPP-4 inhibitors to afford highest potency with low undesirable effect. [111]
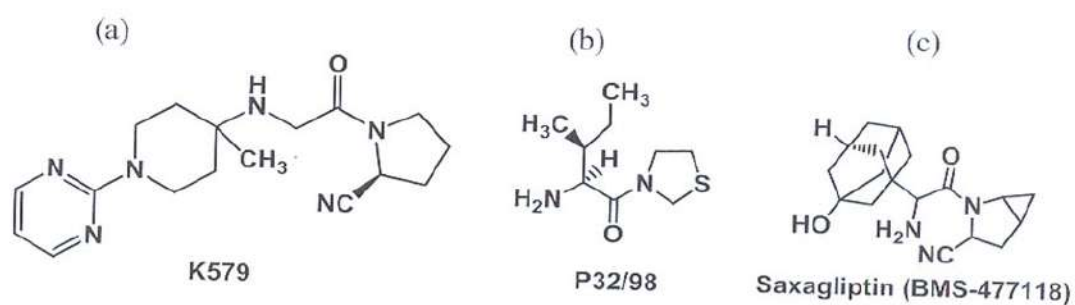

Figure 17 The chemicsl structures of (a) K579, (b) sexagliptin (c) P32/98.

Non-substrate-like inhibitors are non-covalent inhibitors and usually have an aromatic ring that occupies the S1-pocket, instead of the proline mimic. Merch has discovered a β-amino acid piperazine series (β-amino amide derivatives) which was very selective. They found triazolopiperazine compounds in this series showed excellent pharmacokinetic properties and finally led to the discovery of sitagliptin. (Figure 18) Sitagliptin prolongs the activity of proteins that increase the release of insulin after blood sugar rises, such as after a meal. Sitagliptin is a selective inhibitor of the enzyme dipeptidyl peptidase-4 (DPP-4), which metabolizes the naturally occurring incretin hormones glucagon-like peptide-1(GLP-1) and glucose-dependent insulin tropic polypeptide (GIP) resulting in enhanced glucose-dependent insulin secretion from the pancreas and decreased hepatic glucose production. Since GLP-1 enhances insulin secretion in the presence of raised blood glucose levels, inhibiting DPP-IV activity will increase and prolong the action of GLP-1 by reducing its rate of inactivation in plasma. Sitagliptin reduces hemoglobin A1c (HbA1c), fasting and postprandial glucose by glucose-dependent stimulation of insulin secretion and inhibition of glucagon secretion. GLP-1 has other widespread effects including delaying gastric emptying, significantly reducing glucagons levels and possible central effects on the appetite. [112, 113]
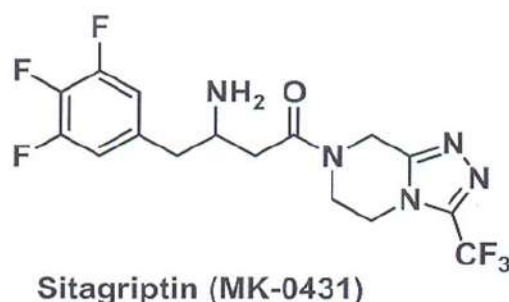
Sitagriptin (MK-0431)

Figure 18 The chemicsl structures ofsitagliptin.

Denagliptin (Figure 18) an advanced compound with a branched side chain at the S2 position, but also has (4S)-fluoro substitution on the cyanopyrrolidine ring. It is a well-known DPP-4 inhibitor developed by GlaxoSmithKline. Biological evaluations have shown that the S-configuration of the amino acid portion is essential for the inhibitory activity since the R-configuration showed reluctantly inhibition. These findings are useful in future for designing and synthesis of DPP-4 inhibitors. [109]

Denagliptin

Figure 19 The chemicsl structures of Denagliptin.

Xanthine-based compound are different class of inhibitors that were identified by high throughput screening (HTS). Aromatic heterocyclic-based DPP-4 inhibitors have gained increased attention recently. The first model is xanthines (Figure 19a) which were devoloped from Boehringer-Ingelheim (BI) and Novo Nordisk. When xanthin based DPP-4 inhibitors are compared with sitagliptin and vildagliptin, they have shown a superior profile. [109, 114]

Quinazolinones based structures (Figure 19b) which have higher potency, long-lasting inhibition and long-lasting improvement of glucose tolerance Alogliptin (Figure 20c) which is a novel DPP-4 inhibitor developed by Takeda Pharmaceutical Company. This compound is a quinazolinone based compound which improves the metabolic stability, potency and selectivity. [109, 114, 115]

Xanthine type   **Quinazolinone based struture**   **Alogliptin**

(a)   (b)   (c)
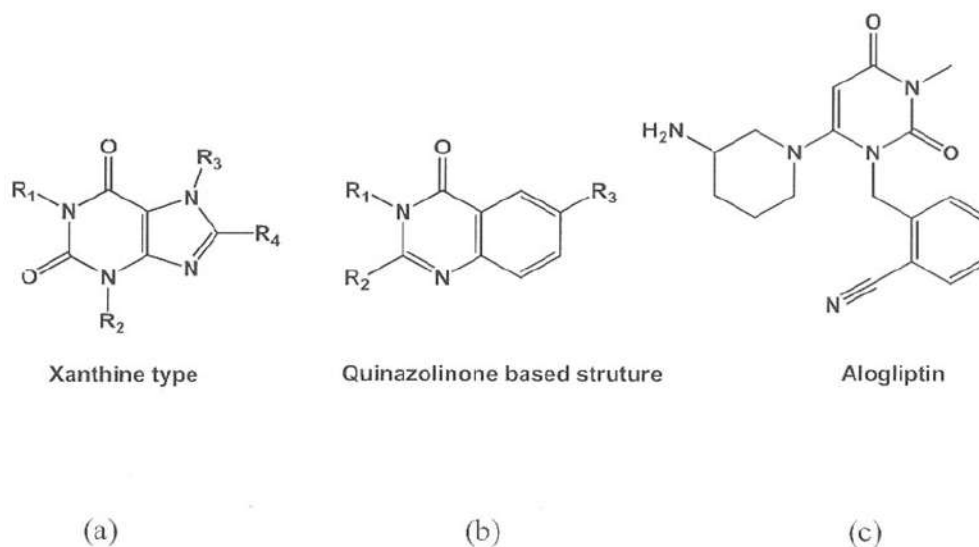
Figure 20 The chemicsl structures of (a) Xanthine type inhibitor, (b)
Quinazolinones based structures ihhibitor (c) alogliptin.

Tremendous efforts have been tried to generate the novel DPP-4 inhibitors, the DPP-4 inhibitors developed during 2007-2011 are displayed in Table 3.

Table 3   **The novel DPP-4 inhibitors developed during 2005-2011.**

Series	Structure	Modification	Gain Property	Ref. (year)
β-Amino amides incorporating fused heterocylcle		From pyrrolidine to fused heterocycles	Improve bioavailability and	(116) (2005)
1-((S)-γ-Substituted prolyl)-(S)-2-cyanopyrrolidine		Substituted at γ position to constrain the conformation	Reduce cyclization	(117) (2005)

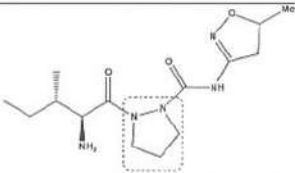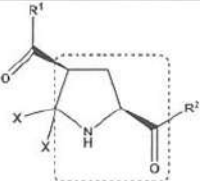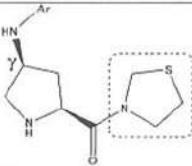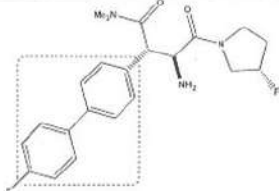## Table 3   The novel DPP-4 inhibitors developed during 2005-2011.
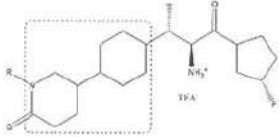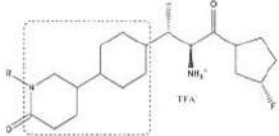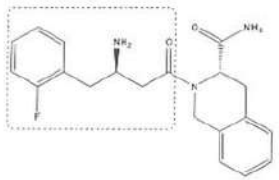
Series	Structure	Modification	Gain Property	Ref. (year)
Pyrazolidine scaffold lacking nitrile group		Pyrazolidine scaffold without cyano group	Avoid instability (improve bioavailability)	(118) (2005)
Substituted pyrrolidine-2,4-dicarboxylic acid amides		Conformationally constaining the P2 portion	Improve potency, selectivity profile	(119) (2005)
(S)-γ-Arylamino)prolyl] thiazolidine compounds		From (S)-2-cyanopyrrolidineto thiazolidine	More stable and remain potent	(120) (2006)
β-Substitued biarylphenylalanine amides		Changing to β-substitued biarylphenylala nine amides	Improve metabolic	(121) (2006)
Anti-substituted β-methyphenylalanine derived amides		To anti-substituted β-methyphenylala nine derived	Improve potentcy and selectivity	(122) (2006)
Anti-substituted β-methyphenylalanine derived amides		To anti-substituted β-methyphenylalanine derived	Improve potentcy and selectivity	(122) (2006)
β-Phenethylamine derivatives		Reverse binding of β-phenethylamine inhibitors of DPP-4	Generate concepts that obviate substrate-like SAR	(123) (2006)

Table 3   **The novel DPP-4 inhibitors developed during 2005-2011.**
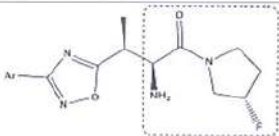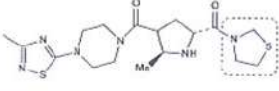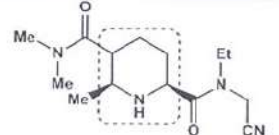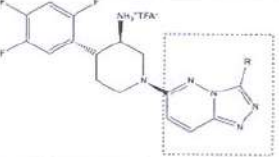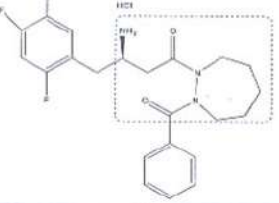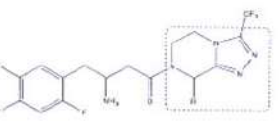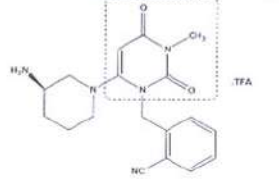
Series	Structure	Modification	Gain Property	Ref. (year)
Oxazodiazole based amides		Replace the central phenyl group in biphenyl series with heterocycle	Generate novel potent series	(124) (2006)
Non-nitrile pyrrolidine		From pyrrolidine to thiazole ring and 5-methyl substituted prolyl	Increase stability in rat plasma	(125) (2007)
(N-Ethyl) aminoacetonitrile		Using (N-ethyl) aminoacetonitrile instead of 2-cyanopyrrolidine	Improve selectivity but decrease potentcy	(126) (2007)
Xanthine		Changing to a novel series xanthine-derivative	Increase potentcy, selectivity and duration of action	(127) (2007)
Series of 3-aminopiperidines		Modified from MK-0431. replacement of the central cyclohexylamine	Good potent and selectivity over other peptidases	(128) (2007)
β-Aminoacyl-containing cyclic hydrazine derivatives		Modified from MK-0431template to structure containing pyrazolidine to cyclic hydrazine	Excellent selectivity, enhance in vivo efficacy	(129) (2007)
β-Aminoamides bearing substituted triazolopiperazine		Modified the series of sitagliptin	High selectivity, good pharmacokinetic profile	(130) (2007)
Quinazolinone based scaffold		Replace the quinazolinone with pyrimidinedione	More potent and selective	(131) (2007)

Table 3   The novel DPP-4 inhibitors developed during 2005-2011.
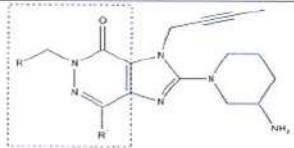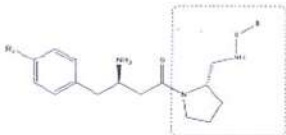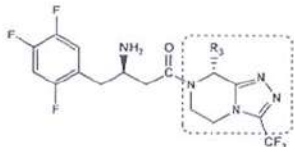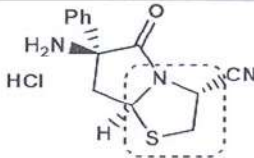
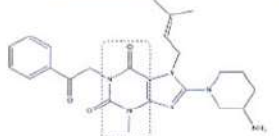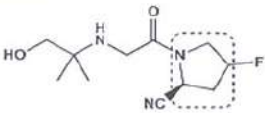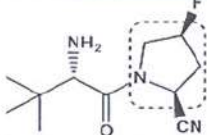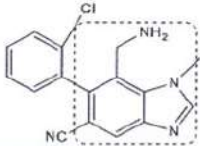| Series	Structure	Modification	Gain Property	Ref. (year)
4-Fluoro-2-cyanopyrrolidine		From 2-cyanopyrrolidine to 4-fluoro-2-cyanopyrrodine	More stable, decrease of potency	(132) (2008)
		Changing isoleucine to L-ter-butyl glycine	More stable and remain potent	(133) (2008)
Benzimidazole		Changing to a novel series benzimidazole-derivative	Increase potentcy and selectivity	(134) (2008)
A series of β-aminoacyl-containing homopiperazine derivatives		Modified the series of β-aminoacyl-derivatives	Potent and more specific without inhibiting CYPs	(135) (2008)
Xanthine scaffold		Development compound BI 1356	A series of highly potent DPP-4 inhibitors	(136) (2008)
β-Homophenylalanine based pyrrolidin-2-ylmethyl amides and sulfonamides		β-Homophenylalanine based pyrrolidin-2-ylmethyl amides and sulfonamides	High potent, selective and most potent is 0.38 nM DPP-4 inhibitors	(137) (2009)
Triazolopiperazine		Substituting methyl or $CH_2(4\text{-fluorophenyl})$ at R_3	Increase potency and half-life in plasma	(138) (2009)
Bicyclic cyanothiazolidines		Changing to novel series cyanothiazolidine	Increase potency	(139) (2009)

Table 3   The novel DPP-4 inhibitors developed during 2005-2011.
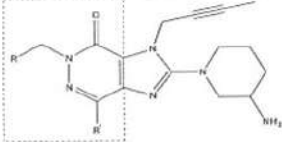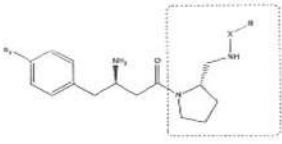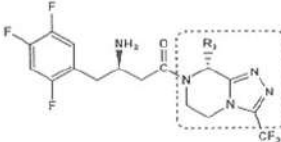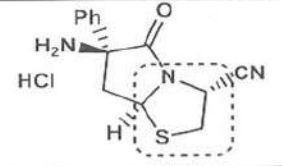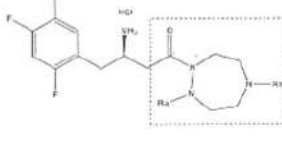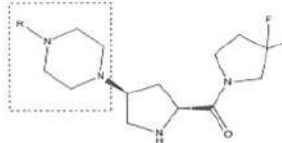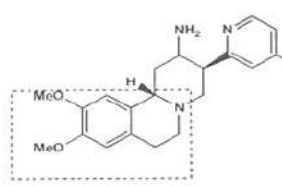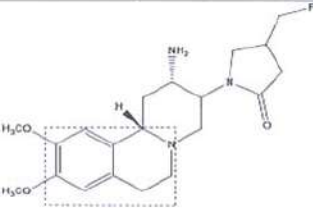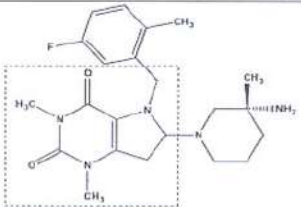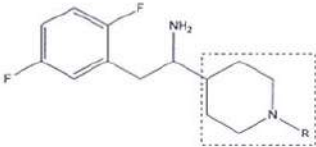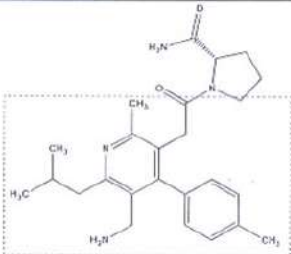
Series	Structure	Modification	Gain Property	Ref. (year)
Xanthine scaffold		Development compound BI 1356	A series of highly potent DPP-4 inhibitors	(136) (2008)
β-Homophenylalanine based pyrrolidin-2-ylmethyl amides and sulfonamides		β-Homophenylalanine based pyrrolidin-2-ylmethyl amides and sulfonamides	High potent, selective and most potent is 0.38 nM DPP-4 inhibitors	(137) (2009)
Triazolopiperazine		Substituting methyl or CH_2(4-fluorophenyl) at R_3	Increase potency and half-life in plasma	(138) (2009)
Bicyclic cyanothiazolidines		Changing to novel series cyanothiazolidine	Increase potency	(139) (2009)
A series of triazepane derivatives		Modified the series of sitagliptin	Good in vitro activity, selectivity without CYP inhibition	(140) (2009)
A series of 4-substituted proline amides		Modified the the series of PF-00734200	Potent, selective and most potent is 13nM DPP-4 inhibitors	(141) (2009)
Aminobenzo[a] quinolizines		Changing aryl-substituted aminobenzo[a]quinolizines based on SAR for occupying in S1 pocket	Increse potency	(142) (2010)

Table 3   **The novel DPP-4 inhibitors developed during 2005-2011.**
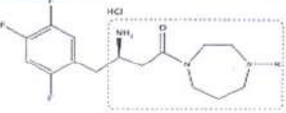
Series	Structure	Modification	Gain Property	Ref. (year)
A series aminobenzo[a] quinolizines		Aminobenzo[a]quinolizines with non-aromatic substituents	Carmegliptin exhibits a unique pharmacokinetic profile, with no metabolism	(143) (2010)
(R)-3-amino-3-methylpiperidine		Modified the series xanthine scaffold	Potent DPP-4 inhibitors with good bioavailability	(144) (2010)
		Combination of of sitagliptin and substituted 4-amino cyclohexyl glycine	Good potent and selectivity DPP-4 inhibitor	(145) (2011)
Novel nicotinic acid derivative		Modified the series 3-pyridylacetamide derivatives.	Potent and selective DPP-4 inhibitor	(146) (2011)

The DPP-4 inhibition is a novel and promising therapy for T2DM. The novel DPP-4 inhibitor is not essential to be proline-like structure and proline structure is not always occupied in S1 pocket. So, the target of innovation is merely design structures that can fit to S1 and S2 pockets and are orally active, safe and well tolerated. Moreover the optimal inhibitor results in a sustained robust and clinically significant improvement in glycaemia both in monotherapy and in combination with metformin and thaizolidinediones.

DPP-4 inhibition works through preventing the inactivation of the incretin hormone GLP-1 and there by increases and prolongs the action of the incretin hormone. DPP-4 inhibitors eventually assist the stimulation of insulin secretion and reduction in glucagons secretion with a potential also of increased β-cell mass.

Besides improvement in glucose metabolism.[147] At present, there are more than 10 agents being evaluated in clinical trials by different pharmaceutical companies. [148]

From the clinical studies, DPP-4 inhibitors are likely to be potential therapy in diabetes. However, there are some concerns about long-term inhibition of DPP-4 which lead to significant unwanted side effects. Therefore, the development of DPP-4 inhibitors has been concentrated on the specificity and duration of action.

CHAPTER III
EXPERIMENTAL

A. *In Silico* Experiment

1. Materials

1.1 Software AutoGrid 4 and AutoDock 4 (The Scripps Research Institute)

1.2 Software ChemOffice 8.0 for Windows (CambridgeSoft Corporation, USA)

1.3 Dipeptidyl peptidase IV (Protein Data Bank entry code: 1X70, 2IIT, 3G0B and 1RWQ

2. Methods

2.1 DPP-4 Template Preparation

A crystallographic structure of human dipeptidyl peptidase IV (DPP-4, PDB entry code: 1X70) bound to the inhibitor 715 (sitagliptin) was selected for the preparation of DPP-4 template. The bound crystal was solved by X-ray diffraction techniques with a resolution of 2.10 Å. In the preparation of the DPP-4 template, the ligand and crystallographic water were removed. The polar hydrogens were added add Gasteiger charges were computed and then non-polar hydrogens were merged by using AutoDockTools 1.5.2 (ADT). The grid maps for every atom type in the ligand were added an electrostatics ('e'map) and a desolvation map ('d'map) and were calculated with AutoGrid. The dimentions of the grid were 52 x 50 x 42grid points with a spacing of 0.375 Å between the grid points. The grid box was centered on the coordinates 40.926 x 50.522 x 34.843 Å. This grid map parameters were used for further DPP-4 model validation and docking experiments. Four DPP-4 bound ligands from the available X-ray crystallographic data were used to validate the constructed DPP-4 template. A validated by re-docking ligand 715, 872, T22 and 5AP (PDB code: 1X70, 2IIT, 3G0B and 1RWQ and finally by visualizing the re-docked poses were determined. The criteria to evaluate whether the template was the appropriate DPP-4 model were the cluster distribution character from docking and the RMSD of the docked conformations. The good results should display (a) one single cluster with higher number of number of members of docked conformations and (b) the docked conformations in the largest cluster were considered to be the same as that of the crystal pose according to RMSD value < 2 Å.

2.2 Ligand Preparation

The combinatory library of 356 structures containing two main fragments linked with imine or amide functions was prepared. The 3D structures of all ligands were initially drawn, cleaned up by the ChemDraw Ultra version 11.0 and Chem 3D Ultra 11.0 program and then energy was minimized by MM2. All hydrogens were added and Gasteiger charges were assigned to each pdb file by using ADT 1.5.2 Gasteiger charge was non-polar hydrogen was merged, aromatic carbons identified, Later, the rigid root and rotatable bonds were defined. The compounds in the library were docked with the constructed DPP-4 template.

2.3 Molecular Docking

The AutoDock 4.1 run parameters in docking studies were as follows: the number of Genetic Algorithm (GA) runs was 100; the population size was 150; the maximum number of energy evaluations was increased to 15,000,000 per run; and the maximum number of generation was 27,000. The jobs were run on Bluefish at The Scripps Research Institute. After jobs were run completely, the docked poses were clustered at 2 Å RMSD for grouping the similarity of their final docked conformations. The cluster of highest members with lowest docking energy was chosen and its binding energy was recorded for the evaluation. Ultimately, the docking result i.e. the docked pose or binding mode, RMSD against the bound crystal structure and binding energy were analyzed to evaluate the interaction between the ligand and the active site of macromolecule.

B. Synthesis
1. Equipment and Chemicals
1.1 Equipment

Analytical balance	Satorius 2842, USA
Elemental analyzer	Perkin Elmer CHNS/O 2400, USA
Fourier Transform Infrared Spectrometer	Perkin-Elmer model 2000
Infarred spectrophotometer	Nicolet FTIR 550, USA
Magnetic stirrer	Heidolph MR 3001K, Germany
Mass spectrophotometer (EI)	Thermo Finnigan, USA
Mass spectrophotometer (ESI)	BrukerMicroTof, Switzerland
Melting point apparatus	Electrothemal®, UK
Micropipet	Pipetman Gilson, France

Nuclear Magnetic Resonance (NMR)	BrukerAvance 300 MHz, Switzerland
Rotary evaporator	Eyela, Japan
Stirring hot plate	ThermolyneCimarec®, USA
Thin layer ChromatographyReader 240 C/F	Spectroline model ENF-

1.2 Chemicals and reagent

Molecular sieve 4 Å beads 8-12 mesh	Aldrich, Germany
Silica gel 60 (0.063-0.200 mm)	Merck, Germany
TLC Silica gel 60 F254	Merck, Germany
Sand low ion stable	Fischer Scientific, UK
Fmoc-Cys(4Mbzl)-OH	Carbiochem-Novabiochem, USA
Boc-Cys(4Mbzl)-OH	AnaSpecInc, USA
Boc-Cys(pMeOBzl)-OH	AnaSpecInc, USA
Acetone	Labscan, Thailand
Absolute ethanol	Labscan, Thailand
3-amino-6-chloropyridazine	Combi-Blocks, Inc
2-amino-3-formyl-6-methyl-chromone	Oakwood, India
Benzylamine	Fluka, Switzerland
N-Boc-piperazine	AK Scientific, Inc
3-Chromone carbaldehyde	Wako, Japan
Chloroform AR	Labscan, Thailand
Chloroform-d 99.8 atom % D	Aldrich, Germany
N,N'-carbonyldiimidazole (CDI)	Wako, Japan
N,N'-diisopropylcarbodiimide (DIC)	Sigma Aldrich, Germany
Dichloromethane (DCM)	Labscan, Thailand
DMSO-d6 99.9 atom % D	Cambridge Tsotope Laboratories, USA
4-Dimethylaminopyridine AR (DMAP)	Sigma, Germany
Ether AR	JT baker, USA
Ethyl acetate AR	Labscan, Thailand
3-formyl-4-oxo-4H-chromen-7-yl acetate	Indofine chemical, Inc, USA
p-Fluorobenzylamine	WaKO, Japan
Hexane AR	Labscan, Thailand
Hydrocholric acid 37%	Labscan, Thailand
p-Methylbenzylamine	WaKO, Japan
6-methyl-4-oxo-4H-chromene-3-carbaldehyde	Oakwood, India

Methanol AR	Labscan, Thailand
Methylsulfoxide-d6 (99.9 atom% D)	Aldrich, Germany
3-picolylamine	Sigma, USA
Piperidine	Sigma, Germany
Potassium bromide(for IR spectroscopy)	Merck, Germany
Potassium dihydrogen phosphate	Unilab, Australia
Sodium bicarbonate AR	Sigma, Germany
Sodium chlorite 80% pure, unstabilized	Acros organics, Belgium
Sodium chloride	M&B, England
Sodium hydroxide AR	Analar, England
Sodium sulfate, anhydrous	Merck, Germany
Sulphamic acid AR	M &B , England
Sulfuric acid	Labscan, Thailand
Seasand	Ferak, Germany
Silicagel 60 No. 1.07734	Merck, Germany
Silicagel 60 F254 (0.2 mm)	Merck, Germany
Tetrahydrofuran AR	Labscan, Thailand

2. Methods

The preparation of series imine. The structures of six chromone imines **1-6** were synthesized by condensation of chromones and 3 hydrazides in methanol as shown in **Scheme 1**.
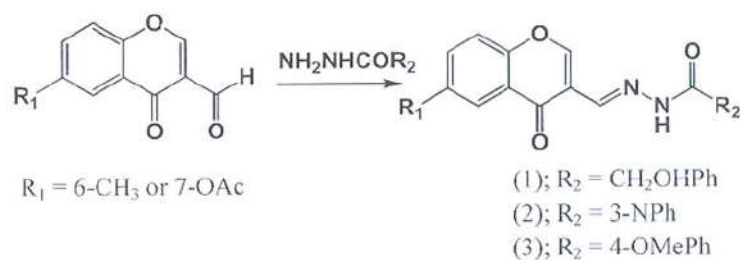
$R_1 = 6\text{-}CH_3$ or 7-OAc

(1); $R_2 = CH_2OHPh$
(2); $R_2 = 3\text{-}NPh$
(3); $R_2 = 4\text{-}OMePh$

Scheme 1 Synthesis of chromone imines **1-6**. Chromone derivatives with various hydrazides in methanol, stir 3-5 hr., RT.

The preparation of series amide. The structures cysteine amides **7-26** and $L(-)$-tryptophan amides **27-33** were synthesized by condensation of cysteine and amine with the aid of peptide coupling agents, CDI as shown in **Scheme 2** and **Scheme 3** respectively.

$R_1 = H$ or CH_3

(1); $R_2 =$ 3-picolylamine
(2); $R_2 =$ morpholine
(3); $R_2 = p$-fluorobebzylamine
(4); $R_2 =$ 4-hydrazinylbenzonitrile
(5); $R_2 =$ 6-methoxybenzo[d]thiazol-2-amine
(6); $R_2 =$ 6-methylbenzo[d]thiazol-2-amine
(7); $R_2 =$ phenylhydrazinehydrochloride
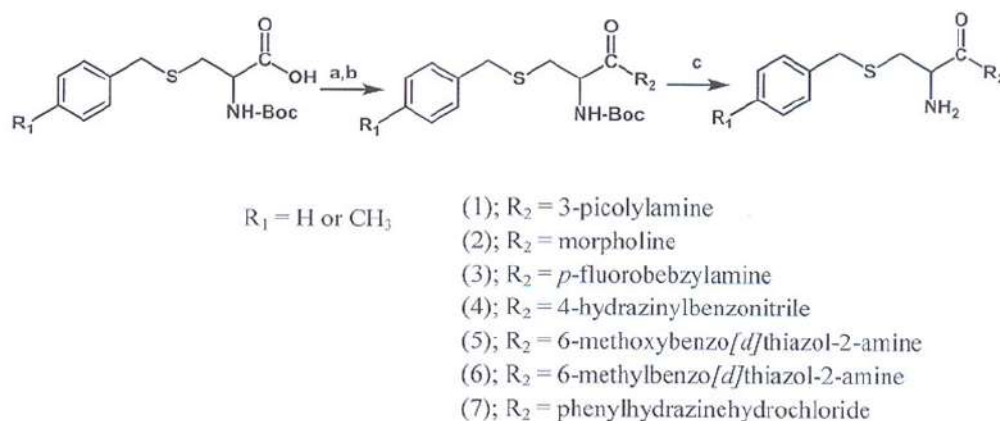
Scheme 2 Synthesis of cysteine amides **7-26** (a) CDI, CH_2Cl_2, stir 1 hr, RT; (b) add R_2NH_2, stir overnight, RT; (c) TFA, CH_2Cl_2, stir 1 hr., 0 ^{0}C.

(1); $R_1 =$ phenylhydrazine hydrochloride
(2); $R_1 =$ morpholine
(3); $R_1 =$ 6-methoxybenzo[d]thiazol-2-amine
(4); $R_1 =$ 6-methylbenzo[d]thiazol-2-amine

Scheme 3 Synthesis of $L(-)$-tryptophan amides **26-33** (a) Boc$_2$O, NaOH (aq), THF, H_2O, stir overnight, RT; (b) CDI, THF, stir 1 hr, RT; (c) add R_1NH_2, stir overnight, RT; (d) TFA, THF, stir 1 hr., 0 ^{0}C.

The structure of the synthesized compounds were elucidated by melting point, infrared (IR) spectrum, mass spectrum (MS), nuclear magnaticresonace spectra (NMR) and/or elemental analysis. Meltingpoint of all compounds were determined on an Electrothermal model 9100 capillary melting point apparatus. Infrared spectra were run on FTIR Nicolet 6700 in the 4000-400 cm^{-1} region by using the potassium bromide (KBr) pellet or attenuated total reflectance (ATR) technique. Proton nuclear resonance (^{1}H NMR) spectra were obtained from BrukerAvance (300 MHz). The ^{1}H NMR solvent were deuterated chloroform (CDCl$_3$, & C$\underline{H}$Cl$_3$ = 7.25 ppm) or deurateddimethylsulfoxide (DMSO-d6, & (C$\underline{H}_3$)$_2$SO) = 2.5 ppm, absorbed water &$\underline{H}_2$O = 0.4 ppm). Mass spectra were run on Thermo Finnigan. Elemental analyses of all compounds were performed on Perkin Elmer CHNS/O 2400 or high resolution mass spectrometer model microTOFBruker for the determination of molecular weight.

(E)-2-Hydroxy-*N'*-((6-methyl-4-oxo-4*H*-chromen-3-yl)methylene)-2-phenylacetohydrazide [1]
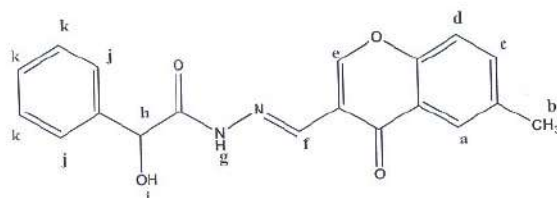
1

3-Formyl-6-methylchromone (0.1882 g, 1.0001 mmol) was dissolved in 20 ml of methanol in 250 mL round bottom flask until completely dissolved. The mixture of mandelic acid hydrazide (0.1662 g, 1.0001 mmol) in 20 ml of methanol was added in reaction solution. This solution was stirred at room temperature for 5 hours to give an orange precipitate and after filtration and washing with methanol to give *(E)-2-hydroxy-N'-((6-methyl-4-oxo-4H-chromen-3-yl)methylene)-2-phenylacetohydrazide* [1] as white crystalline power (0.2643 g, 0.7458 mmol, 74.58% yield); m.p. 215-217 ^{0}C; IR (KBr)(cm^{-1}): 3399.50, 3268.74 (N-H st), 3084.86 (aromatic C-H st), 3031.73 (aliphatic C-H st), 1626.05 (C=O st), 1519.81 (N-H bending), 1458.51 (aromatic C=C st), 1058.06 (C-O st); ^{1}H NMR (300 MHz, DMSO-*d6*): δ 11.64 (s, 1H, N-N<u>H</u>-CO), δ 8.68 (s, 1H, C-C<u>H</u>=N), δ 8.56 (s, 1H, O-C<u>H</u>=C), δ 7.88 (s, 1H, chromone-<u>H</u>$_a$), δ 7.47-7.67 (m, 4H, chromone-<u>H</u>$_{c-d, j}$), δ 7.30 (m, 3H, Ph-<u>H</u>$_k$), δ 6.31 (d, J = 4.46 Hz, 1H, OC-C<u>H</u>-Ph), δ 5.06 (d, J = 4.36 Hz, 1H, Ph-CH-O<u>H</u>), δ 2.42 (s, 3H, Ph-C<u>H</u>$_3$); TLC (silica gel GF ethyl acetate/hexanes/ethanol [2:2:0.5]) ; R$_f$ of *(E)-2-hydroxy-N'-((6-methyl-4-oxo-4H-chromen-3-yl)methylene)-2-phenylacetohydrazide* = 0.27.

(E)-2-Hydroxy-*N'*-((4-oxo-4*H*-chromen-3-yl)methylene)-2-phenylacetohydrazide [2]

2

Chromone-3-carboxaldehyde (0.1742 g, 1.0002 mmol) was dissolved in 20 ml of methanol in 250 mL round bottom flask until completely dissolved. The mixture of mandelic acid hydrazide (0.1663 g, 1.0002 mmol) in 20 ml of methanol was added in reaction solution. This solution was stirred at room temperature for 5 hours to give an orange precipitate and after filtration and washing with methanol to give *(E)-2-*

hydroxy-*N'*-((4-oxo-4*H*-chromen-3-yl)methylene)-2-phenylacetohydrazide **[2]** as white crystalline power (0.2494 g, 0.7246 mmol, 72.62% yield); m.p. 210-213 ^{0}C; IR (KBr)(cm^{-1}): 3464.88, 3256.48 (N-H st), 3064.42 (aromatic C-H st), 2888.71 (aliphatic C-H st), 1634.22 (C=O st), 1519.81 (N-H bending), 1478.94 (aromatic C=C st), 1074.40(C-O st); ^{1}H NMR (300 MHz, DMSO-*d6*): δ 11.65 (s, 1H, N-N$\underline{H}$-CO), δ 8.71 (s, 1H, C-C$\underline{H}$=N), δ 8.56 (s, 1H, O-C$\underline{H}$=C), δ 8.09 (d, J = 7.84 Hz, 1H, chromone-$\underline{H}_a$) δ 7.82 (t, J = 7.84 Hz, J = 8.29 Hz chromone-$\underline{H}_b$), δ 7.69 (t, J = 7.17 Hz, J = 8.17 Hz chromone-$\underline{H}_c$), δ 7.47-7.54 (m, 3H, chromone-$\underline{H}_{d,j}$), δ 7.21-7.36 (m, 3H, OC-C$\underline{H}$-Ph), δ 6.31 (d, J = 4.38 Hz, 1H, Ph-C$\underline{H}$-OH), δ 5.06 (d, J = 4.61 Hz, 1H, Ph-CH-O$\underline{H}$); TLC (silica gel GF ethyl acetate/hexanes/ethanol [2:2:0.5]) ; R$_f$ of *(E)*-2-hydroxy-*N'*-((4-oxo-4*H*-chromen-3-yl)methylene)-2-phenylacetohydrazide = 0.22.

(E)-N'-((4-Oxo-4*H*-chromen-3-yl)methylene)nicotinohydrazide [3]

3

Chromone-3-carboxaldehyde (0.1742 g, 1.002 mmol) was dissolved in 20 ml of methanol in 250 mL round bottom flask until completely dissolved. The mixture of nicotinic acid hydrazide (0.1372 g, 1.0002 mmol) in 20 ml of methanol was added in reaction solution. This solution was stirred at room temperature for 5 hours to give an orange precipitate and after filtration and washing with methanol to give *(E)-N'*-((4-oxo-4*H*-chromen-3-yl)methylene)nicotinohydrazide **[3]** as pale yellowish crystalline powder (0.146 g, 0.5126 mmol, 51.26% yield); m.p. 200-203 ^{0}C; IR (KBr)(cm^{-1}): 3448.54, 3256.48 (N-H st), 3056.25 (aromatic C-H st), 2815.16 (aliphatic C-H st), 1671.00,1626.05 (C=O st), 1540.24 (N-H bending), 1458.51 (aromatic C=C st), 1143.87 (C-O st); ^{1}H NMR (300 MHz, DMSO-*d6*): δ 12.11 (s, 1H, N-N$\underline{H}$-CO), δ 9.07 (s, 1H, C=C$\underline{H}$-N), δ 8.85 (s, 1H, C-C$\underline{H}$-O), δ 8.76 (d, J = 4.47 Hz, 1H, N=C$\underline{H}$-CH), δ 8.61 (s, 1H, C-C$\underline{H}$-O-), δ 8.26 (d, J = 7.9 Hz, 1H, C-C$\underline{H}$=CH) , δ 8.12 (d, J = 7.8 Hz, 1H, chromone-$\underline{H}_a$), δ 7.85 (t, 1H, CH=C$\underline{H}$-CH), δ 7.71 (d, J = 8.45 Hz, 1H, chromone-$\underline{H}_c$) , δ 7.55 (m, 2H, chromone-$\underline{H}_{b,d}$); TLC (silica gel GF ethyl acetate/hexanes/ethanol [2:2:0.5]) ; R$_f$ of *(E)-N'*-((4-oxo-4*H*-chromen-3-yl)methylene)nicotinohydrazide = 0.22.
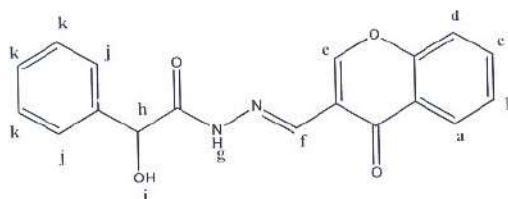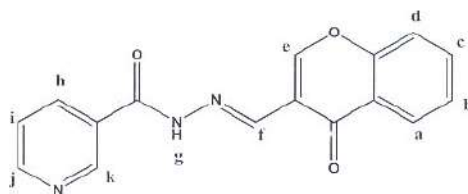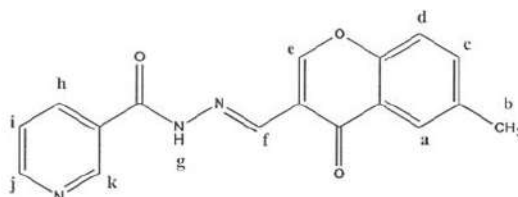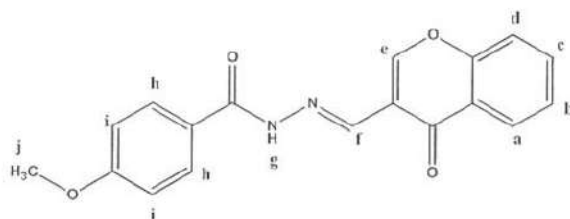
(E)-N'-((6-Methyl-4-oxo-4*H*-chromen-3-yl)methylene)nicotinohydrazide [4]

4

3-Formyl-6-methylchromone (0.1882 g, 1.001 mmol) was dissolved in 20 ml of methanol in 250 mL round bottom flask until completely dissolved. The mixture of nicotinic acid hydrazide (0.1372 g, 1.0001 mmol) in 20 ml of methanol was added in reaction solution. This solution was stirred at room temperature for 5 hours to give an orange precipitate and after filtration and washing with methanol to give *(E)-N'-((6-methyl-4-oxo-4H-chromen-3-yl)methylene)nicotinohydrazide* [4] as pale yellowish crystalline powder (0.132 g, 0.3725 mmol, 37.25% yield); m.p. 208-210 ^{0}C; IR (KBr)(cm^{-1}): 3391.33, 3260.57 (N-H st), 3093.03 (aromatic C-H st), 2359.23 (aliphatic C-H st), 1671.00, 1630.14 (C=O st), 1564.76 (N-H bending), 1519.81 (aromatic C=C st), 1229.68 (C-O st); ^{1}H NMR (300 MHz, DMSO-*d6*): δ 11.65 (s, 1H, N-N$\underline{H}$-CO), δ 8.72 (s, 1H, C=C$\underline{H}$-N), δ 8.56 (s, 1H, C-C$\underline{H}$-O), δ 8.09 (d, J = 7.84 Hz, 1H, chromone-$\underline{H}_a$), δ7.82 (t, J = 7.19 Hz, J = 8.32 Hz, 1H, chromone-$\underline{H}_c$), δ 7.69 (t, J = 7.17 Hz, J = 8.17 Hz, 1H,chromone-$\underline{H}_t$), δ 7.47-7.54 (m, 3H, Ph-C$\underline{H}_3$), δ 7.21-7.36 (m, 2H, chromone-$\underline{H}_{d,i,j}$), δ 6.32 (d, J = 4.38 Hz, 1H,C-C$\underline{H}$-N), δ 5.06 (d, J = 4.61 Hz, 1H,C-C$\underline{H}$-C); TLC (silica gel GF ethyl acetate/hexanes/ethanol [2:2:0.5]) ; R$_f$ of *(E)-N'-((6-methyl-4-oxo-4H-chromen-3-yl)methylene)nicotinohydrazide* = 0.42.

(E)-4-Methoxy-N'-((4-oxo-4H-chromen-3-yl)methylene)benzohydrazide [5]

5

Chromone-3-carboxaldehyde (0.1742 g, 1.002 mmol) was dissolved in 20 ml of methanol in 250 mL round bottom flask until completely dissolved. The mixture of 4-methoxybenzhydrazide 0.1662 g, 1.0002 mmol) in 20 ml of methanol was added in reaction solution. This solution was stirred at room temperature for 5 hours to give an orange precipitate and after filtration and washing with methanol to give *(E)-4-methoxy-N'-((4-oxo-4H-chromen-3-yl)methylene)benzohydrazide* [5] as pale yellowish crystalline powder (0.1520 g, 0.4428 mmol, 44.28% yield); m.p. 213-215 ^{0}C; IR

(KBr)(cm^{-1}): 3460.79, 3264.65 (N-H st), 3027.65 (aromatic C-H st), 2357.50 (aliphatic C-H st), 1679.71, 1634.22 (C=O st), 1503.46 (N-H bending), 1454.43 (aromatic C=C st), 1254.20 (C-O st); ^{1}H NMR (300 MHz, DMSO-*d6*): δ 11.82 (s, 1H, N-N$\underline{H}$-CO), δ 8.81 (s, 1H, C-C$\underline{H}$=N), δ 8.61 (s, 1H, C-C$\underline{H}$-O), δ 8.13 (d, J = 8.12 Hz, 1H, chromone-$\underline{H}_a$), δ 7.82-7.93 (m, 3H, chromone-$\underline{H}_{c,h}$), δ 7.72 (d, J = 8.41 Hz, 1H, chromone-$\underline{H}_d$) , δ 7.54 (t, J = 7.50 Hz, J = 7.51 Hz, 1H,chromone-$\underline{H}_b$), δ 7.05 (d, J = 8.76 Hz, 2H,Ph-C$\underline{H}$-C); TLC (silica gel GF ethyl acetate/hexanes/ethanol [2:2:0.5]) ; R$_f$ of *(E)-4-methoxy-N'-((4-oxo-4H-chromen-3-yl)methylene)benzohydrazide* = 0.31.

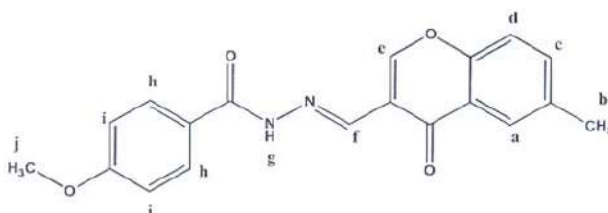### *(E)-4- Methoxy-N'-((6-methyl-4-oxo-4H-chromen-3yl)methylene)benzohydrazide* [6]


6

3-Formyl-6-methylchromone (0.1882 g, 1.001 mmol) was dissolved in 20 ml of methanol in 250 mL round bottom flask until completely dissolved. The mixture of 4-methoxybenzhydrazide 0.1662 g, 1.0002 mmol) in 20 ml of methanol was added in reaction solution. This solution was stirred at room temperature for 5 hours to give an orange precipitate and after filtration and washing with methanol to give *(E)-4-methoxy-N'-((6-methyl-4-oxo-4H-chromen-3-yl)methylene)benzohydrazide* [6] as pale yellowish crystalline powder (0.2132 g, 0.6017 mmol, 60.17% yield); m.p. 220-222 ^{0}C; IR (KBr)(cm^{-1}): 3419.93, 3252.39 (N-H st), 3043.99 (aromatic C-H st), 2835.59, 2841.50 (aliphatic C-H st), 1638.31, 1605.62 (C=O st), 1507.55 (N-H bending), 1470.77 (aromatic C=C st), 1254.20 (C-O st); ^{1}H NMR (300 MHz, DMSO-*d6*): δ 11.81 (s, 1H, N-N$\underline{H}$-CO), δ 8.78 (s, 1H, C-C$\underline{H}$=N), δ 8.60 (s, 1H, C-C$\underline{H}$-O), δ 7.91 (d, J = 8.61 Hz, 3H, chromone-$\underline{H}_{a,c,d}$), δ 7.58-7.66 (m, 2H, C-C$\underline{H}$-Ph), δ 7.04 (d, J = 8.59 Hz, 2H, Ph-C$\underline{H}$); TLC (silica gel GF ethyl acetate/hexanes/ethanol [2:2:0.5]) ; R$_f$ of *(E)-4-methoxy-N'-((6-methyl-4-oxo-4H-chromen-3-yl)methylene)benzohydrazide* = 0.46.

(R)-2-Amino-3-(4-methylbenzylthio)-*N*-(pyridin-3-ylmethyl)propanamide
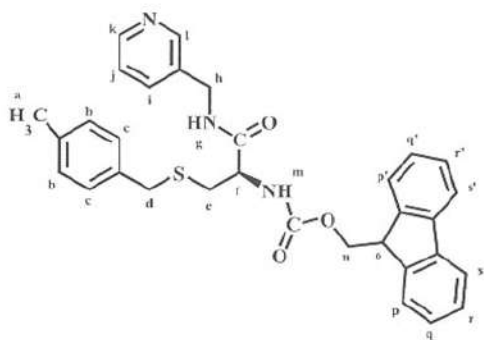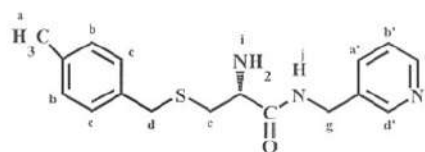
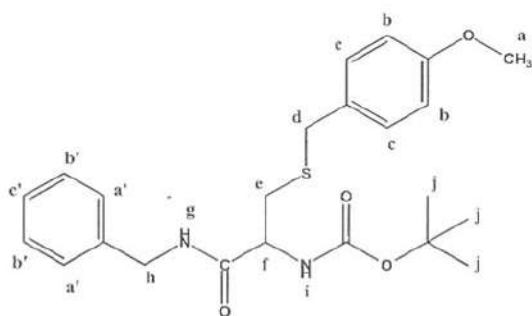(7)   (8)

Fmoc-Cys (PMeBzl)-OH (0.6012 g, 1.3423 mmol) was dissolved in 25 ml of dichloromethane in 250-ml round bottom flask until completely dissolved. After cooling to 0 ^{0}C with the aid of an ice-water bath, a solution of *N,N*-diisopropylcarbodiimide (DIC, 0.1961 g, 1.5565 mmol) in 20 ml of dichloromethane and 3-picolyamine (0.1601g, 1.4809 mmol) in 20 ml of dichloromethane and the reaction mixture was allowed to warm to room temperature and stirred overnight. The mixture was evaporated under reduced atmospheric pressure to dryness. The obtained residue was chromatographed on a silica gel column eluted with ethyl acetate/hexanes/ethanol: (3:2:1)to give *(R)*-(9*H*-fluoren-9-yl)methyl 3-(4-methylbenzylthio)-1-oxo-1-(pyridin-3-ylmethylamino)propan-2-ylcarbamate [7] as white crystalline powder (0.7015 g, 1.2636 mmol, 94.14% yield); m.p. 126-128 °C; IR (KBr)(cm^{-1}): 3338.26, 3290.77 (N-H st), 3024.80 (aromatic C-H st), 2967.81, 2920.32 (aliphatic C-H st), 1691.82 (C=O st), 1546.17 (N-H bend), 1527.18 (aromatic C=C st); TLC (silica gel GF ethyl acetate/hexanes/ethanol [3:2:1]); R$_f$ of [7] = 0.52.

The solution of piperidine in DMF (3:1) was added drop wise to the solution of [7] (0.6012 g, 1.0829 mmol) in 10 ml of dichloromethane and stirred for 60 min under room temperature. The resulting solution was evaporated under reduced atmospheric pressure to dryness. The residue was chromatographed on a silica gel column eluted with ethyl acetate/hexanes/ethanol [3:2:1]) to give *(R)*-2-amino-3-(4-methylbenzylthio)-*N*-(pyridin-3-ylmethyl)propanamide, C$_{17}$H$_{21}$N$_3$OS [8], as colorless or slightly yellow liquid (0.2538 g, 0.8057 mmol, 74.40% yield); IR (KBr)(cm^{-1}): 3325.38 (N-H st), 3040.46 (aromatic C-H st), 2916.99 (aliphatic C-H st), 1663.33 (C=O st), 1511.37 (N-H bend), 1425.89 (aromatic C=C st); ^{1}H NMR (300 MHz, CDCl$_3$-*d*): δ 8.53 (m, 2H, Ph-H$_{c',d'}$), δ 7.84 (s, 1H, OC-NH-CH$_2$), δ 7.63 (d, J = 7.79 Hz, 1H, Ph-H$_{a'}$), δ 7.13-7.27 (m, 5H, Ph- H$_{b, c, b'}$), δ 4.46 (d, J = 6.13 Hz, 2H, NH-CH$_2$-Ph), δ 3.69 (s, 2H, S-CH$_2$-Ph), δ 3.51 (m, 1H, NH$_2$-CH-CO) , δ 2.99 (dd, J = 13.65 Hz, J = 3.89 Hz,

1H, S-CH$_2$-CH), δ 2.72 (dd, J = 13.66 Hz, J = 8.28 Hz, 1H, S-CH$_2$-CH), δ 2.33 (s, 3H, Ph-CH$_3$), δ 2.33 (s, 2H, CH-NH$_2$); TLC (silica gel GF ethyl acetate/hexanes/ethanol [3:2:1]); R$_f$ of [7] = 0.52. and R$_f$ of [8] = 0.31

2-Amino-*N*-benzyl-3-(4-methoxybenzylthio)propanamide
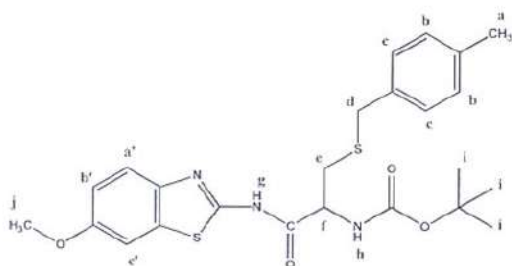

(9)   (10)
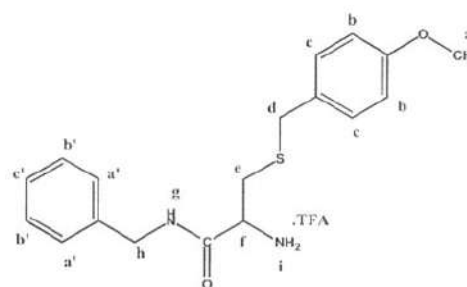
Boc-Cys(4Mbzl)-OH (0.5001 g, 1.4650 mmol) was dissolved in 25 ml of dichloromethane in 250 mL round bottom flask until completely dissolved. After cooling to 0 ^{0}C with the aid of an ice-water bath, a solution of *N*,*N*'-carbonyldiimidazole (CDI, 0.3551 g, 2.1901 mmol) in 20 ml of dichloromethane and phenylmethanamine (0.2036 g, 1.902 mmol) in 20 ml of dichloromethane and the reaction mixture was allowed to warm to room temperature and stirred overnight. The mixture was evaporated under reduced atmospheric pressure to dryness. The obtained residue was chromatographed on a silica gel column eluted with ethyl acetate/hexanes/ethanol: (3:2:1) to give *tert*-butyl 1-(benzylamino)-3-(4-methoxybenzylthio)-1-oxopropan-2-ylcarbamate [9] as white crystalline powder (0.5403 g, 1.2548 mmol, 85.95% yield); m.p. 132-135 °C; IR (KBr)(cm^{-1}): 3354.16, 3309.21 (N-H st), 2916.98 (aromatic C-H st), 2353.15 (aliphatic C-H st), 1691.28 (C=O st), 1617.72 (N-H bend), 1527.83 (aromatic C=C st); TLC (silica gel GF ethyl acetate/hexanes/ethanol [3:2:1]); R$_f$ of [9] = 0.42.

The solution of trifuoroacetic acid in dichloromethane (2:3) was added drop wise to the solution of [9] (0.3505 g, 0.8434 mmol) in 5 ml of dichloromethane in ice bath and stirred for 60 min under 0°C to room temperature. The resulting solution was evaporated under reduced atmospheric pressure to dryness. The obtained precipitates were washed with cool ether for 3-4 times and washed with cool hexane to give 2-

amino-*N*-benzyl-3-(4-methoxybenzylthio)propanamide, $C_{18}H_{22}N_2O_2S$.TFA **[10]**, as a white crystalline powder or crystal (0.1321 g, 0.3090 mmol, 36.64% yield); m.p. 150-153 °C; IR (KBr)(cm^{-1}): 3432.01 (br, N-H st), 3125.54 (aromatic C-H st), 1597.28 (C=O st), 1515.55, 1413.39 (aromatic C=C st); ^{1}H NMR (300 MHz, DMSO-*d6*): δ 9.28 (s, 1H, OC-N<u>H</u>-CH$_2$), δ 8.50 (s, 2H, CH-N<u>H$_2$</u>), δ 7.45-7.12 (m, 9H, Ph-<u>H</u>), δ 4.18-4.40 (m, 2H, NH-C<u>H$_2$</u>-Ph), δ 4.05 (m, 1H, NH-C<u>H</u>-CO), δ 2.85 (d, J =5.91 Hz, 2H, S-C<u>H$_2$</u>-CH), δ 2.25 (s, 3H, Ph-C<u>H$_3$</u>); TLC (silica gel GF ethyl acetate/hexanes/ethanol [3:2:1]) ; R$_f$ of **[9]** = 0.42 and R$_f$ of **[10]** = 0.25.

2-Amino-*N*-(6-methoxybenzo[d]thiazol-2-yl)-3-(4-methylbenzylthio)propanamide
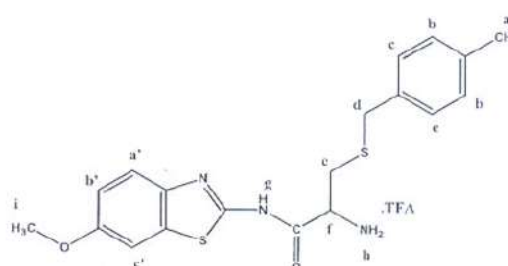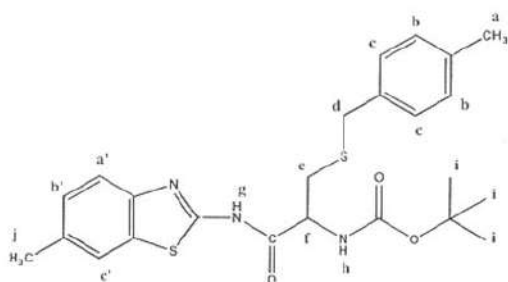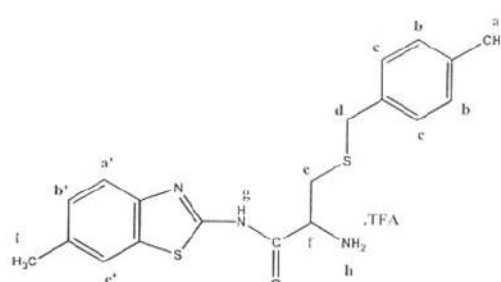

(11)   (12)

Boc-Cys(pMeOBzl)-OH (0.5001 g, 1.5366 mmol) was dissolved in 25 ml of dichloromethane in 250 mL round bottom flask until completely dissolved. After cooling to 0 ^{0}C with the aid of an ice-water bath, a solution of *N,N'*-carbonyldiimidazole (CDI, 0.32391 g, 1.9976 mmol) in 20 ml of dichloromethane and 6-methoxybenzo[*d*]thiazol-2-amine (0.3317 g, 1.8404 mmol) in 20 ml of dichloromethane and the reaction mixture was allowed to warm to room temperature and stirred overnight. The mixture was evaporated under reduced atmospheric pressure to dryness. The obtained residue was chromatographed on a silica gel column eluted with ethyl acetate/hexanes: (2:3) to give *tert*-butyl 1-(6-methoxybenzo[*d*]thiazol-2-ylamino)-3-(4-methylbenzylthio)-1-oxopropan-2-ylcarbamate **[11]** as white crystalline powder (0.3548 g, 0.7017mmol, 45.66% yield); m.p. 93-95 °C; IR (KBr)(cm^{-1}): 3338.21, 3203.36 (N-H st), 2978.61 (aromatic C-H st), 1908.00 (aliphatic C-H st), 1666.91 (C=O st), 1556.58 (N-H bend), 1518.72 (aromatic C=C st); TLC (silica gel GF ethyl acetate/hexanes [2:3]); R$_f$ of **[11]** = 0.46.

The solution of trifuoroacetic acid in dichloromethane (2:3) was added drop wise to the solution of **[11]** (0.1095 g, 0.2166 mmol) in 5 ml of dichloromethane in ice bath and stirred for 60 min under 0°C to room temperature. The resulting solution was evaporated under reduced atmospheric pressure to dryness. The obtained precipitates were washed with cool ether for 3-4 times and washed with cool hexane to give 2-amino-N-(6-methoxybenzo[d]thiazol-2-yl)-3-(4-methylbenzylthio)propanamide, $C_{19}H_{21}N_3O_2S_2$.TFA **[12]**, as a white crystalline powder or crystal (0.0524 g, 0.1354 mmol, 62.51% yield); m.p. 185-187°C; IR (KBr)(cm^{-1}): 3444.45 (br, N-H st), 3199.27 (aromatic C-H st), 1679.17 (C=O st), 1572.93, 1511.63 (aromatic C=C st); ^{1}H NMR (300 MHz, DMSO-$d6$) δ 8.35 (s, 2H, CH-N$\underline{H}_2$), δ 7.05-7.40 (m, 9H, Ph-$\underline{H}_{a-c,a',b'}$), δ 4.38 (d, J =4.99 Hz, 2H, NH-C$\underline{H}_2$-Ph), δ 4.05 (m, 1H, CH, NH$_2$-C$\underline{H}$-CO), δ 3.79 (s, 2H, S-C$\underline{H}_2$-Ph), δ 2.70-2.92 (m, 2H, S-C$\underline{H}_2$-CH); TLC (silica gel GF ethyl acetate/hexanes [2:3]) ; R$_f$ of **[11]** = 0.46 and R$_f$ of **[12]** = 0.16

2-Amino-N-(6-methylbenzo[d]thiazol-2-yl)-3-(4-methylbenzylthio)propanamide

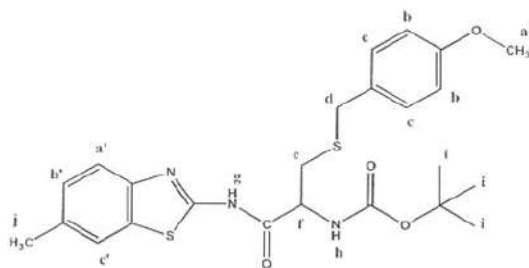(13)   (14)

Boc-Cys(pMeOBzl)-OH (0.5001 g, 1.5366 mmol) was dissolved in 25 ml of dichloromethane in 250 mL round bottom flask until completely dissolved. After cooling to 0^0 C with the aid of an ice-water bath, a solution of N,N'-carbonyldiimidazole (CDI, 0.3239 g, 1.9976 mmol) in 20 ml of dichloromethane and 6-methylbenzo[d]thiazol-2-amine (0.3022 g, 1.8404 mmol) in 20 ml of dichloromethane and the reaction mixture was allowed to warm to room temperature and stirred overnight. The mixture was evaporated under reduced atmospheric pressure to dryness. The obtained residue was chromatographed on a silica gel column eluted with ethyl acetate/hexanes: (2:3) to give $tert$-butyl 1-(6-methylbenzo[d]thiazol-2-ylamino)-3-(4-

methylbenzylthio)-1-oxopropan-2-ylcarbamate **[13]** as white crystalline powder (0.1354 g, 0.2765mmol, 17.99% yield); m.p. 178-180 °C; IR (KBr)(cm^{-1}): 3227.88, 3093.03 (N-H st), 2978.61, 2925.49 (aromatic C-H st), 1908.00 (aliphatic C-H st), 1691.43 (C=O st), 1548.41 (N-H bend), 1470.77 (aromatic C=C st); TLC (silica gel GF ethyl acetate/hexanes [2:3]); R$_f$ of **[13]** = 0.32

The solution of trifuoroacetic acid in dichloromethane (2:3) was added drop wise to the solution of **[13]** (0.0783 g, 0.1599 mmol) in 5 ml of dichloromethane in ice bath and stirred for 60 min under 0°C to room temperature. The resulting solution was evaporated under reduced atmospheric pressure to dryness. The obtained precipitates were washed with cool ether for 3-4 times and washed with cool hexane to give 2-amino-N-(6-methylbenzo[d]thiazol-2-yl)-3-(4-methylbenzylthio)propanamide, C$_{19}$H$_{21}$N$_3$OS$_2$.TFA **[14]**, as a white crystalline powder or crystal (0.0312 g, 0.0665 mmol, 41.64% yield); m.p. 168-170°C; IR (KBr)(cm^{-1}): 3342.29 (br, N-H st), 2966.35 (aromatic C-H st), 1613.79 (C=O st), 1454.43, 1356.36 (aromatic C=C st); ^{1}HNMR (300 MHz, DMSO-*d6*): δ 8.95 (s, 2H, CH-N$\underline{H}_2$), δ7.30 (m, 10H, Ph-$\underline{H}$ $_{a-c,\,a'-c'}$), δ 7.00 (s, 4H, Ph-$\underline{H}_j$), δ 4.50 (br, 1H, Ph-O$\underline{H}$), δ4.35 (s, 2H, N-C$\underline{H}_2$.Ph), δ 3.40 (q, J =6.89 Hz, 1H, NH$_2$-C$\underline{H}$-CO-N), δ 3.05 (d, J =6.04 Hz, 2H, S-C$\underline{H}_2$-CH); TLC (silica gel GF ethyl acetate/hexanes [2:3]) ; R$_f$ of **[13]** = 0.32 and R$_f$ of **[14]** = 0.25.

2-amino-3-(4-methoxybenzylthio)-N-(6-methylbenzo[d]thiazol-2-yl)propanamide
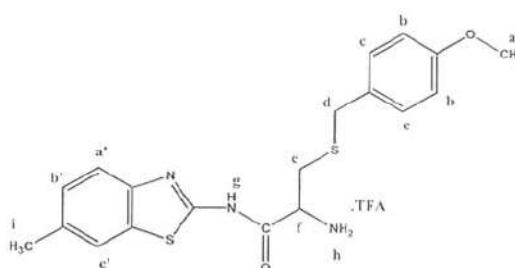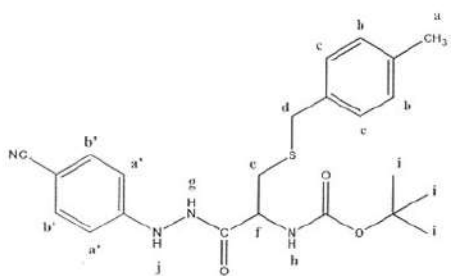

(15)   (16)

Boc-Cys(4Mbzl)-OH (0.5001 g, 1.4650 mmol) was dissolved in 25 ml of dichloromethane in 250 mL round bottom flask until completely dissolved. After cooling to 0^0 C with the aid of an ice-water bath, a solution of *N,N'*-carbonyldiimidazole (CDI, 0.3088 g, 1.9045 mmol) in 20 ml of dichloromethane and 6-methylbenzo[d]thiazol-2-amine (0.2887 g, 1.7580 mmol) in 20 ml of dichloromethane
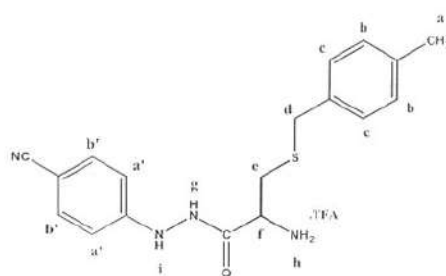
and the reaction mixture was allowed to warm to room temperature and stirred overnight. The mixture was evaporated under reduced atmospheric pressure to dryness. The obtained residue was chromatographed on a silica gel column eluted with ethyl acetate/hexanes/ethanol (3:2:0.5) to give *tert*-butyl-3-(4-methoxybenzylthio)-1-(6-methylbenzo[*d*]thiazol-2-ylamino)-1-oxopropan-2-ylcarbamate **[15]** as white crystalline powder (0.6102 g, 1.2068 mmol, 82.37% yield); m.p. 125-127 °C; IR (KBr)(cm^{-1}): 3320.55, 3202.60 (N-H st), 2978.95, 2930.15 (aromatic C-H st), 2356.74(aliphatic C-H st), 1665.40 (C=O st), 1510.87 (N-H bend), 1453.95 (aromatic C=C st); TLC (silica gel GF ethyl acetate/hexanes/ethanol [3:2:0.5]); R_f of **[15]** = 0.53

The solution of trifuoroacetic acid in dichloromethane (2:3) was added drop wise to the solution of **[15]** (0.2321 g, 0.4590 mmol) in 5 ml of dichloromethane in ice bath and stirred for 60 min under 0 °C to room temperature. The resulting solution was evaporated under reduced atmospheric pressure to dryness. The obtained precipitates were washed with cool ether for 3-4 times and washed with cool hexane to give 2-amino-3-(4-methoxybenzylthio)-N-(6-methylbenzo[d]thiazol-2-yl)propanamide, $C_{19}H_{21}N_3O_2S_2$.TFA **[16]**, as a white crystalline powder or crystal (0.1561 g, 0.3288 mmol, 71.63% yield); m.p. 132-135 °C; IR (KBr)(cm^{-1}): 3442.55 (br, N-H st), 2942.35 (aromatic C-H st), 1669.47 (C=O st), 1510.87, 1429.53 (aromatic C=C st); ^{1}HNMR (300 MHz, DMSO-*d6*): δ 9.20 (s, 1H, OC-N<u>H</u>-CH$_2$), δ 8.48 (s, 2H, CH-N<u>H$_2$</u>), δ 7.18-7.42 (m, 10H, Ph-<u>H</u>), δ 4.48 (t, J =5.50 Hz, 2H, NH-C<u>H$_2$</u>-Ph), δ 4.05 (m, 1H, NH$_2$-C<u>H</u>-CO), δ 2.80-2.93 (m, 2H, S-C<u>H$_2$</u>-CH); TLC (silica gel GF ethyl acetate/hexanes/ethanol [3:2:0.5]) ; R_f of **[15]** = 0.53 and R_f of **[16]** = 0.21.

2-Amino-*N'*-(4-cyanophenyl)-3-(4-methylbenzylthio)propanehydrazide

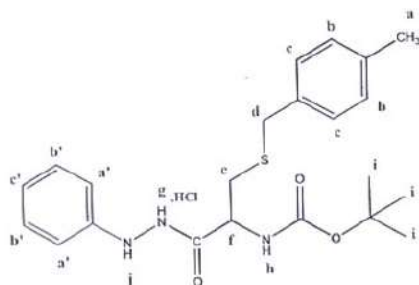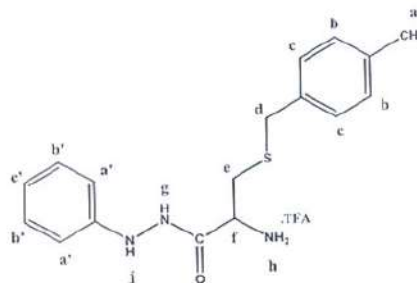(17)   (18)

Boc-Cys(pMeOBzl)-OH (0.5001 g, 1.5366 mmol) was dissolved in 25 ml of dichloromethane in 250 mL round bottom flask until completely dissolved. After cooling to 0 ^{0}C with the aid of an ice-water bath, a solution of N,N'-carbonyldiimidazole (CDI, 0.3239 g, 1.9976 mmol) in 20 ml of dichloromethane and 4-hydrazinylbenzonitrile (0.3122 g, 1.8404 mmol) in 20 ml of dichloromethane and the reaction mixture was allowed to warm to room temperature and stirred overnight. The mixture was evaporated under reduced atmospheric pressure to dryness. The obtained residue was chromatographed on a silica gel column eluted with ethyl acetate/hexanes (1:2) to give *tert*-butyl 3-(4-methylbenzylthio)-1-oxo-1-(2-phenylhydrazinyl)propan-2-ylcarbamate [17] as w crystalline powder (0.4856 g, 0.9809 mmol, 63.96% yield); m.p. 70-73 °C; IR (KBr)(cm^{-1}): 3340.89, 3259.55 (N-H st), 2974.88, 2922.01 (aromatic C-H st), 2248.17 (aliphatic C-H st), 1677.60 (C=O st), 1510.87 (N-H bend), 1368.53 (aromatic C=C st); TLC (silica gel GF ethyl acetate/hexanes [1:2]); R$_f$ of [17] = 0.51

The solution of trifuoroacetic acid in dichloromethane (2:3) was added drop wise to the solution of [17] (0.2278 g, 0.4602 mmol) in 5 ml of dichloromethane in ice bath and stirred for 60 min under 0 °C to room temperature. The resulting solution was evaporated under reduced atmospheric pressure to dryness. The obtained precipitates were washed with cool ether for 3-4 times and washed with cool hexane to give 2-amino-N'-(4-cyanophenyl)-3-(4-methylbenzylthio)propanehydrazide, $C_{18}H_{20}N_4OS$.TFA [18], as a white crystalline powder or crystal (0.1673 g, 0.3825 mmol, 83.12% yield); m.p. 130-132 °C; IR (KBr)(cm^{-1}): 3332.75 (br, N-H st), 2922.01 (aromatic C-H st), 1693.87 (C=O st), 1596.27, 1506.80 (aromatic C=C st); ^{1}HNMR (300 MHz, CDCl$_3$): δ 8.65 (m, 1H, OC-N$\underline{H}$-CH$_2$), δ 8.28 (s, 2H, CH-N$\underline{H}_2$), δ 7.75 (d, J =8.22 Hz, 2H, Ph-$\underline{H}$), δ 7.45 (d, J =8.18 Hz, 2H, Ph-$\underline{H}$), δ 4.35 (m, 2H, NH-C$\underline{H}_2$-Ph), δ 3.70 (s, 2H, S-C$\underline{H}_2$-Ph), δ 2.65 (dd, J =13.25 Hz, 5.76 Hz, 1H, S-C$\underline{H}_2$-CH) δ 2.55 (dd, J =13.22 Hz, 6.96 Hz, 1H, S-C$\underline{H}_2$-CH); TLC (silica gel GF ethyl acetate/hexanes [1:2]) ; R$_f$ of [17] = 0.51 and R$_f$ of [18] = 0.18.

2-Amino-3-(4-methylbenzylthio)-*N'*-phenylpropanehydrazide
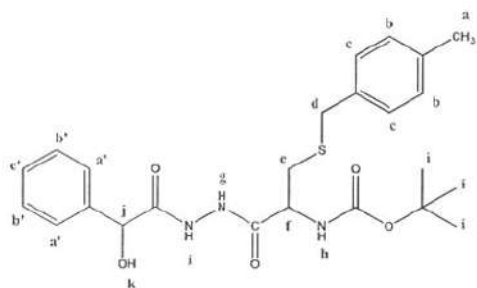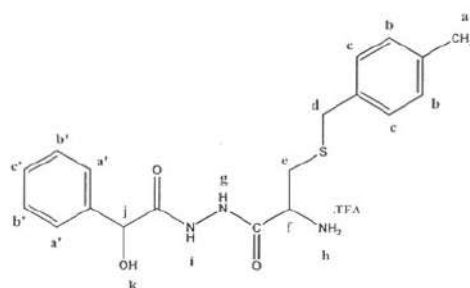

(19)   **(20)**

Boc-Cys(pMeOBzl)-OH (0.5001 g, 1.5366 mmol) was dissolved in 25 ml of dichloromethane in 250 mL round bottom flask until completely dissolved. After cooling to 0^0C with the aid of an ice-water bath, a solution of *N,N'*-carbonyldiimidazole (CDI, 0.3239 g, 1.9976 mmol) in 20 ml of dichloromethane and phenylhydrazine (0.2661 g, 1.8404 mmol) in 20 ml of dichloromethane and the reaction mixture was allowed to warm to room temperature and stirred overnight. The mixture was evaporated under reduced atmospheric pressure to dryness. The obtained residue was chromatographed on a silica gel column eluted with ethyl acetate/hexanes/ethanol (3:2:0.5) to give *tert*-butyl 1-(2-(4-cyanophenyl)hydrazinyl)-3-(4-methylbenzylthio)-1-oxopropan-2-ylcarbamate **[19]** as white crystalline powder (0.5066 g, 1.0778 mmol, 70.14% yield); m.p. 108-110 °C; IR (KBr)(cm^{-1}): 3342.29, 3313.69 (N-H st), 2974.53, (aromatic C-H st), 2365.67 (aliphatic C-H st), 1662.83 (C=O st),1515.72 (N-H bend), 1360.44 (aromatic C=C st); TLC (silica gel GF ethyl acetate/hexanes/ethanol [3:2:0.5]); R$_f$ of **[19]** = 0.77

The solution of trifuoroacetic acid in dichloromethane (2:3) was added drop wise to the solution of **[19]** (0.1155 g, 0.2457 mmol) in 5 ml of dichloromethane in ice bath and stirred for 60 min under 0 °C to room temperature. The resulting solution was evaporated under reduced atmospheric pressure to dryness. The obtained precipitates were washed with cool ether for 3-4 times and washed with cool hexane to give 2-Amino-3-(4-methylbenzylthio)-*N'*-phenylpropanehydrazide, C$_{17}$H$_{21}$N$_3$OS.TFA **[20]**, as a white crystalline powder or crystal (0.0597 g, 0.0.1894 mmol, 77.09% yield); m.p. 148-150 °C; IR (KBr)(cm^{-1}): 3305.52 (br, N-H st), 2913.23 (aromatic C-H st), 1679.17 (C=O st), 1597.45, 1491.20 (aromatic C=C st); ^{1}H NMR (300 MHz, DMSO-*d6*): δ 7.84 (s, 1H, OC-N**H**-CH$_2$), δ 6.99-7.28 (m, 8H, Ph-**H**), δ 4.41 (d, J = 6.02 Hz, 2H, CH$_2$-N**H**$_2$-CO), δ 3.70 (s, 2H, Ph-C**H**$_2$), δ 3.51 (m, 1H, CH$_2$-C**H**-NH$_2$), δ 3.01 (dd, J = 13.87, Hz, J = 3.86 Hz, 1H, S-C**H**$_2$-CH), δ 2.72 (dd, J = 13.66, Hz, J = 8.37 Hz, 1H, S-C**H**$_2$-CH), δ 2.34 (s, 3H, Ph-C**H**$_3$);TLC (silica gel GF ethyl acetate/hexanes/ethanol [3:2:0.5]) ; R$_f$ of **[19]** = 0.51 and R$_f$ of **[20]** = 0.20.

2-Amino-*N*'-(2-hydroxy-2-phenylacetyl)-3-(4-methylbenzylthio)propanehydrazide

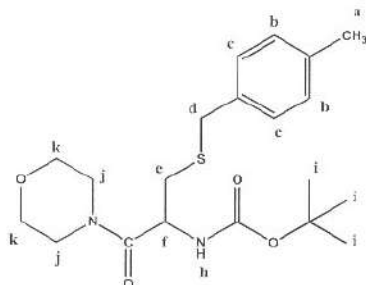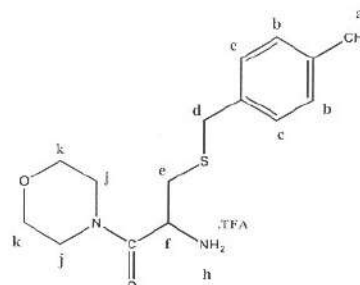**(21)**   **(22)**

Boc-Cys(pMeOBzl)-OH (0.5001 g, 1.5366 mmol) was dissolved in 25 ml of dichloromethane in 250 mL round bottom flask until completely dissolved. After cooling to 0 ^{0}C with the aid of an ice-water bath, a solution of *N,N'*-carbonyldiimidazole (CDI, 0.3239 g, 1.9976 mmol) in 20 ml of dichloromethane and 2-hydroxy-2-phenylacetohydrazide (0.3058 g, 1.8404 mmol) in 20 ml of dichloromethane and the reaction mixture was allowed to warm to room temperature and stirred overnight. The mixture was evaporated under reduced atmospheric pressure to dryness. The obtained residue was chromatographed on a silica gel column eluted with ethyl acetate/ chloroform (2:3) to give *tert*-butyl 1-(2-(2-hydroxy-2-phenylacetyl)hydrazinyl)-3-(4-methylbenzylthio)-1-oxopropan-2-ylcarbamate **[21]** as a white crystalline powder (0.2304 g, 0.4686 mmol, 30.50% yield); m.p. 124-125 °C; IR (KBr)(cm^{-1}): 3309.60, 3244.22 (N-H st), 2970.44, 2917.30 (aromatic C-H st), 2332.98 (aliphatic C-H st), 1683.26 (C=O st), 1617.88 (N-H bend), 1368.61 (aromatic C=C st); TLC (silica gel GF ethyl acetate/chloroform [2:3]); R$_f$ of **[21]** = 0.62

The solution of trifuoroacetic acid in dichloromethane (2:3) was added drop wise to the solution of **[21]** (0.1004 g, 0.2042 mmol) in 5 ml of dichloromethane in ice bath and stirred for 60 min under 0 °C to room temperature. The resulting solution was evaporated under reduced atmospheric pressure to dryness. The obtained precipitates were washed with cool ether for 3-4 times and washed with cool hexane to give 2-amino-N'-(2-hydroxy-2-phenylacetyl)-3-(4-methylbenzylthio)propanehydrazide, $C_{19}H_{23}N_3O_3S$.TFA **[22]**, as a white crystalline powder or crystal (0.0512 g, 0.1089 mmol, 53.33% yield); m.p. 140-142 °C; IR (KBr)(cm^{-1}): 3219.70 (br, N-H st), 2925.49 (aromatic C-H st), 1666.91 (C=O st), 1515.72, 1433.99 (aromatic C=C st); ^{1}HNMR (300 MHz, DMSO-*d6*): δ 7.82 (br, 2H, CH-N$\underline{H}_2$; exchangeable with D$_2$O), δ 7.20-7.40 (m, 5H, Ph-$\underline{H}$), δ 4.45 (d, J = 5.94 Hz, 2H, NH-C$\underline{H}_2$-Ph), δ 3.75 (dd, J =9.03 Hz, 3.72 Hz, 1H, S-C$\underline{H}_2$-CH), δ 3.32 (dd, J =13.54 Hz, 3.77 Hz, 1H, S-C$\underline{H}_2$-CH), δ 2.80 (m, 1H, NH$_2$-C$\underline{H}$-CO), δ 1.35 (s, 9H, C-C$\underline{H}_3$); TLC (silica gel GF ethyl acetate/ chloroform [2:3]) ; R$_f$ of **[21]** = 0.62 and R$_f$ of **[22]** = 0.20.

2-Amino-3-(4-methylbenzylthio)-1-morpholinopropan-1-one

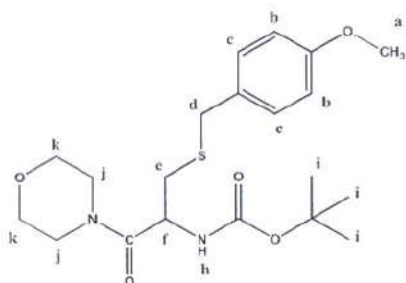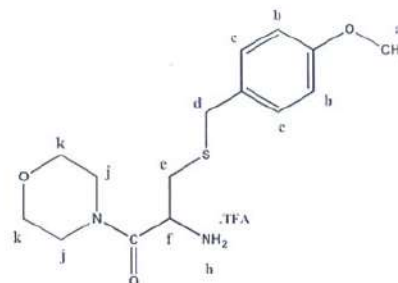
(23)   **(24)**

Boc-Cys(pMeOBzl)-OH (0.4002 g, 1.2312 mmol) was dissolved in 25 ml of dichloromethane in 250 mL round bottom flask until completely dissolved. After cooling to 0 ^{0}C with the aid of an ice-water bath, a solution of N,N'-carbonyldiimidazole (CDI, 0.2997 g, 1.8500 mmol) in 20 ml of dichloromethane and morpholine (0.1394 g, 1.6002 mmol) in 20 ml of dichloromethane and the reaction mixture was allowed to warm to room temperature and stirred overnight. The mixture was evaporated under reduced atmospheric pressure to dryness. The obtained residue was chromatographed on a silica gel column eluted with ethyl acetate/hexane/ethanol (5:2:0.5) to give *tert*-butyl-3-(4-methylbenzylthio)-1-morpholino-1-oxopropan-2-ylcarbamate **[23]** as a colorless or slightly yellow liquid (0.4950 g, 1.1999 mmol, 97.55 % yield); TLC (silica gel GF ethyl acetate/hexane/ethanol [5:2:0.5]); R_f of **[23]** = 0.55

The solution of trifuoroacetic acid in dichloromethane (2:3) was added drop wise to the solution of **[23]** (0.4950 g, 1.1999 mmol) in 5 ml of dichloromethane in ice bath and stirred for 60 min under 0 °C to room temperature. The resulting solution was evaporated under reduced atmospheric pressure to dryness. The obtained precipitates were washed with cool ether for 3-4 times and washed with cool hexane to give 2-amino-3-(4-methylbenzylthio)-1-morpholinopropan-1-one, $C_{15}H_{22}N_2O_2S$.TFA **[24]**, as a colorless or slightly yellow liquid (0.2462 g, 0.6289 mmol, 52.41% yield); IR (KBr)(cm^{-1}): 3321.86 (br, N-H st), 2974.53, 2921.40 (aromatic C-H st), 1654.65 (C=O st), 1515.72, 1442.17 (aromatic C=C st); ^{1}HNMR (300 MHz, DMSO-*d6*): δ 8.33 (s, 2H, NH$_2$-CH-CO), δ 6.87-7.25 (m, 4H, Ph-H$_{b, c}$), δ 4.53 (s, 1H, C-CH-CO), δ 3.38-3.85, (m, 14H, Ph-H$_{a, d, j, k}$) δ 2.72 (dd, J = 16.03 Hz, J = 6.21 Hz, 1H, S-CH$_2$-CH); TLC (silica gel GF ethyl acetate/hexane/ethanol [5:2:0.5]) ; R_f of **[23]** = 0.55 and R_f of **[24]** = 0.24.

2-Amino-3-(4-methoxybenzylthio)-1-morpholinopropan-1-one

**(25)**   **(26)**

Boc-Cys(4Mbzl)-OH (0.5001 g, 1.4650 mmol) was dissolved in 25 ml of dichloromethane in 250 mL round bottom flask until completely dissolved. After cooling to $0\,^{\circ}$C with the aid of an ice-water bath, a solution of N,N'-carbonyldiimidazole (CDI, 0.3551 g, 1.1901 mmol) in 20 ml of dichloromethane and morpholine (0.1655 g, 1.902 mmol) in 20 ml of dichloromethane and the reaction mixture was allowed to warm to room temperature and stirred overnight. The mixture was evaporated under reduced atmospheric pressure to dryness. The obtained residue was chromatographed on a silica gel column eluted with ethyl acetate/hexane/ethanol (5:2:0.5) to give *tert*-butyl 3-(4-methylbenzylthio)-1-morpholino-1-oxopropan-2-ylcarbamate **[25]** as a colorless or slightly yellow liquid (0.5310 g, 1.2945 mmol, 88.36 % yield); TLC (silica gel GF ethyl acetate/hexane/ethanol [5:2:0.5]); R_f of **[25]** = 0.54

The solution of trifuoroacetic acid in dichloromethane (2:3) was added drop wise to the solution of **[25]** (0.5310 g, 1.2945 mmol) in 5 ml of dichloromethane in ice bath and stirred for 60 min under 0 °C to room temperature. The resulting solution was evaporated under reduced atmospheric pressure to dryness. The obtained precipitates were washed with cool ether for 3-4 times and washed with cool hexane to give 2-Amino-3-(4-methoxybenzylthio)-1-morpholinopropan-1-one, $C_{15}H_{22}N_2O_3S$.TFA **[26]**, as a colorless or slightly yellow liquid (0.2758 g, 0.6769 mmol, 52.29 % yield); IR (KBr)(cm^{-1}): 3317.77 (br, N-H st), 2974.53, 2925.49, 2856.02 (aromatic C-H st), 1658.74 (C=O st), 1515.72, 1470.77 (aromatic C=C st); ^{1}HNMR (300 MHz, DMSO-$d6$): δ 6.86-7.28 (m, 4H, Ph-H$_{b,c}$), δ 4.39 (t, 1H, C-CH-CO), δ 3.47-3.81, (m, 14H, Ph-H$_{a,d,j,k}$) δ 3.14 (d, J = 22.44 Hz, 2H, S-CH$_2$-CH), δ 2.81 (d, J = 5.92 Hz, 2H, NH-C-CO);; TLC (silica gel GF ethyl acetate/hexane/ethanol [5:2:0.5]) ; R_f of **[25]** = 0.54 and R_f of **[26]** = 0.22.

***Tert*-butyl-3-(1*H*-indol-3-yl)-1-(6-methoxybenzo[*d*]thiazol-2-ylamino)-1-oxopropan-2-ylcarbamate**
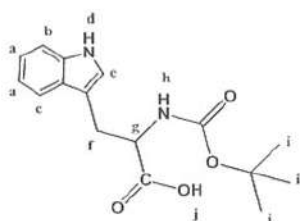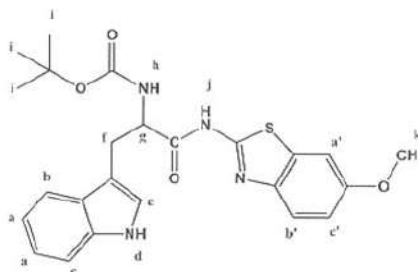
(27)   (28)

Sodium hydroxide (0.2584 g, 6.4632 mmol) and Boc$_2$O (0.9617 g, 4.4067 mmol) were add to a stirred solution of *L*(-)-Tryptophan (0.6001 g, 2.9378 mmol) in THF/H$_2$O (v/v, 10 ml: 10 ml) and the reaction mixture was allowed to warm to room temperature and stirred for 18 hr. The mixture was evaporated under reduced atmospheric pressure and the aqueous layer was extracted with dichloromethane. The aqueous layer was acidified with HCl (1N) to pH 4 and then extracted with dichloromethane 3-4 times and extracted with ethyl acetate 3-4 times. The organic phase was dried over Na$_2$SO$_4$ and the solvent was evaporator under reduced atmospheric pressure to dryness. The obtained residue obtained residue was chromatographed on a silica gel column eluted with ethyl acetate/hexane/ethanol (3:2:0.5) to give 2-(*tert*-butoxycarbonylamino)-3-(1*H*-indol-3-yl)propanoic acid [27] as a white crystalline powder or crystal (0.8521 g, 1.8278 mmol, 62.23 % yield); m.p. 112-115 °C; IR (KBr)(cm^{-1}): 3342.29 (N-H st), 2966.35, 2933.66 (aromatic C-H st), 2872.37 (aliphatic C-H st), 1613.79 (C=O st),1568.84 (N-H bend), 1380.87 (aromatic C=C st); ^{1}H NMR (300 MHz, DMSO-*d6*): δ 12.65 (br, 1H, CH-CO-OH), δ 10.84 (s, 1H, CH-NH-CH), δ 6.99-7.55 (m, 7H, Ph-H$_{a, b, c, e, h'}$), δ 4.17 (s, 1H, CH$_2$-CH-NH), δ 3.07 (d, J = 39.17 Hz, 2H, C-CH$_2$-CH), δ 1.28 (d, J = 34.57 Hz, 9H, O-C-CH$_3$); TLC (silica gel GF ethyl acetate/hexane/ethanol [3:2:0.5]); R$_f$ of [27] = 0.12
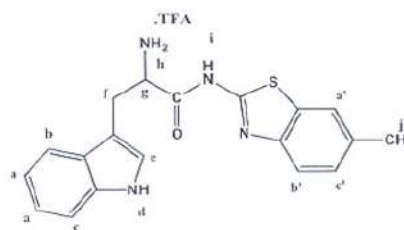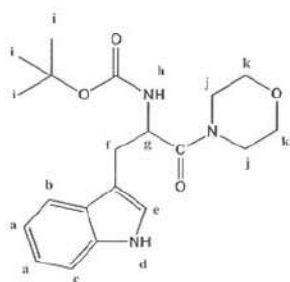
2-(*Tert*-butoxycarbonylamino)-3-(1*H*-indol-3-yl)propanoic acid [27] (0.2565 g, 0.8428 mmol) was dissolved in 25 ml of THF in 250 mL round bottom flask until completely dissolved. After cooling to 0 °C with the aid of an ice-water bath, a solution of *N,N'*-carbonyldiimidazole (CDI, 0.1776 g, 1.0956 mmol) in 20 ml of THF and 6-methoxybenzo[d]thiazol-2-amine (0.1822 g, 1.0114 mmol) in 20 ml of THF and the reaction mixture was allowed to warm to room temperature and stirred overnight. The mixture was evaporated under reduced atmospheric pressure to dryness. The obtained residue was chromatographed on a silica gel column eluted with ethyl acetate/hexane/ethanol (3:2:0.5) to give *tert*-butyl-3-(1H-indol-3-yl)-1-(6-methoxybenzo[d]thiazol-2-ylamino)-1-oxopropan-2-ylcarbamate [28] as a white

crystalline powder (0.3112 g, 0.6675 mmol, 79.21 % yield); m.p. 132-135 °C; IR (KBr)(cm^{-1}): 3342.29, (N-H st), 2925.49, 2851.94 (aromatic C-H st), 2357.50 (aliphatic C-H st), 1687.34 (C=O st), 1654.65 (N-H bend), 1307.32 (aromatic C=C st); ^{1}H NMR (300 MHz, DMSO-$d6$): δ 7.82 (br, 2H, CH-N$\underline{H}_2$), δ 7.20-7.40 (m, 5H, Ph-$\underline{H}$), δ 4.45 (d, J = 5.94 Hz, 2H, NH-C$\underline{H}_2$-Ph), δ 3.75 (dd, J =9.03 Hz, 3.72 Hz, 1H, S-C$\underline{H}_2$-CH), δ 3.32 (dd, J =13.54 Hz, 3.77 Hz, 1H, S-C$\underline{H}_2$-CH), δ 2.80 (m, 1H, NH$_2$-C$\underline{H}$-CO), δ 1.35 (s, 9H, C-C$\underline{H}_3$); TLC (silica gel GF ethyl acetate/hexane/ethanol [3:2:0.5)]); R$_f$ of **[28]** = 0.54.

2-Amino-3-(1H-indol-3-yl)-N-(6-methylbenzo[d]thiazol-2-yl)propanamide
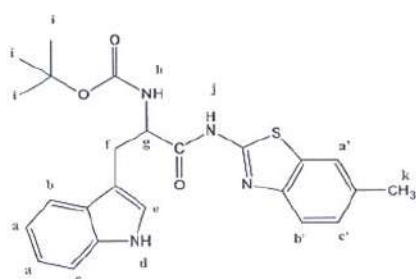
(29)   **(30)**

2-(*Tert*-butoxycarbonylamino)-3-(1H-indol-3-yl)propanoic acid **[27]** (0.4121 g, 1.3143 mmol) was dissolved in 25 ml of THF in 250 mL round bottom flask until completely dissolved. After cooling to 0 °C with the aid of an ice-water bath, a solution of N,N'-carbonyldiimidazole (CDI, 0.2771 g, 1.7086 mmol) in 20 ml of THF and 6-methoxybenzo[d]thiazol-2-amine (0.2589 g, 1.5768 mmol) in 20 ml of THF and the reaction mixture was allowed to warm to room temperature and stirred overnight. The mixture was evaporated under reduced atmospheric pressure to dryness. The obtained residue was chromatographed on a silica gel column eluted with ethyl acetate/hexane/ethanol (2:5:0.5) to give *tert*-butyl 3-(1H-indol-3-yl)-1-(6-methylbenzo[d]thiazol-2-ylamino)-1-oxopropan-2-ylcarbamate **[29]** as a white crystalline powder (0.2797 g, 0.6213 mmol, 47.27 % yield); m.p. 120-123 °C; IR (KBr)(cm^{-1}): 3411.76 (N-H st), 2974.53, 2921.40 (aromatic C-H st), 2365.67 (aliphatic C-H st), 1691.43 (C=O st), 1605.62 (N-H bend), 1270.54 (aromatic C=C st); TLC (silica gel GF ethyl acetate/hexane/ethanol [2:5:0.5)]); R$_f$ of **[29]** = 0.63
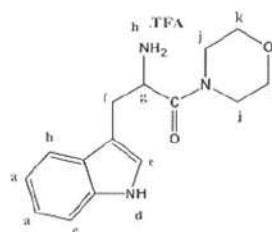
The solution of trifluoroacetic acid in THF (2:3) was added drop wise to the solution of **[29]** (0.2222 g, 0.4931 mmol) in 5 ml of THF in ice bath and stirred for 60 min under 0 °C to room temperature. The resulting solution was evaporated under reduced atmospheric pressure to dryness. The obtained precipitates were washed with cool ether for 3-4 times and washed with cool hexane to give 2-amino-3-(1H-indol-3-

---

yl)-1-morpholinopropan-1-one, $C_{15}H_{19}N_3O_2$.TFA **[32]**, as a white crystalline powder or crystal (0.2120 g, 0.5728 mmol, 45.58% yield); m.p. 170-173 °C; IR (KBr)(cm^{-1}): 3317.77 (br, N-H st), 2966.35, 2925.49 (aromatic C-H st), 1630.14 (C=O st), 1515.72 (aromatic C=C st); δ 7.40-7.10 (m, 9H, Ph-H), δ 6.50 (br, 1H, OC-NH-CH$_2$), δ 5.28 (br, 1H, OC-NH-CH), δ 4.42 (m, 2H, NH-CH$_2$-Ph), δ 4.27 (br, 1H, NH-CH-CO), δ 3.75 (dd, J =13.44 Hz, 2.54 Hz, 2H, S-CH$_2$-Ph), δ 2.95 (dd, J =13.97 Hz, 5.65 Hz, 1H, S-CH$_2$-CH), δ 2.78 (dd, J =13.95 Hz, 6.84 Hz, 1H, S-CH$_2$-CH) ,δ 2.35 (s, 3H, Ph-CH$_3$) ,δ 1.45 (s, 9H, C-CH$_3$); TLC (silica gel GF ethyl acetate/hexanes/ethanol [2:5:0.5]) ; R$_f$ of **[31]** = 0.70 and R$_f$ of **[32]** = 0.21.

Tert-butyl-3-(1H-indol-3-yl)-1-oxo-1-(2-phenylhydrazinyl)propan-2-ylcarbamate
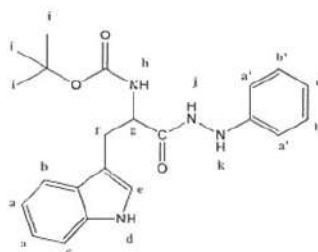
(33)

2-(*Tert*-butoxycarbonylamino)-3-(1*H*-indol-3-yl)propanoic acid **[27]** (0.4001 g, 1.3143 mmol) was dissolved in 25 ml of THF in 250 mL round bottom flask until completely dissolved. After cooling to 0 °C with the aid of an ice-water bath, a solution of *N,N'*-carbonyldiimidazole (CDI, 0.2271 g, 1.7086 mmol) in 20 ml of THF and phenylhydrazine (0.2281 g, 1.5772 mmol) in 20 ml of THF and the reaction mixture was allowed to warm to room temperature and stirred overnight. The mixture was evaporated under reduced atmospheric pressure to dryness. The obtained residue was chromatographed on a silica gel column eluted with ethyl acetate/hexane/ethanol (2:5:0.5) to give *tert*-butyl 3-(1*H*-indol-3-yl)-1-oxo-1-(2-phenylhydrazinyl)propan-2-ylcarbamate **[33]** as a white crystalline powder (0.3656 g, 0.9268 mmol, 70.51 % yield); m.p. 126-128 °C; IR (KBr)(cm^{-1}): 3432.19, (N-H st), 2978.61, 2921.40 (aromatic C-H st), 2365.67 (aliphatic C-H st), 1703.69 (C=O st), 1630.14 (N-H bend), 1364.53 (aromatic C=C st); δ 8.42 (br, 2H, CH-NH$_2$), δ 7.12 (q, J = 7.75 Hz, 4H, Ph-H$_{g,h}$), δ 4.22 (br, 2H, NH-CH$_2$-Ph), δ3.00 (dd, J = 7.45, 5.21 Hz, 1H, S-CH$_2$-CH), δ 2.82 (dd, J = 7.54 Hz, 4.87 Hz, 1H, S-CH$_2$-CH), δ 2.22 (s, 3H, Ph-CH$_3$), δ 1.25 (s, 9H, C-CH$_3$)); TLC (silica gel GF ethyl acetate/hexane/ethanol [2:5:0.5)]); R$_f$ of **[33]** = 0.42.

C.   *In Vitro* Dipeptidyl Peptidase IV Activity Assay

1. Materials

Equipment

Analytical balance	Satorius BP211D, Germany
	ae Adam AFA-210LC, UK
Vortex mixer	Vortex-genie K550GE, USA)
pH meter	Orion 720A
Micropipettes 0.5-10 μl	Biohit, Finland
Micropipettes 2-20 μl, 20-200 μl	Gilson, France
Micropipettes 100-1000 μl	Nichiryo, Japan
Multichanel pipette 20-200 μl	High Tech Lab, Poland
96-Black well plate	Serowell, UK

Chemicals

Dipeptidyl peptidase IV, Human,	Calbiochem, USA
Recombinant, *Spodopterafrugiperda*	
Dimethyl sulfoxide (DMSO)	Lab-Scan, Thailand
Hydrochloric acid (HCl)	Lab-Scan ,Thailand
Tris (hydroxymethyl)-aminomethaneHCl	Fisher Scientific, UK
Gly-Pro-7-amido-4-methylcoumarin HBr	Sigma-Aldrich, USA
(Gly-Pro-AMC)	

2. Methods

2.1 Dipeptidyl Peptidase IV Activity Assay

2.1.1 Screening Test

The activity test was based on the concept that the specificity of DPP-4 is characterized to preferentially release dipeptide from the amino terminus of polypeptides with proline or alanine in the penultimate position. The substrate of this assay is gly-pro-7 amido-4-methylcoumarin (Gly-Pro-AMC) which AMC is a fluorogenic probe. When DPP-4 cleaves AMC moiety from the N-terminus of the peptide substrate, free AMC is released and can be detected its fluorescent intensity at wavelength of 380 nm (excitation) and 460 nm (emission)

Preparation of 50 mMTrisBuffer (pH 7.5): The 100 ml of distilled water was added to 0.6057 g of Tris-HCl. When the solution was dissolved completely, pH was adjusted with 1N HCl to pH 7.5. Then, the volume was adjusted to 100 ml with distilled water.

Preparation of Position Control:sitagliptin phosphate (Januvia®), a potent DPP-4 inhibitor was used as positive control. The stock solution was freshly prepared in DMSO at 0.01 mM concentration by dissolving 2.53 mg of sitagliptin in 500 µl DMSO and pipetted 0.1 µl of this solution to 9.9 µl DMSO then mixed and adjusted to 100 µl with Tris–HCl buffer (pH 7.5)to give stock solution. The test solution (0.002mM) was prepared by diluting 20 µl of stock solution with 10% DMSO in Tris–HCl and adjusted to 100 µl.

Preparation of substrate: The 1 mM stock solution of gly-pro-7-amido-4 methylcoumarin(Gly-Pro-AMC)was prepared by dissolving Gly-Pro-AMC 0.14 mg.

Preparation of DPP-4: The Enzyme was dissolven in Tris-HCl buffer (pH 7.5) to obtain the concentration of 2.2 µU/µl. After the dilution, the enzyme was kept in ice bath and used within 90 minutes.

Preparation of Test Compounds 1-33: The stock solutions of test compounds in imine and amide series at 100 mM were freshly prepared in DMSO. The test solution at 100 µM was prepared by diluting 1 µl of stock solution in 9 µl DMSO and adjusted to 90 µl with Tris-HCl buffer (pH 7.5).

DPP-4 inhibitory activity assay: The effects of synthesized compounds on the DPP-4 activity were evaluated in vitro. A fluorometric assay was employed to measure the DPP-4 activity by using Gly-Pro-AMC as substrate. The substrate was cleaves by the enzyme to release the fluorescent aminomethylcoumarin (AMC). The amount of the liberated AMC was measured by the fluorescent emission at wavelength of 380 nm after an excitation at wavelength of 460 nm. The assay was performed in a 96-black well plate and the sequential addition of reagent was buffer, enzyme, and sitagliptin (positive control) or test compounds (Table 4). The assay mixtures were mixed well, and incubated at 37°C for 1 hr. The substrate was added in the final step, the fluorescent intensity (F) was measured and recorded. The percent inhibition was determined using below equation

Table 4 **The composition of the DPP-4 assay mixture in each well**

Sample	TrisHCl buffer (pH 7.5) (µl)	DPP-4 (µl)	Sitagliptin/ test solution (µl)	10% DMSO (µl)	Substrate (µl)
Blank	40	0	0	10	50
Control	25	15	0	10	50
Sitagliptin	25	15	10	0	50
Test compound	25	15	10	0	50

$$\% \text{ Inhibition } = \frac{(F_{control} - F_{test\ compound}) \times 100}{F_{control}}$$

2.1.2   Determination of IC_{50}

Compound 8, 9 in amide series were further assayed to determine IC_{50}. The half maximal inhibitory concentration (IC_{50}) is a measure of the effectiveness of a compound in inhibiting the DPP-4 activity. The procedure was the same as described in the experimental section 2.1.1. The percent inhibition of test compound in 3-5 varied concentrations were determined. The IC_{50} value was obtained from linear regression plot between % inhibitions and concentrations of test compounds.

Preparation of Test Compounds 24, 26 : The stock solutions of test compounds werefreshly prepared in DMSO at 100 mM concentration. The test solution was prepared by diluting 0.5, 0.75, 1, 1.5, 2 µl of stock solution in 9.5, 9.25, 9, 8.5, 8 µl DMSO and adjusted to 90 with Tris-HCl buffer (pH 7.5) to obtain 50, 75, 100, 150, and 200 µM concentrations, respectively.

CHAPTER IV
RESULT AND DISCUSSION

Diabetes (DM) is a syndrome of disordered metabolism, usually due to a combination of hereditary and environmental causes, resulting in abnormally high blood sugar levels (hyperglycemia). The majority of the patients who are diagnosed with diabetes are type 2 diabetes. The goal of type 2 diabetes therapy is to control euglycemia or set the preprandial glycemic level within a 90-130 mg/dl (5.0-7.2 mmol/L) and to maintain HbA1C to lower than 7%. In order to fulfill the goal of DM therapy, most patients have to take medicines in combination to reach euglycemia. Many attempts have been tried to achieve the goal of diabetes mellitus treatment. Apart from the conventional antidiabetic drugs, novel drugs approved by USFDA during 2005-2011 are classified into 3 classes based on drugs target. They are amylin analogues, GLP-1 analogues and dipeptidatse IV (DPP-4) inhibitors. The most interesting target appeared to be DPP-4 inhibitors e.g. sitagliptin and a large numbers in the pipeline. The mechanism of action of DPP-4 inhibitors is inhibition of the enzyme named DPP-4. DPP-4 degraded incretin hormones, especially GLP-1 and GIP. The GLP-1 is a peptide hormone secreted by intestinal L-cells in response to food intake. This hormone stimulates insulin secretion from β-cell, suppresses glucagon secretion, and regulates food intake and gastric emptying. In human, GLP-1 is rapidly N-terminally degraded by the ubiquitous DPP IV, leading to short half lives of GLP-1 after the secretion. Therefore, the DPP-4 inhibitors are very potential in the improvement of type 2 diabetes mellitus treatment.

A large number of Thai medicinal plants possessing antidiabetic activity have been recorded in many folk literatures but they are not recognized as the official regimen in the treatment. For instance, Cysteine and *L*(-)-tryptophan are the active component of *Allium ascaloncu,* and *Allium cepa* Linn. In Alliaceae family. The chromone moiety is one of interesting structure found in many medicinal herbs. In this research, DPP-4 inhibitors were developed based on the information of Thai medicinal plants and structure based drug design. The proposed structures were designed by structural modification of Cysteine, *L*(-)-tryptophan and chromone

scaffold. The AutoDock program was the tool that aided in the design and selection of the potential candidates. There are three main series in the design, series A from chromone, series B from Cysteine and series C from $L(-)$-tryptophan. The hit compounds from docking experiment were selected for synthesis and *in vitro* evaluation.

CHROMONE   CYSTEINE $L(-)$-TRYPTOPHAN
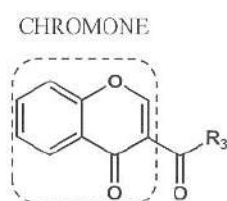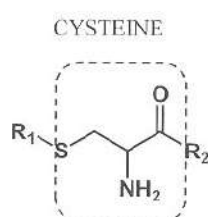
Series A   **Series B**   **Series C**

A. Molecular Modeling (*In Silico*) Experiment

-bond forming between N<u>H</u> of the ligand and <u>C</u>O of the residue Glu205 (2.782), Glu206 (2.461) and <u>O</u>H of the residue Tyr662 (2.545)

The AutoDock program version 4.1 was applied to assess the interaction between enzymes and the designed molecules. The docking program AutoDock allows the ligand flexible of mobility whereas the target or enzyme is conformational rigid.

The docking study started with the preparation of the target protein DPP-4. The selected protein was the crystal structure of PDB entry code 1X70 which bound to the inhibitor 715 or sitagliptin. The enzyme was solved by X-ray diffraction techniques with a resolution of 2.10 Å. The DPP-4 from this PDB is a dimmer containing chain A and B. Chain A was chosen to prepare the DPP-4 template. The bound inhibitor 715 is known as first potent inhibitor launched in worldwide market including Thailand, its trade name is Januvia®. The binding mode between DPP-4 protein and ligand 715 was displayed in **Figur 20**, there is one H-bond forming between N<u>H</u> of the ligand and <u>C</u>O of the residue Glu205 (2.825 Å), Glu206 (2.704 Å) and <u>O</u>H of the residue Tyr662 (2.834 Å)
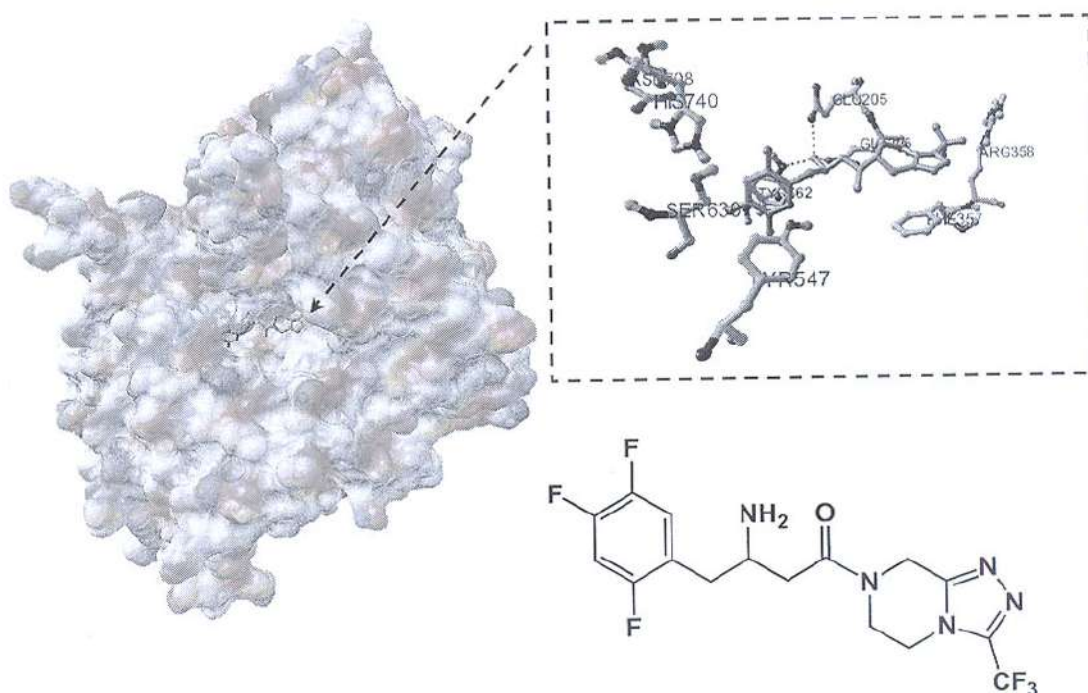
Figure 21 The bound conformation of 715 (sitagliptin) in active site of DPP-4 from PDB entry code 1X70 (chain A) (left) and the H-bond interaction between two N$\underline{H}$ of ligand 715 (green) and $\underline{O}$H of Tyr662 in chain A with 2.834 Å distance and C$\underline{O}$ of Glu205, Glu206 in chain A with 2.825 Å, 2.704 Å distance (right).

This constructed template was initially validated by re-docking ligand 715 back to the prepared template and the docked pose or 3D configuration of ligand 715 obtained from re-docking was compared with the crystallographic pose. In addition to ligand 715 from PDB: 1X70, three ligands (872, T22 and 5AP) from PDB entry codes 2IIT, 3G0B, and 1RWQ respectively were docked into the prepared template. The docked poses of these three ligands were compared with its corresponding crystal poses. The results of template validation were showed in Table 5.

Table 5   **Validation result of the prepared DPP-4 template.**

PDB code	Ligand	Ligand cluster number	%Member in cluster	**(b)** RMSD (Å)
1X70	715	1	82	0.56
2IIT	872	1	56	1.22
3G0B	T22	3	55	1.31
1RWQ	5AP	1	46	1.56

* GA runs = 100, population size = 100, max no. of energy evaluations = 15×10^6 per run

The validation result from re-docking ligand 715 to the template showed cluster of 2 Å RMSD clustering tolerance (82% of the docked conformations). The RMSD between the docked poses in this cluster and the crystal pose of 715 was 0.56 Å. The docked pose from the prepared DPP-4 template was found to be in the same configuration as crystal structure according to RMSD < 2Å (Figure 22). Therefore, the prepared template was suitable to be a model in docking study.
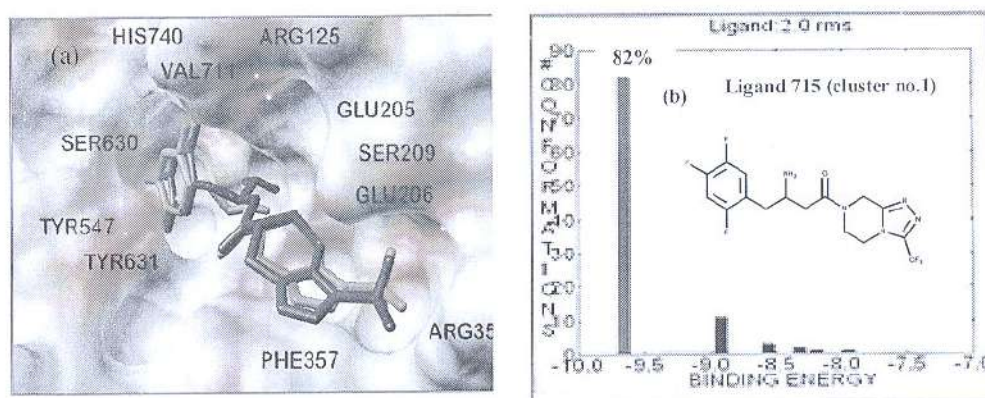
Figure 22   Superimposition between the crystal pose of ligand 715 (blue) and the docked pose (pink) at the binding site (a) and the clustering result (b)

Further validation to assure the suitability of the DPP-4 template was conducted with three crystal ligands 2IIT, 3G0B, and 1RWQ from PDB code 872, T22 and 5AP, respectively. The ligands from these three crystals were docked into the constructed template. The conformations or docked poses with RMSD < 2Å were clustered as displayed in Figure 22. The result of docked ligands 872, T22 and 5AP to the template clearly showed one medium cluster with 56%, 55% and 46% membership of the docked conformations, respectively, The orientations of docked poses of ligand and its corresponding crystallographic poses were displayed in **Figure 23.**
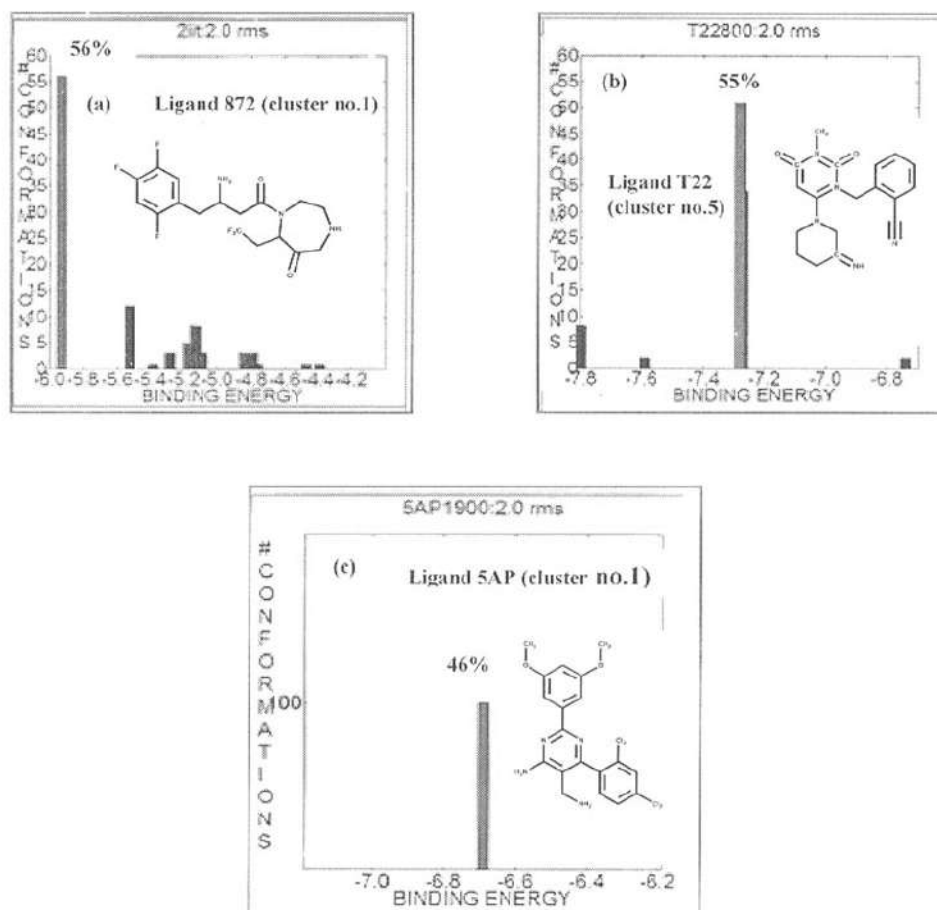
Figure 23   The clustering of docked ligands 872 (a), T22 (b) and 5AP (c) against the constructed template (RMSD < 2 Å clustering tolerance), the clusters of medium number (percent membership) of docked conformations are in red.

The objective of this research is to design and synthesize the novel DPP-4 inhibitors which were modified from the structure of the active compounds of medicinal plant. Chromone, cysteine and $L(-)$-tryptophan naturally occurring compounds especially in plants was found to be the important component or pharmacophores of many biologically active molecules such as antimycobacterial, antifungal, anticonvulsant, antimicrobial and anticancer agents. Hence, chromone, cysteine and $L(-)$-tryptophan was selected to be core structure for the designed compounds. The program AutoDock version 4.1 was used for designing new compounds and for searching the active components. Molecular docking was carried out to investigate the docking energy and binding mode of a crystallographic structure of human dipeptidyl peptidase IV (DPP-4, PDB entry code: 1x70) was used to investigate and validate the docking protocol. Molecular docking of the hit structures with DPP-4 were conducted to identify with increasing binding capacity which leads to potent inhibitory action. The identified hit compounds were synthesized and tested for its inhibition action against DPP-4. The chromone, cysteine and $L(-)$-tryptophan function (S1) was modified by different side chains (S2) to fit DPP-4 was active binding site. The selected twenty top ranking compounds or hit compounds were identified which were 6 chromone imine, 10 cysteine amides and 4 $L(-)$-tryptophan amides. The docked poses and the docking energies are collected and evaluated. The compounds that have good docking and lowest binding energy of biding to DPP-4 were cluster. The obtained nergies from docking were ranked. The docked pose and binding energy of the conformers in the cluster of highest number and analyzed. The compound that had that binding energy lower than -6.0 kcal/mol were selected and the filtered by five parameters: binding energy (<6.5 kcal/mole), ligand efficiency (LE) (<0.6), molecular weight (<470), Log P (<4.5) and % member in highest cluster (>40). The selected compounds for synthesis and its docking results were listed in Table 6, Table 7 and Table 8.

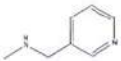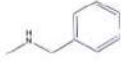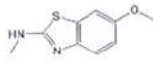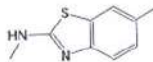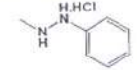Table 6   Docking results of the hit compounds in series A.
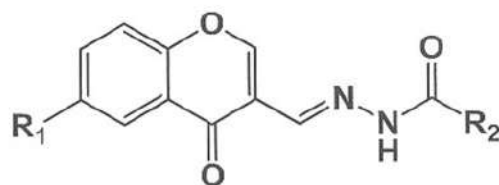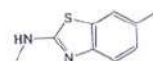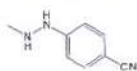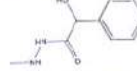
Cpds	R_1	R_2	MW	Log P	$\Delta G^{[a]}$ (kcal/mol)	%Member in highest cluster	$LE^{[b]}$
1	H	CH_2OHPh	322.31	1.40	-8.62	69	-0.35
2	6-Me	CH_2OHPh	336.34	1.89	-9.01	80	-0.36
3	H	3-NPh	293.28	0.77	-6.79	40	-0.31
4	6-Me	3-NPh	307.30	1.26	-7.30	69	-0.32
5	H	4-OMePh	322.31	1.99	-8.32	40	-0.35
6	6-Me	4-OMePh	336.34	2.47	-7.07	42	-0.28

[a] Free energy of binding [b] LE (Ligand Efficiency) = ΔG / HA. ΔG = free energy of ligand binding, N = the number of non-hydrogen atoms.

Table 7   **Docking results of the hit compounds in series B.**
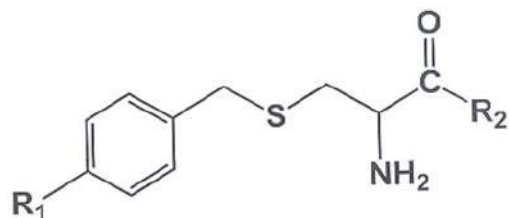
Cpds	R₁	R₂	MW	Log P	ΔG[a] (kcal/mol)	%Member in highest cluster	LE[b]
8	Me		315.43	1.53	-10.56	40	-0.36
10	OMe		330.44	2.26	-10.47	43	-0.39
12	Me		387.52	3.87	-10.56	44	-0.41
14	Me		371.52	4.48	-10.71	41	-0.43
16	OMe		387.52	3.87	-11.59	40	-4.45
18	Me		340.44	2.35	-9.97	42	-0.42
20	Me		315.43	2.32	-10.99	47	-0.49
22	Me		373.47	1.55	-11.11	42	-0.43
24	Me		294.41	0.97	-10.56	70	-0.58
26	OMe		310.41	0.36	-10.03	75	-0.48

[a] Free energy of binding [b] LE (Ligand Efficiency) = ΔG / HA. ΔG = free energy of ligand binding. N = the number of non-hydrogen atoms.

Table 8   **Docking results of the hit compounds in series C.**

Cpds	R₁	R₂	MW	Log P	$\Delta G^{[a]}$ (kcal/mol)	%Member in highest cluster	LE[b]
28		-	466.55	4.03	-8.78	43	-0.42
30		-	350.44	3.25	-10.06	41	-0.40
32		-	273.15	-0.26	-11.95	42	-0.39
33		-	394.47	2.48	-10.16	48	-0.35

[a] Free energy of binding [b] LE (Ligand Efficiency) = ΔG / HA. ΔG = free energy of ligand binding, N = the number of non-hydrogen atoms.

The binding energies were in the range of -6.79 to -11.95 kcal/mol and the membership in the highest clusters were considerably high (40-80%). The chromone, cysteine and L(-)-tryptophan scaffolds were found to locate either in S_1 pocket or S_2 pocket depending on the introduced moiety (R^2). Therefore, the interaction in S1 hydrophobic pocket was relatively weak as the phenyl ring did not accomodate an interaction with any acid residues in S-1 pocket. Table 9, 10 and Table 11 showed results of the docking study presented as superposition over sitagliptin crystal pose binding mode and H-bond interacted residue of all compounds.

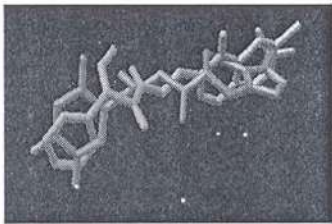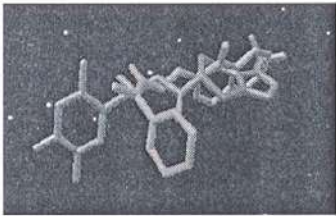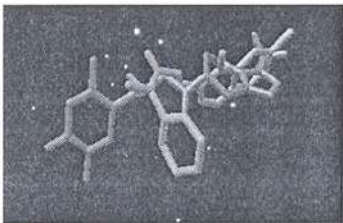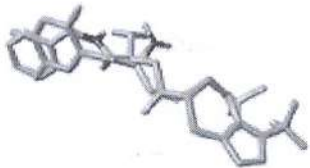Table 9   The docking results of synthesized compounds in series A.
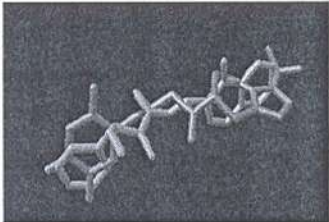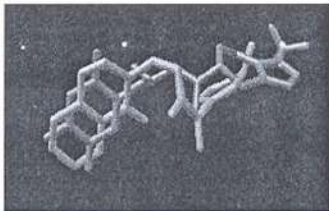
Cpd	superposition over sitagliptin crystal pose (pink)	H-bond interacted residue	distance, Å
1		Tyr547	2.013
2		Glu205	1.838
3		Glu206	2.145
4		Glu205	1.755
5		Arg 125	2.151

Table 9   The docking results of synthesized compounds in series A.
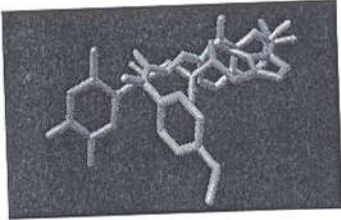
Cpd	superposition over sitagliptin crystal pose (pink)	H-bond interacted residue	distance, Å
6		Glu205	2.344

Table 9   The docking results of synthesized compounds in series B.
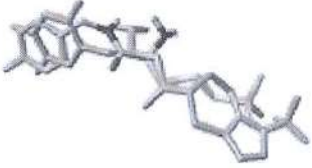
Cpd	superposition over sitagliptin crystal pose (green)	H-bond interacted residue	distance, Å
8		Glu205	2.051
		Glu206	2.212
10		Tyr662	3.210
		Glu205	2.013
		Glu206	2.201
12		Glu206	2.131
14		Glu206	2.310

Table 10 The docking results of synthesized compounds in series B.

Cpd	superposition over sitagliptin crystal pose (green)	H-bond interacted residue	distance, Å
16		Glu205	2.502
		Glu206	2.001
18		Tyr662	2.513
		Glu205	1.812
		Glu206	2.523
20		Glu205	2.420
22		Glu206	1.920

Table 10   The docking results of synthesized compounds in series B.
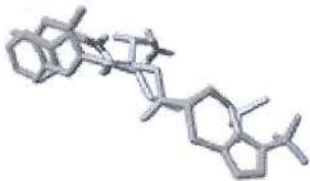
Cpd	superposition over sitagliptin crystal pose (green)	H-bond interacted residue	distance, Å
24		Glu205	1.834
		Glu206	1.790
26		Glu205	1.834
		Glu206	1.880

Table 11   The docking results of synthesized compounds in series C.
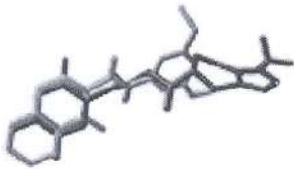
Cpd	superposition over sitagliptin crystal pose (blue)	H-bond interacted residue	distance, Å
28		His740	3.021
		Glu205	1.832
		Glu206	2.112
30		Glu205	1.922
32		Ser	3.225

Table 11   The docking results of synthesized compounds in series C.

Cpd	superposition over sitagliptin crystal pose (blue)	H-bond interacted residue	distance, Å
33		GLU205	1.880

B. Synthesis

The hit compounds (Figure 24) in three series of chromone imines, cysteine amides and $L(-)$-tryptophan amides were synthesized as described in experimental section (Scheme 1-3). The main chemical reaction in the synthesis of compounds in chromone imines series **1-6** from primary amines and aldehydes compound was nucleophilic addition. It began with a hemiaminal forming, followed by a dehydration to generate an imine (Schiff bases). The synthesis of compounds cysteine amides and $L(-)$-tryptophan amides series amide **7-33** was carried out by the reaction between acid and amine to form amide linkage by the aid of various coupling reagent. The reactivity of the carbonyl carbon in carboxylic acid moiety increased with the coupling agent which led to the easily attack by various amines to form amide bond. The coupling reagent used in these reactions was 1,1'-carbonyldiimidazole (CDI) which was generally soluble in most organic solvents.
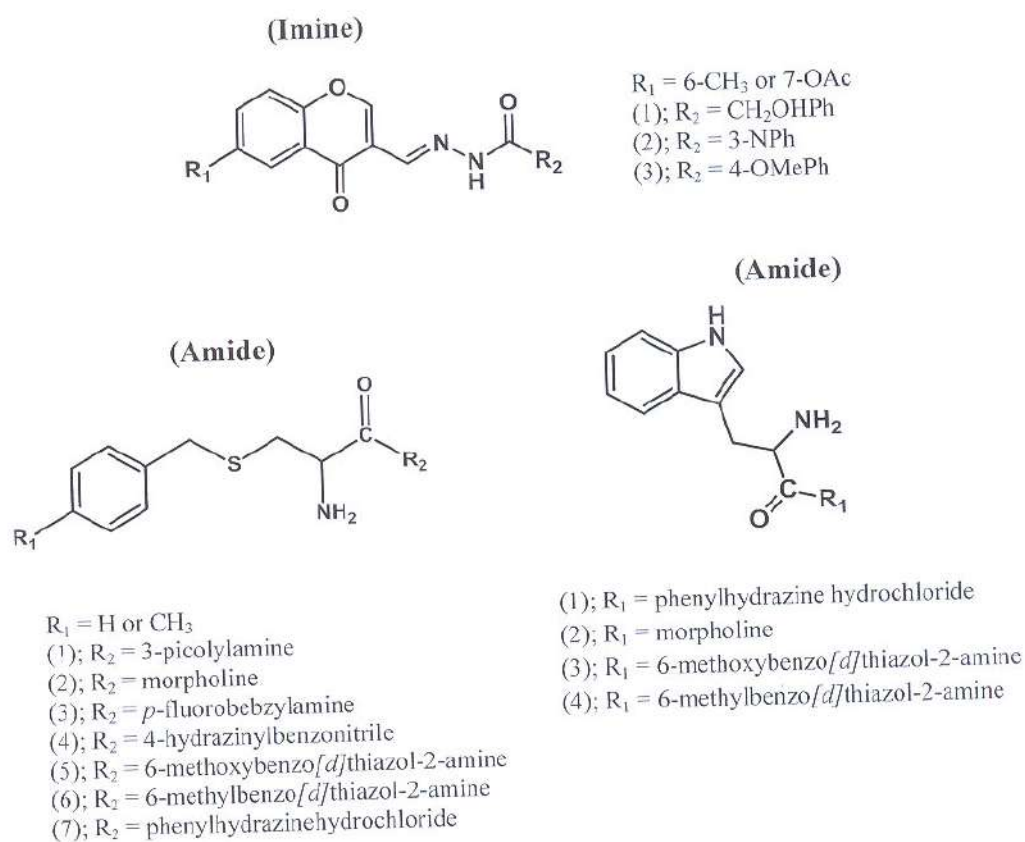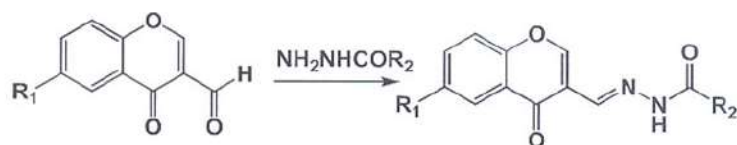
(Imine)

R_1 = 6-CH$_3$ or 7-OAc
(1); R_2 = CH$_2$OHPh
(2); R_2 = 3-NPh
(3); R_2 = 4-OMePh

(Amide)

(Amide)

R_1 = H or CH$_3$
(1); R_2 = 3-picolylamine
(2); R_2 = morpholine
(3); R_2 = p-fluorobebzylamine
(4); R_2 = 4-hydrazinylbenzonitrile
(5); R_2 = 6-methoxybenzo[d]thiazol-2-amine
(6); R_2 = 6-methylbenzo[d]thiazol-2-amine
(7); R_2 = phenylhydrazinehydrochloride

(1); R_1 = phenylhydrazine hydrochloride
(2); R_1 = morpholine
(3); R_1 = 6-methoxybenzo[d]thiazol-2-amine
(4); R_1 = 6-methylbenzo[d]thiazol-2-amine

Figure 24 The structures of twenty hit compounds.

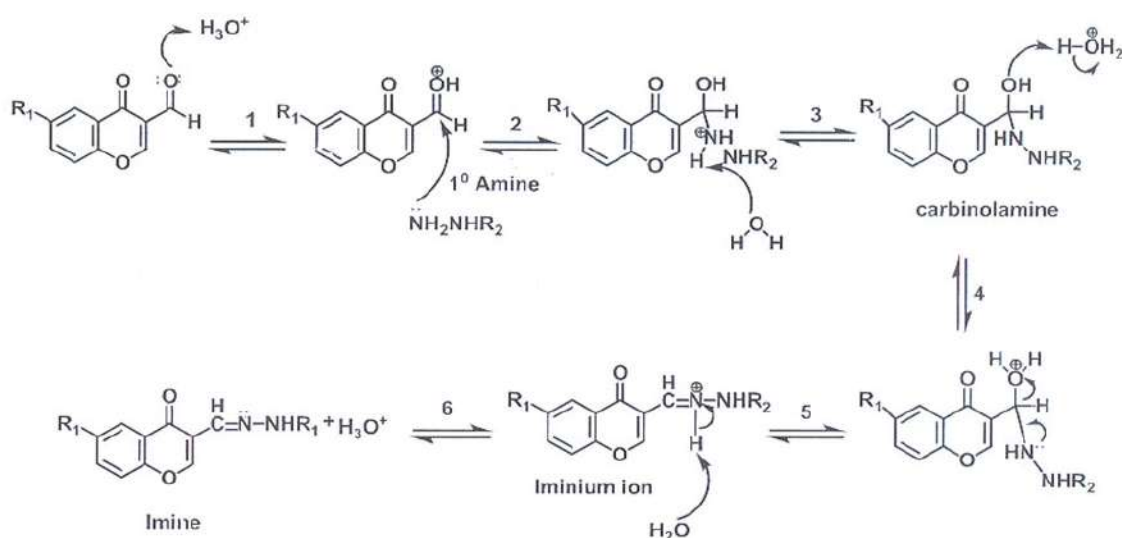## 1. Synthesis of Compounds in Imine Series

1.1 Synthesis of Compounds in Imine Series

The six chromone imine **1-6** were synthesized by condensation of chromone-3-carbocxaldehyde and 3-Formy-6-methylchromone with 3 hydrazides in methanol as shown in **Scheme 1**. The percentage yield of compound 1-6 were medium to high (37.25-75.58%).

Scheme 1 Synthesis of chromone imines **[1]-[6]**. Chromone derivatives with various hydrazides in methanol, stir 3-5 hr., RT.

The mechanism of reaction in **Scheme 2** showed that imines are typically prepared by the condensation of primary amines and aldehydes. In terms of mechanism, such reactions proceed via the nucleophilicaddition giving a hemiaminal–C(OH)(NHR)- intermediate, followed by an elimination of water to yield the imine. The equilibrium in this reaction usually favors of the carbonyl compound and amine, so that azeotropic distillation or use of a dehydrating agent such as molecular sieves is required to push the reaction in favor of imine formation. The final products were recrystallized from methanol.


Scheme 2 The mechanism of chemical reaction in the synthesis of chromone imines [1]-[6].

1.2 Synthesis of Compounds in Amide Series

The ten cysteine amides **7-26** and four L(-)-tryptophan amides **27-33** were synthesized by condensation of cysteine and amine with the aid of peptide coupling

agents, CDI as shown in Scheme 3 and Scheme 4 respectively. The percentage yield of compound 1-6 were medium to high (36.64)
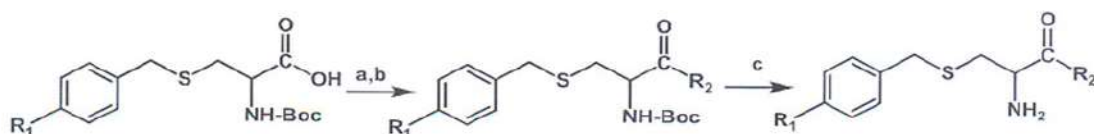

Scheme 3 Synthesis of cysteine amides **[7]-[26]** (a) CDI, CH_2Cl_2, stir 1 hr, RT; (b) add R_2NH_2, stir overnight, RT; (c) TFA, CH_2Cl_2, stir 1 hr., 0 ^{0}C.


Scheme 4 Synthesis of L(-)-tryptophan amides **[27]-[33]**(a) Boc_2O, NaOHaq, THF, H_2O, stir overnight, RT; (b) CDI, THF, stir 1 hr, RT; (c) add R_1NH_2, stir overnight, RT; (d) TFA, THF, stir 1 hr., 0 ^{0}C.

The mechanism of reaction in Scheme 5 showed that the acid group of starting material was attacked by the lone pair electron of nitrogen on CDI. Then, imidazole and carbon dioxide released. From the coupling, the carbonyl carbon of the forming intermediate was more reactive and the imidazole was a better leaving group than the hydroxyl function of the carboxylic acid. Therefore, the nucleophilic nitrogen of amine can readily attack and form amide bond in mid condition yielding Boc according to two distinct advantages; it not only acts as catalyst to increase the yield and rate of reactions but also allows the milder running conditions, thereby reducing unwanted side effects, e.g., racemization. The Boc, the amino protected group was cleaved by mild condition of 4M hydrochloric acid in dichloromethane to produce the desired products **[27]-[33]** (**Scheme 5**). The final products were separated by column chromatography.
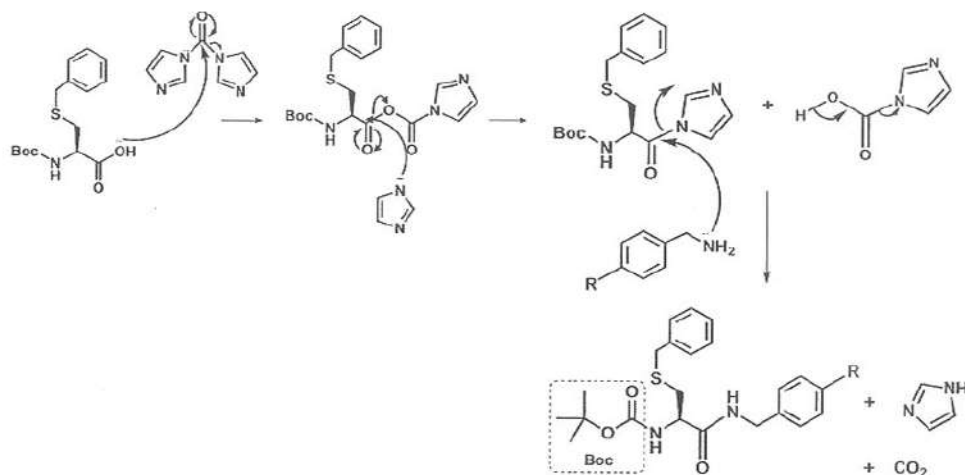
Scheme 5 The mechanism of chemical reaction in the synthesis of the intermediates of compounds **7-26.**
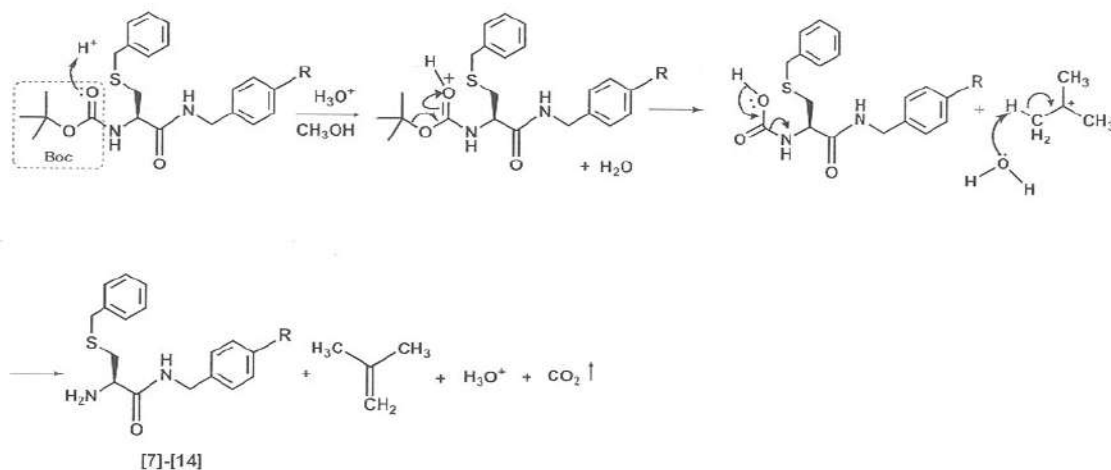
Scheme 6 Cleavage of Boc protecting group from the intermediates to obtain the desired compounds **7-26.**

2. Structure Elucidation

The properties of the intermediates and the designed compounds were determined by infrared spectroscopy (IR), nuclear magnetic resonance spectroscopy (NMR), mass spectroscopy (MS), melting points and elemental analyses.

The IR spectra of compounds **1–6** in imine series and **7–33** in amide series showed the similar pattern in functional group stretchings and bendings. For

example, IR spectra of **1**, **24** and **32** (**Figure 25-27.**) showed the frequency of O-H stretching at 3600-3200 cm⁻¹, N-H stretching at 3500-3000 cm⁻¹, C-H stretching at 3100-3000 cm⁻¹, C=O stretching at 1761-1643 cm⁻¹, C=C aromatic stretching at 1600, 1500, 1450 cm⁻¹, N-H bending vibration at 1575-1508 cm⁻¹, C-N stretching at 1300, 1200 cm⁻¹, aromatic C-H bending at 900-670 cm⁻¹. IR spectrum of compound **[1]** (**Figure 25.**) showed very strong bands at 3268.74 cm⁻¹ and 1626.05 cm⁻¹ which are attributed to N-H stretching and C=O stretching respectively.

IR spectra of compounds **[7]**-**[33]** in amide series (**Figure 26, 27.**) displayed two strong bands at 1716-1617 cm⁻¹ which corresponded to C=O stretching of 2 carbonyl groups, one in cysteine, *L*(-)-tryptophan and another one in amide function. The cysteine amide **[24]** and *L*(-)-tryptophan amide showed N-H stretching at 3241cm⁻¹ and C=O stretching at 1716-1617 cm⁻¹ due to intermolecular H-bonding with amino group.

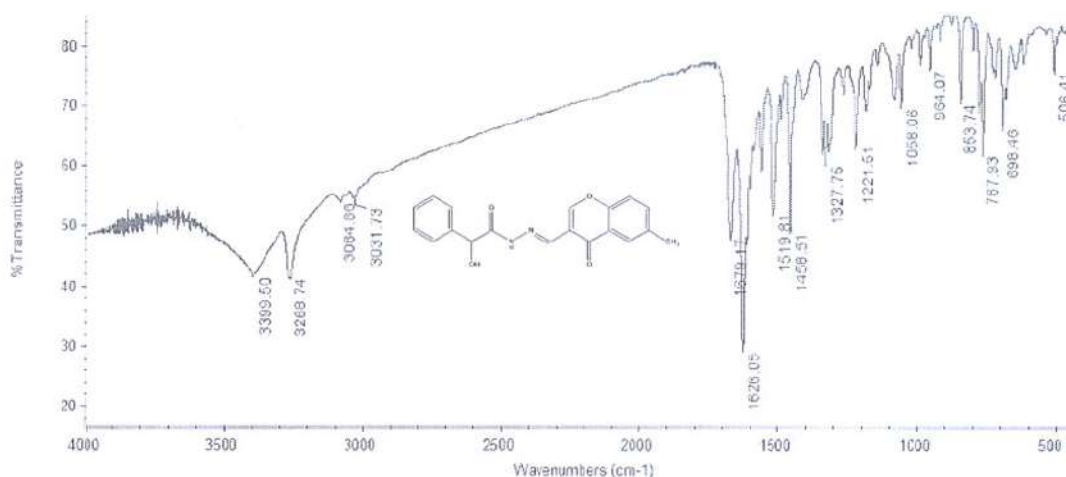**Figure 25**   IR spectrum of *(E)*-2-Hydroxy-*N'*-((6-methyl-4-oxo-4*H*-chromen-3-yl)methylene)-2-phenylacetohydrazide **[1]**.
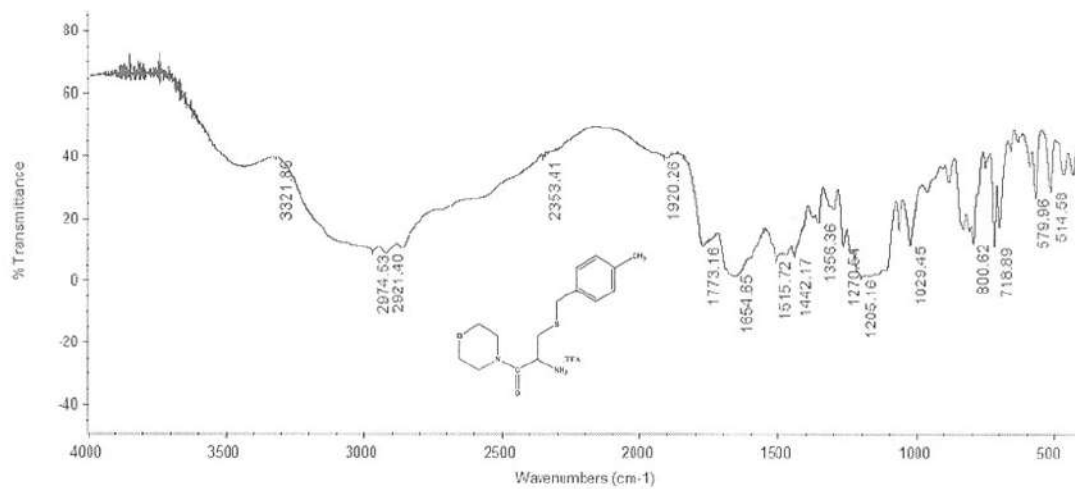
Figure 26 IR spectrum of 2-Amino-3-(4-methylbenzylthio)-1-morpholinopropan-1-one [24].
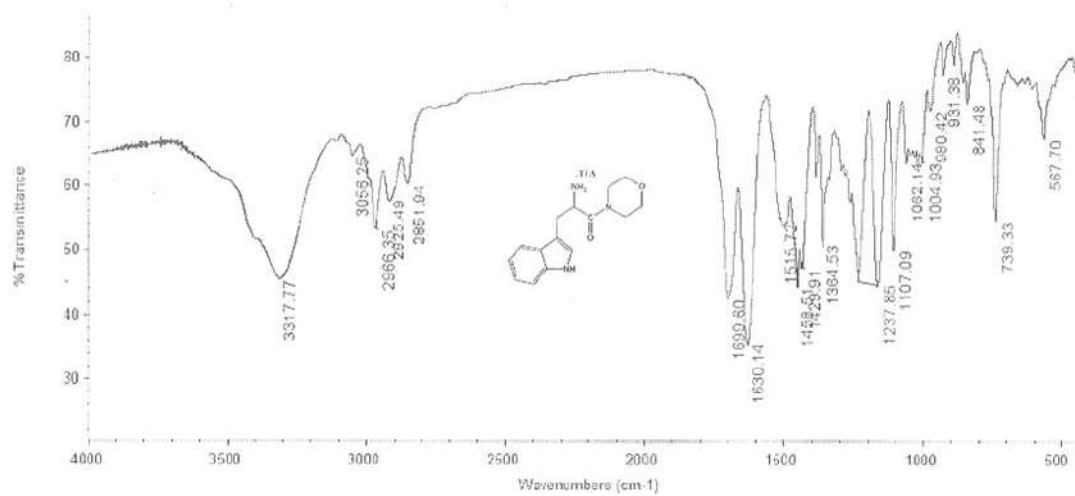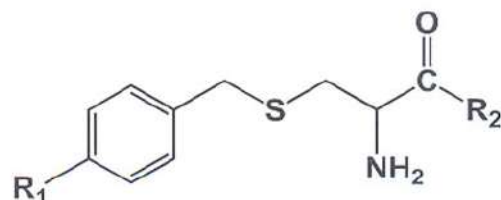

Figure 27 IR spectrum of 2-Amino-3-(1*H*-indol-3-yl)-1-morpholinopropan-1-one [32].

Table 13 Effect of cysteine amide on DPP-4 [a].

Cpds	R$_1$	R$_2$	%Inhibition (100μM)	IC$_{50}$ (μM)[b]
8	Me		12.05	ND
10	OMe		10.20	ND
12	Me		10.15	ND
14	Me		8.56	ND
16	OMe		12.52	ND
18	Me		2.32	ND
20	Me		20.45	ND
22	Me		7.89	ND
24	Me		52.85	95.19
26	OMe		51.97	96.80

[a] Data for each compound was determined in triplicate.

[b] IC$_{50}$ of sitagliptin was nM, ND=Not determined.

Table 14   **Effect of *L*(-)-tryptophan amide on DPP-4 [a].**
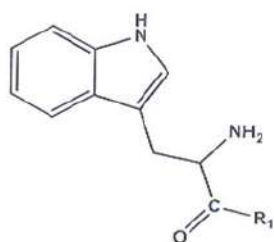
Cpds	R₁	%Inhibition (100μM)	IC$_{50}$ (μM)[b]
28		20.12	ND
30		8.23	ND
32		23.30	ND
33		2.22	ND

[a] Data for each compound was determined in triplicate.

[b] IC$_{50}$ of sitagliptin was nM, ND=Not determined.

Eleven compounds with percent inhibition more than 30% were selected for the determination of IC_{50}, (Table 15). The linear regression plots between the percent inhibitions of DPP-4 activity versus concentrations of test compounds were displayed in Figure 28, r^2 values from all compounds were in the range of 0.9931 – 0.9936.

Table 15   Percent inhibition of hits compounds against DPP-4.

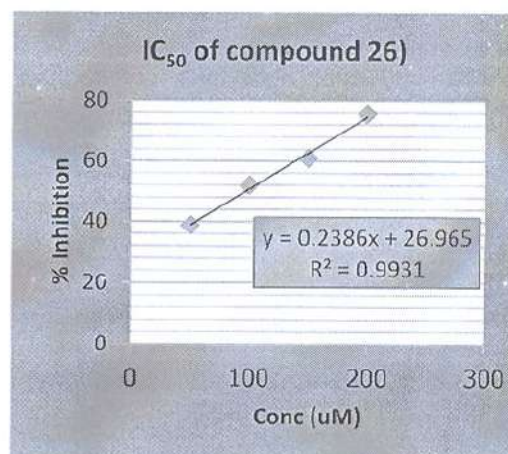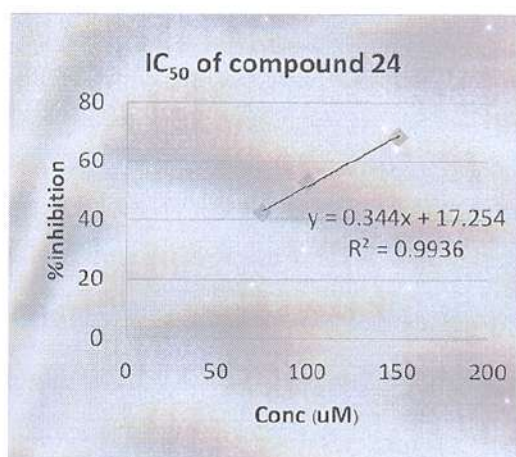| Compound	Conc (µM)	% Inhibition (n= 3 or 4)	SD
24	75	42.26	1.12
	100	52.85	0.29
	150	68.46	0.69
26	50	38.71	2.85
	100	51.97	3.37
	150	61.03	1.27
	200	75.46	1.32

Figure 28 The linear regression plots between the percent inhibitions of DPP-4 activity versus concentrations of test compounds.

Table 16   IC$_{50}$ and docking results the cysteine amide of compound 24 and 26

	24	26
Binding energy (kcal/mol)	-10.10	-10.03
% Member in cluster	70	75
Interacted amino acids(hydrophobic)	Val207, Ser209, Phe357, Ser630, Val656,Tyr662, Tyr666, Arg669, Val711	Phe357, Arg358, Ser630,Val656, Tyr662, Try666,
H-bond (distance Å)	Glu205(1.834) Glu206(1.790)	Glu205(1.834) Glu206(1.880)
IC$_{50}$ (µM)	95.19	96.80

The binding mode of compound **24** and **26** with human DPP-4 in the active site were shown in Figure 29-30. The secondary amide made H-bonds to Glu205 and Glu206. For the cysteine core flipped vertically, turning its locaion in S2-pocket. The structure of compound **24** and **26** to fit DPP-4 was active binding site showed in Figure 29-30.

Figure 29 The binding modes of compound 24 (pink) in the active site of DPP-4.

Figure 30 The binding modes of compound 26 (green) in the active site of DPP-4.

Figure 31 The overlay docked poses of 24 (pink), 26 (green) and sitagliptin (blue) showing the location of morpholine in S1 pocket.

CHAPTER V

CONCLUSION

Target based drug design was performed in searching for new lead of antidiabetic drug. In this research study, the dipeptidyl peptidase IV (DPP-4), a new promising target for diabetic treatment, was selected as drug target. The cysteine, L(-)-tryptophan and chromone, the potential scaffolds in medicinal plants, were used as the core structures in the design of novel DPP-4 inhibitors. The research was divided into three parts, *in silico* docking, synthesis and *in vitro* tests. Series of compounds were designed by the aid of molecular modeling. AutoDock program version 4.1 was the tool for docking study and hit identification. The binding modes of hit compounds to DPP-4 were determined. The hit compounds were synthesized and tested for the inhibitory action against DPP-4. The performed studies are summarized below.

1. A dipeptidyl peptidase IV (DPP-4) template was constructed from sitagliptin bound crystal (PDB code 1X70) and validated (RMSD 0.56 Å). The constructed template was further validated with three bound ligands 872, T22 and 5AP from the crystals (PDB codes: 2IIT, 3G0B, and 1RWQ) respectively were docked into the prepared template. The docked poses of these three ligands were compared with its corresponding crystal poses according to RMSD values 2.29, 1.31 and 1.56 respectively. The validation result from re-docking indicated that the prepared DPP-4 template is a good model for docking studies.

2. Twenty compounds were designed which were 356 structures of The cysteine, L(-)-tryptophan and chromone (series A, B and C), 6 structures of chromones (series A), 10 structures of cysteine and 4 tructures of L(-)-tryptophan. All were screened virtually by docking with the validated DPP-4 template and the thirteen hit compounds were identified.

3. The binding energies of hit compounds, were −6.79 to -9.01 kcal/mol in series A, -9.97 to -11.59 kcal/mol in series B and -10.06 to -11.95 kcal/mol

in series C. The binding energy of compound [32] in series C was the best (-11.95 kcal/mol) and that of compound [3] in series A was the worst (-6.79 kcal/mol).

4. Three series of chromone imines, cysteine amides and L(-)-tryptophan amides were designed and screened in silico. Twenty top ranking compounds or hit compounds were identified hit compounds were synthesized and screened in vitro at 100 μM for their inhibitory action against human DPP-4 with sitagliptin as positive control, and the results are reported as concentrations for 50% inhibition (IC_{50}).

5. Compound 24 and 26 was the most potent in this study with IC_{50} of 95.19 μM and 96.80 μM. The biding mode showed five hydrogen bond interactions: Glu205, Glu206, in the S1, S2 and S3 pockets of catalytic site.
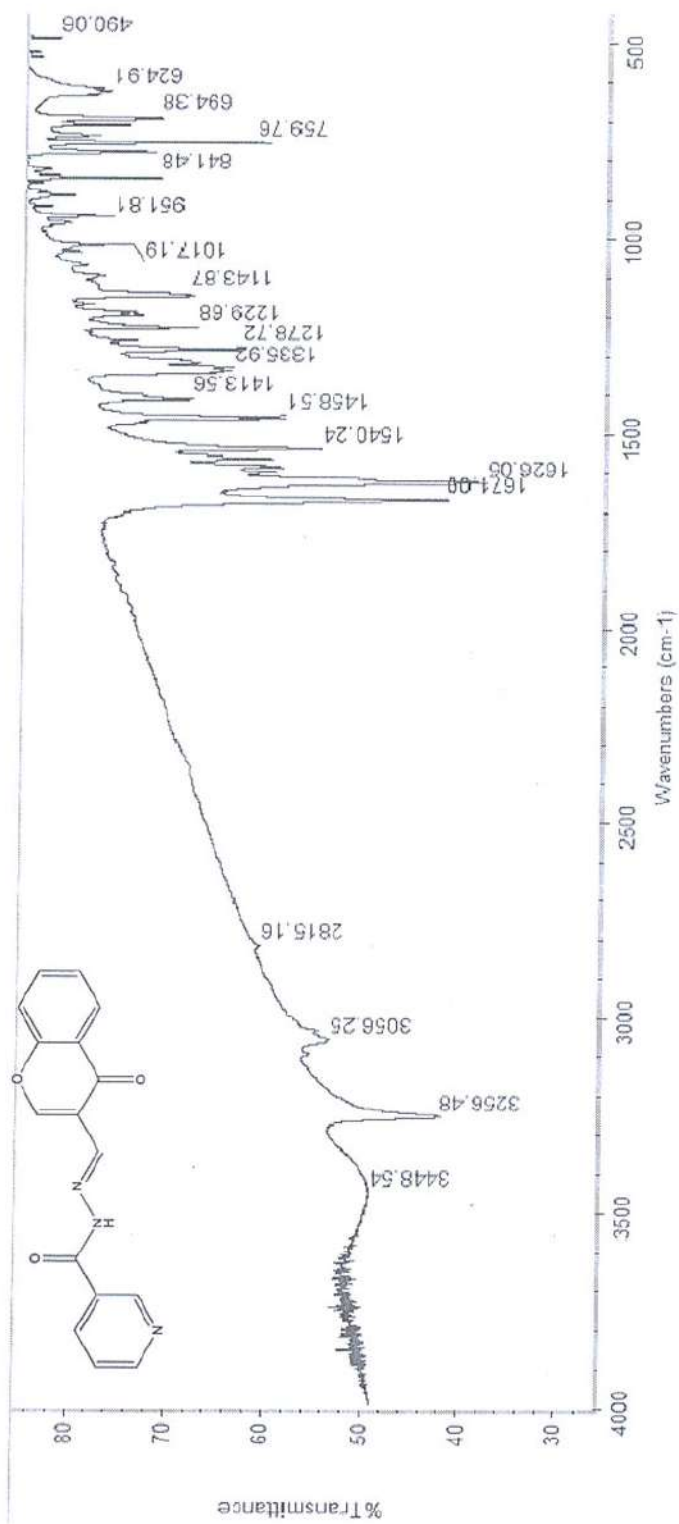
APPENDICES
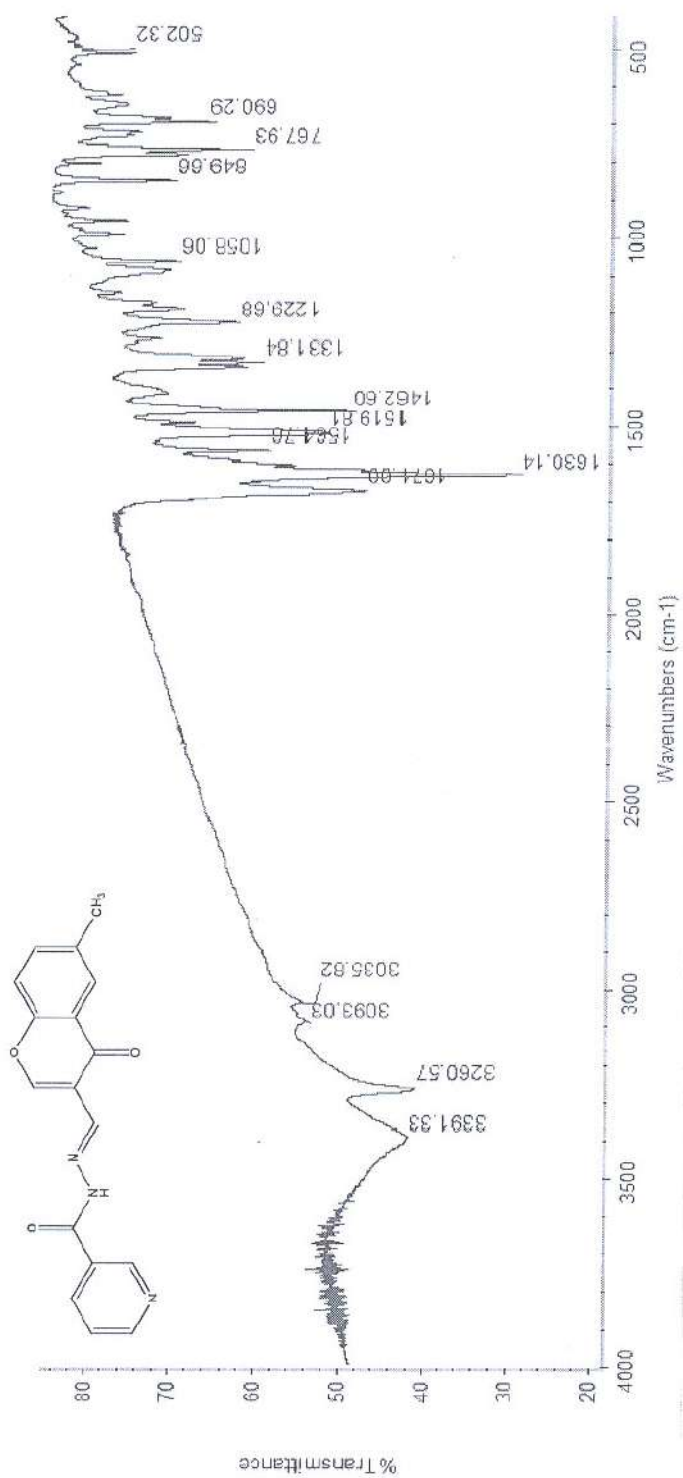
APPENDIX A

(Structure Elucidation)
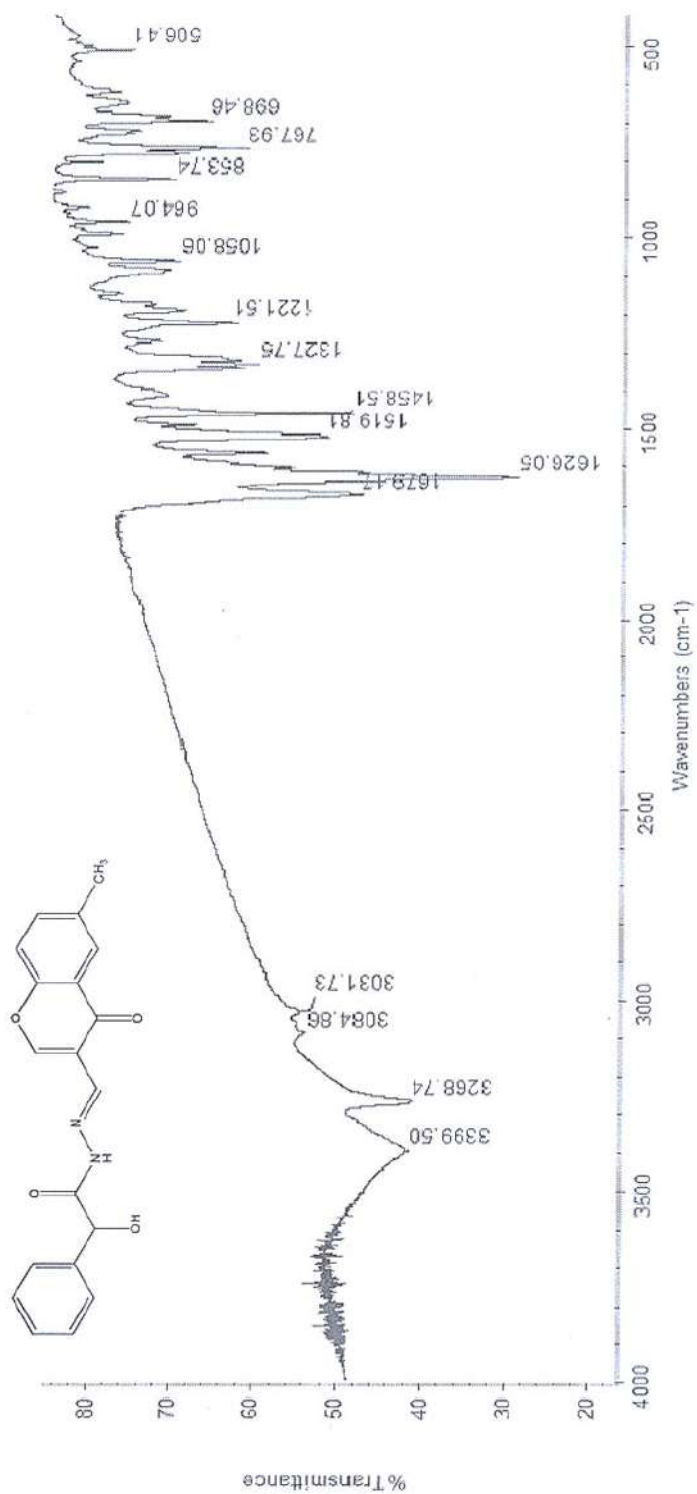
Infrared absorption spectrum of compound [1] as a potassium bromide pellet

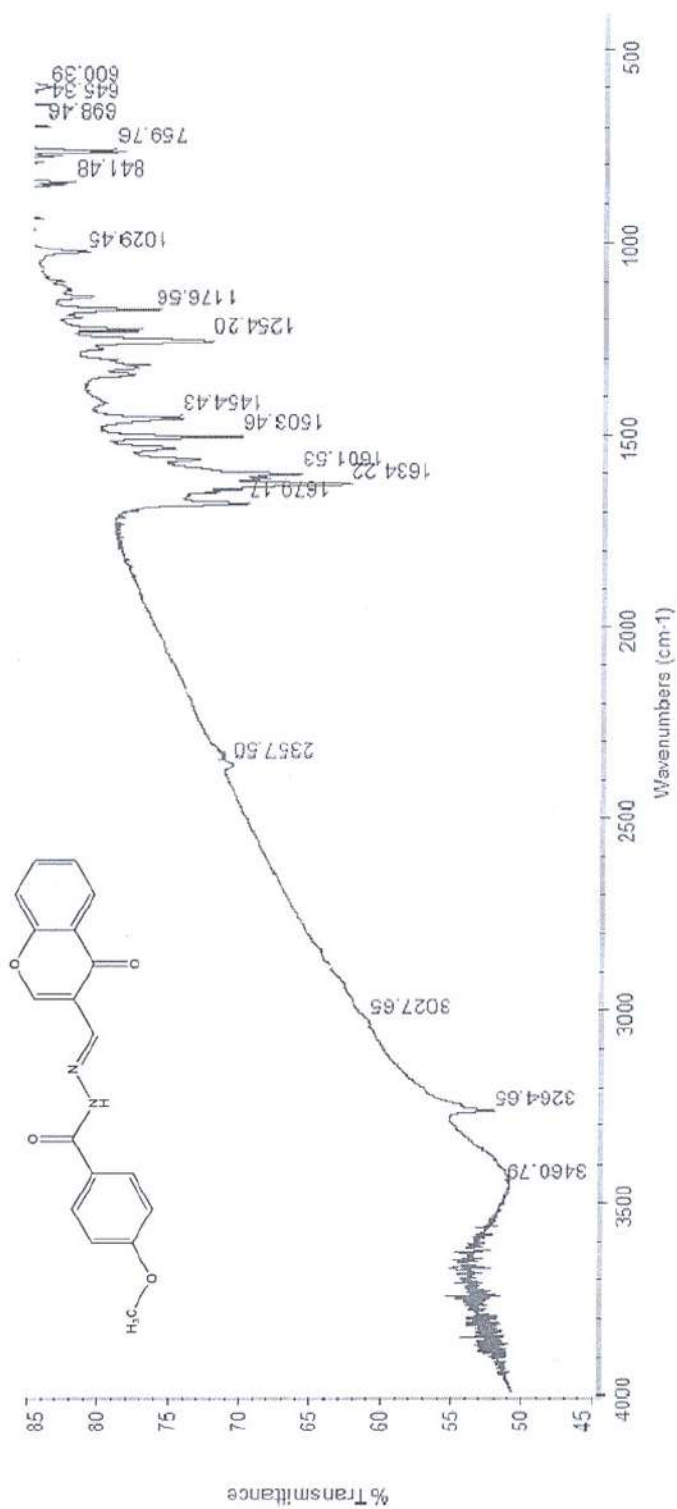Infrared absorption spectrum of compound [2] as a potassium bromide pellet
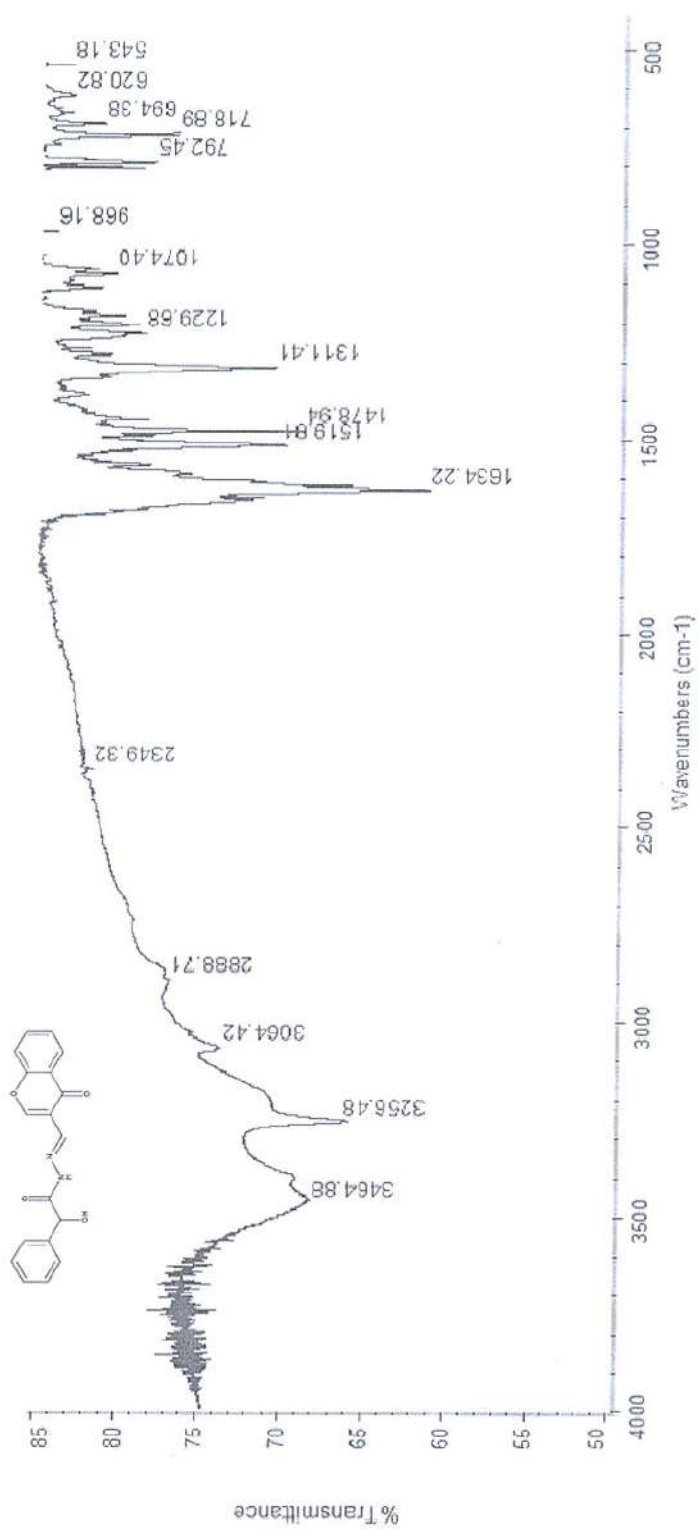
Infrared absorption spectrum of compound [3] as a potassium bromide pellet

Infrared absorption spectrum of compound [4] as a potassium bromide pellet

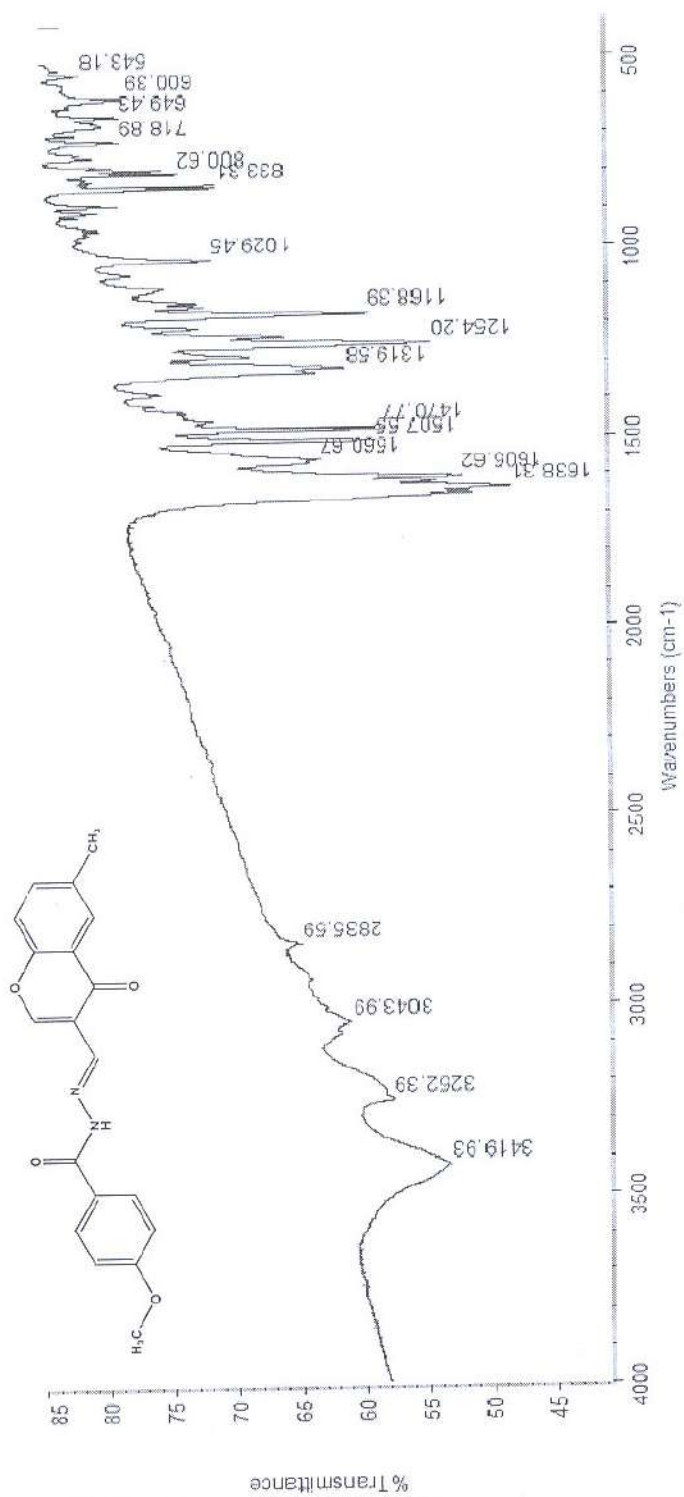Infrared absorption spectrum of compound [5] as a potassium bromide pellet

Infrared absorption spectrum of compound [6] as a potassium bromide pellet

Infrared absorption spectrum of compound [7] as a potassium bromide pellet

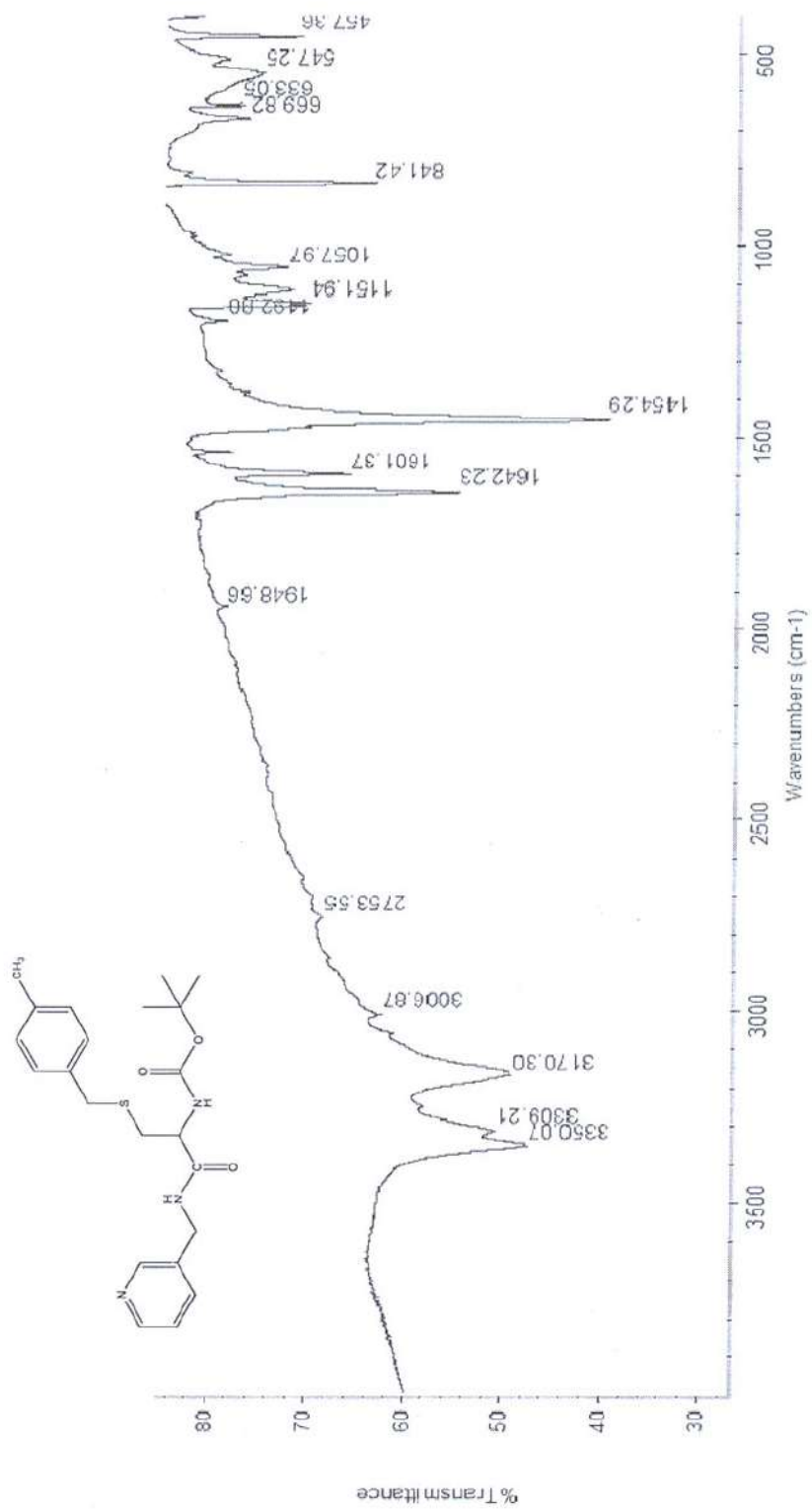Infrared absorption spectrum of compound [8] by using ATR-ZnSe technique

Infrared absorption spectrum of compound [9] as a potassium bromide pellet

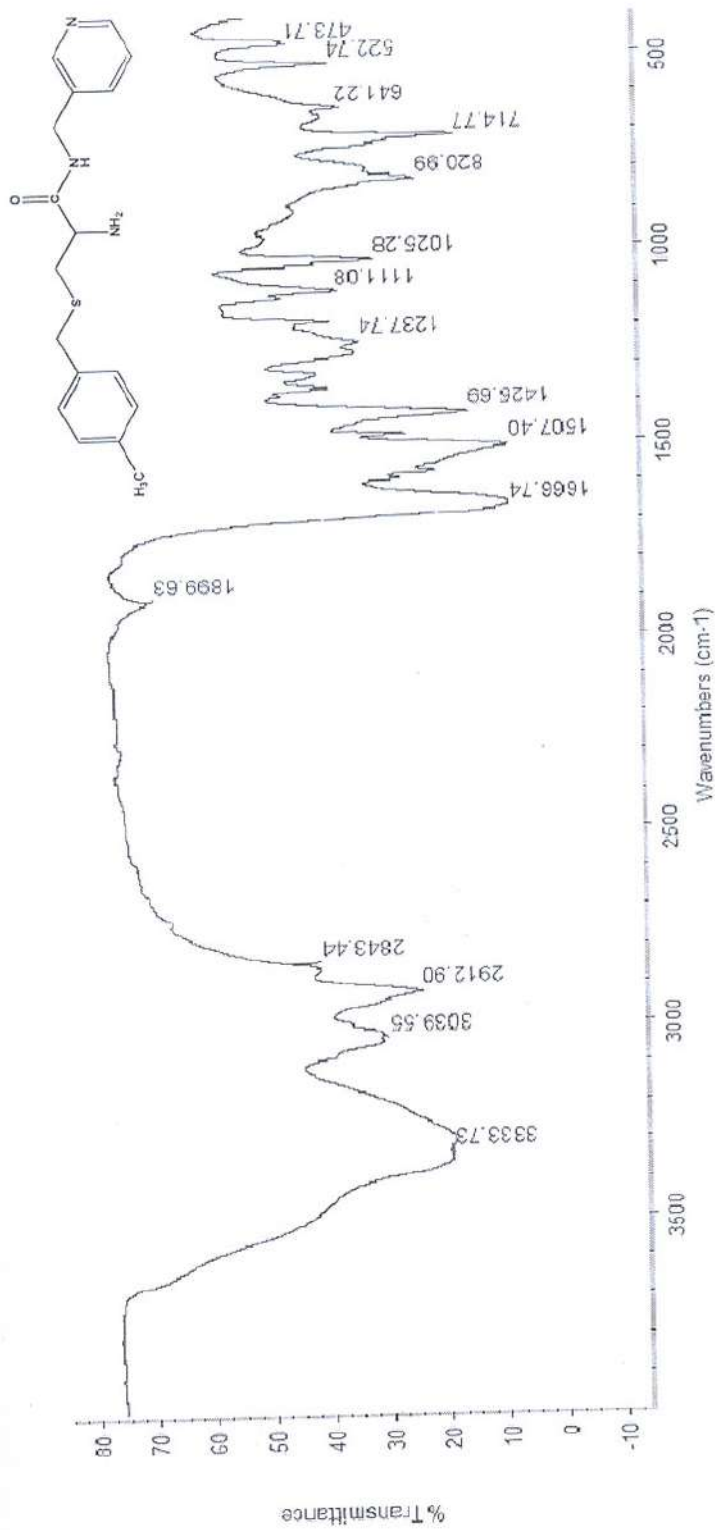Infrared absorption spectrum of compound [10] as a potassium bromide pellet

Infrared absorption spectrum of compound [11] as a potassium bromide pellet

Infrared absorption spectrum of compound [12] as a potassium bromide pellet

Infrared absorption spectrum of compound [13] as a potassium bromide pellet

Infrared absorption spectrum of compound [14] as a potassium bromide pellet

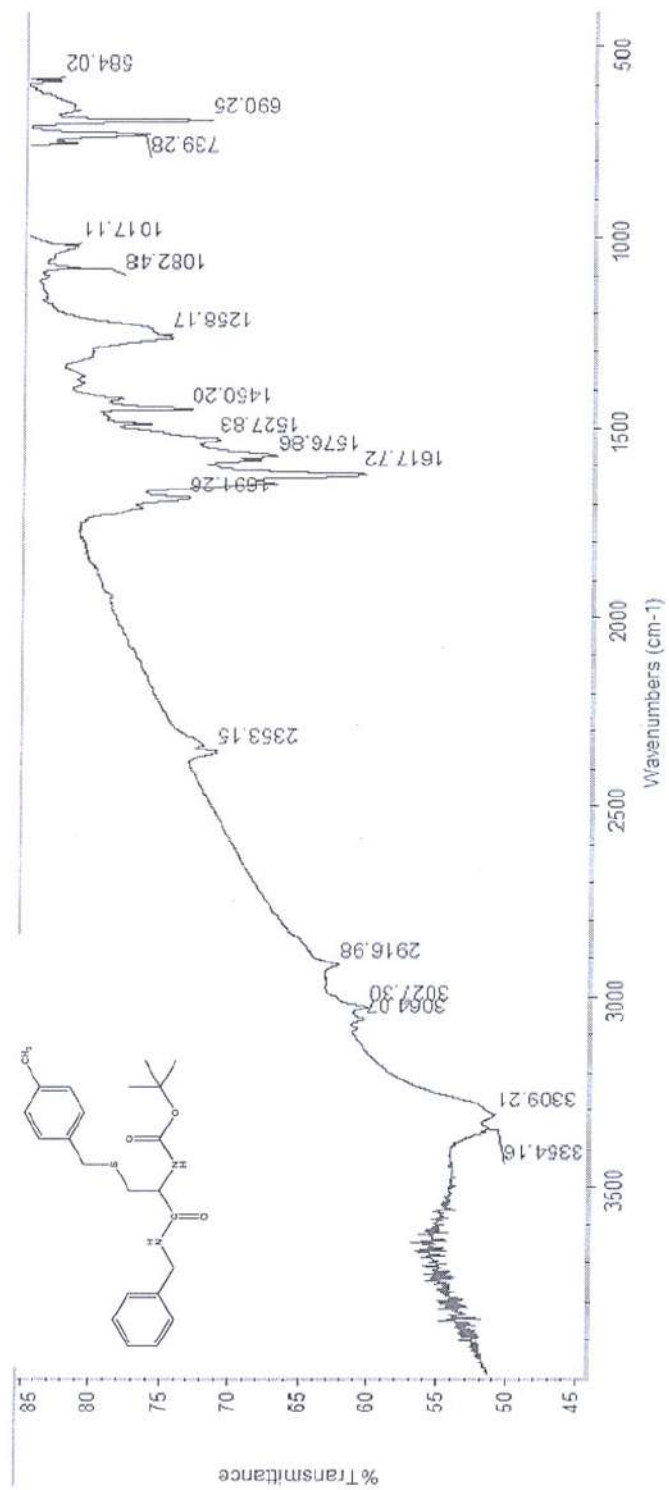Infrared absorption spectrum of compound [15] as a potassium bromide pellet

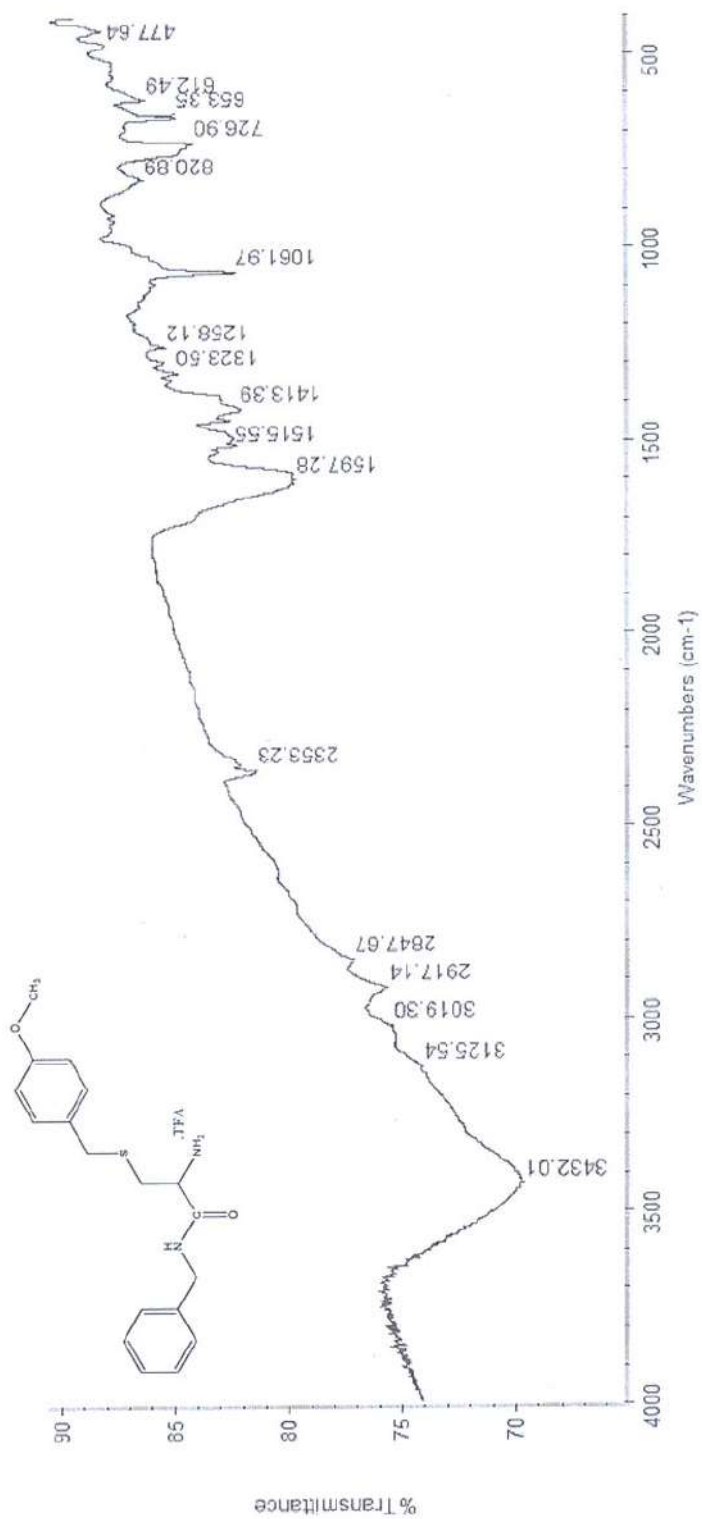Infrared absorption spectrum of compound [16] as a potassium bromide pellet

122
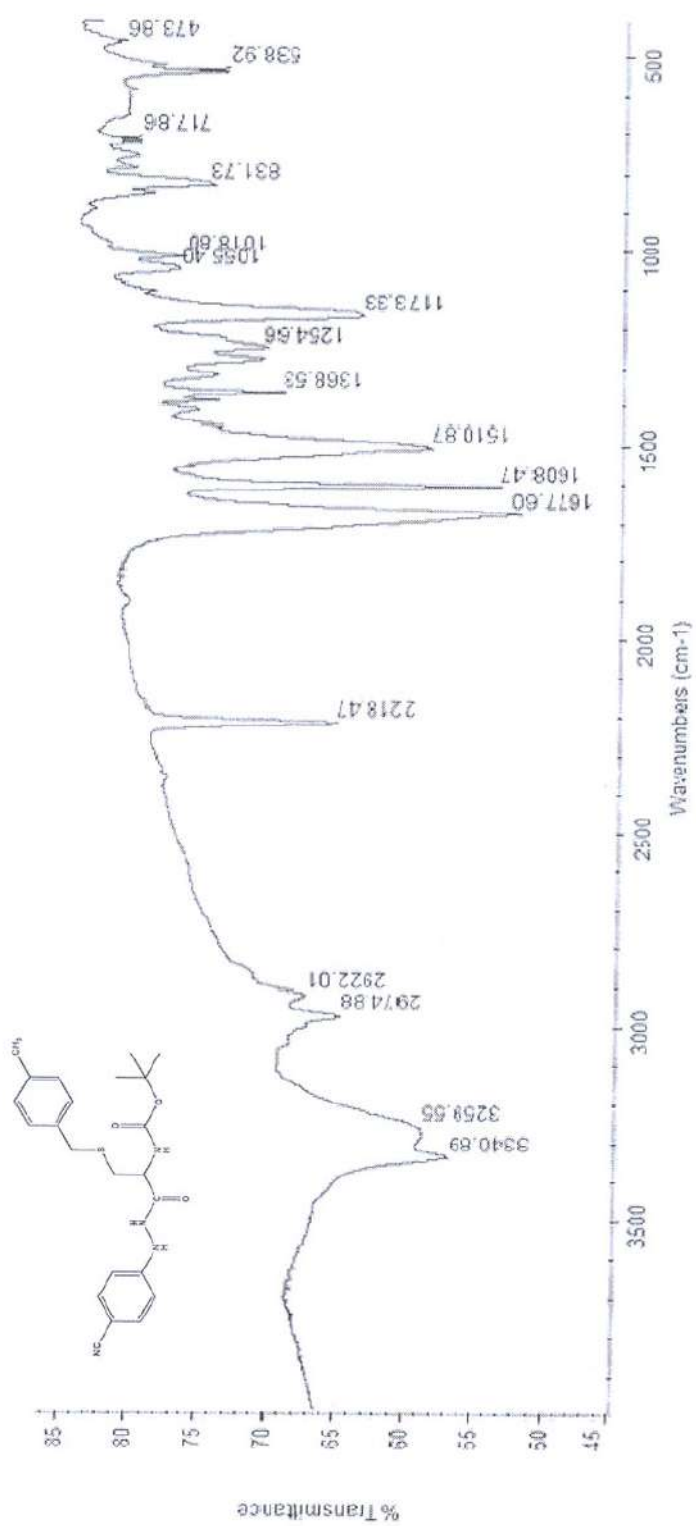
Infrared absorption spectrum of compound [17] as a potassium bromide pellet
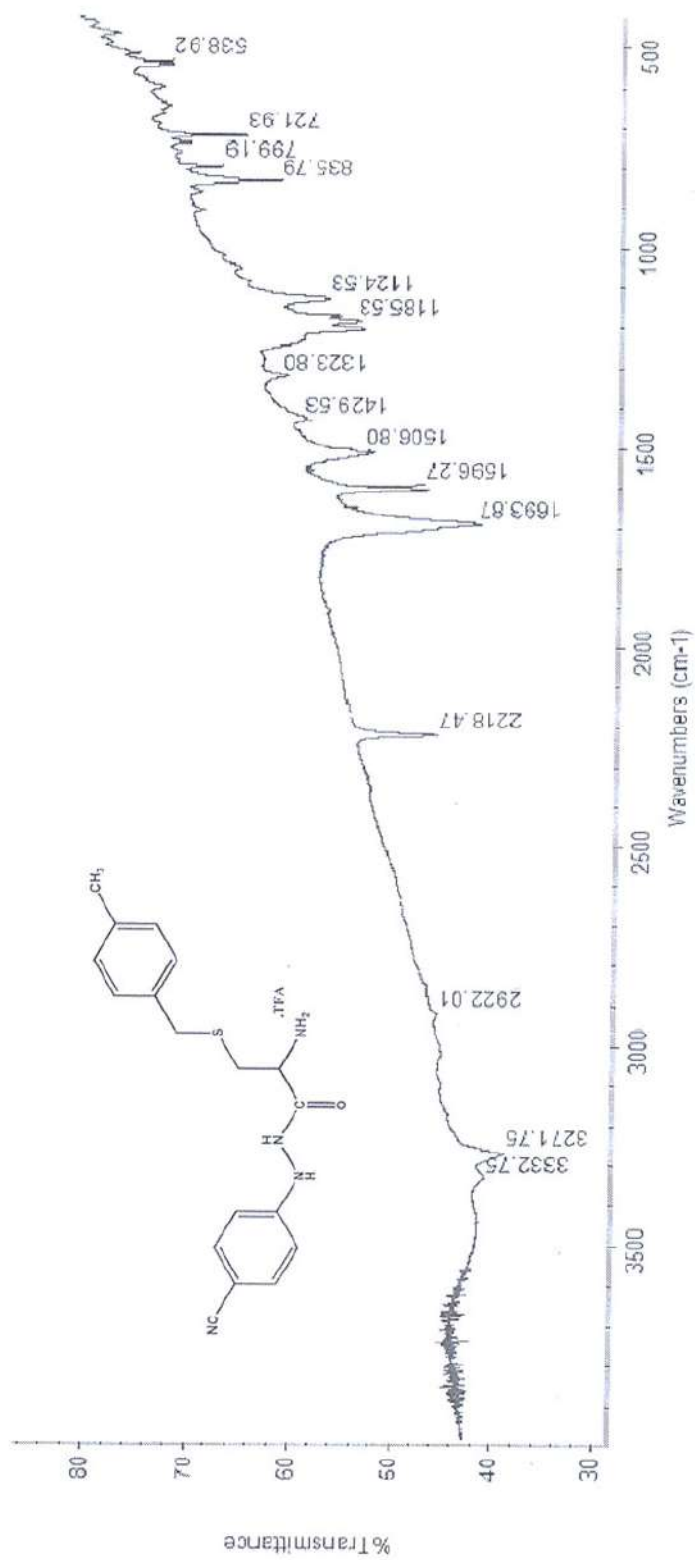
Infrared absorption spectrum of compound [18] as a potassium bromide pellet
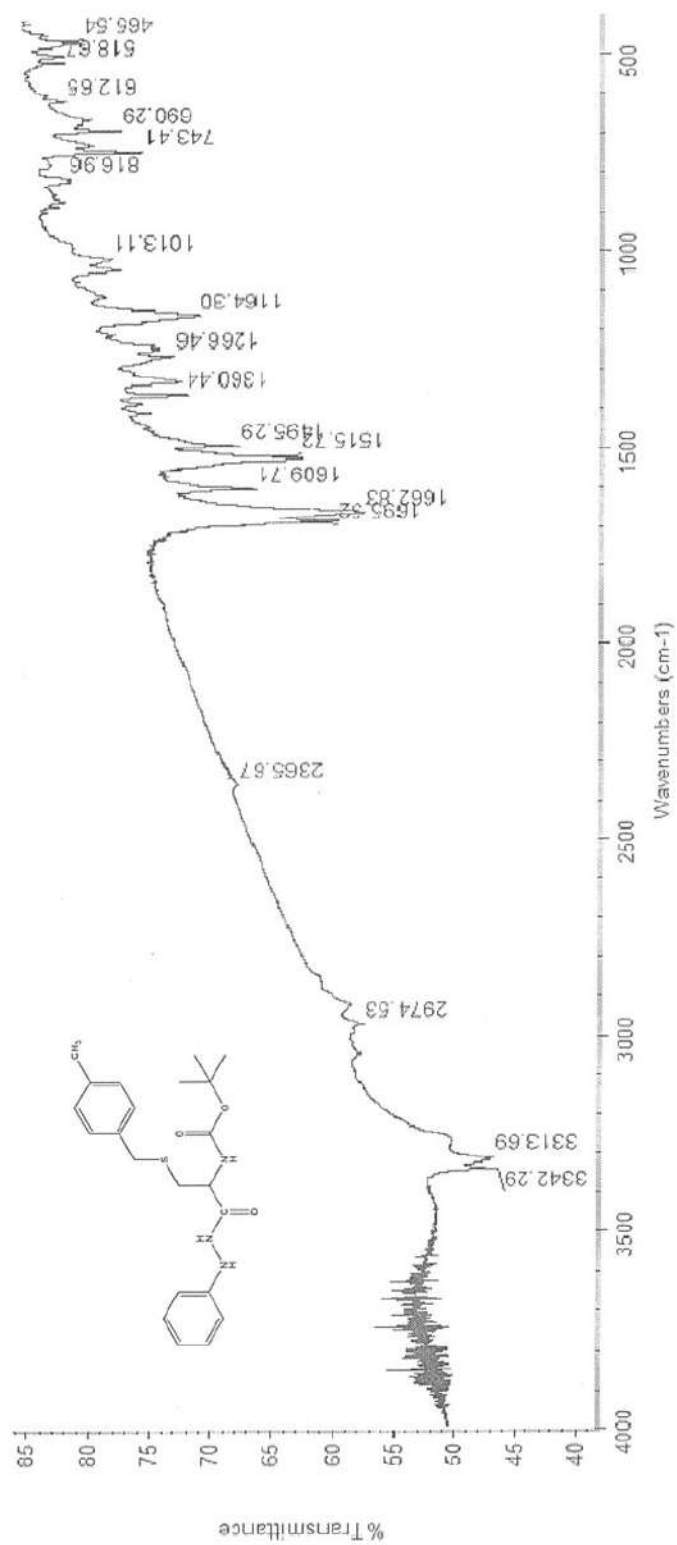
Infrared absorption spectrum of compound [19] as a potassium bromide pellet

125
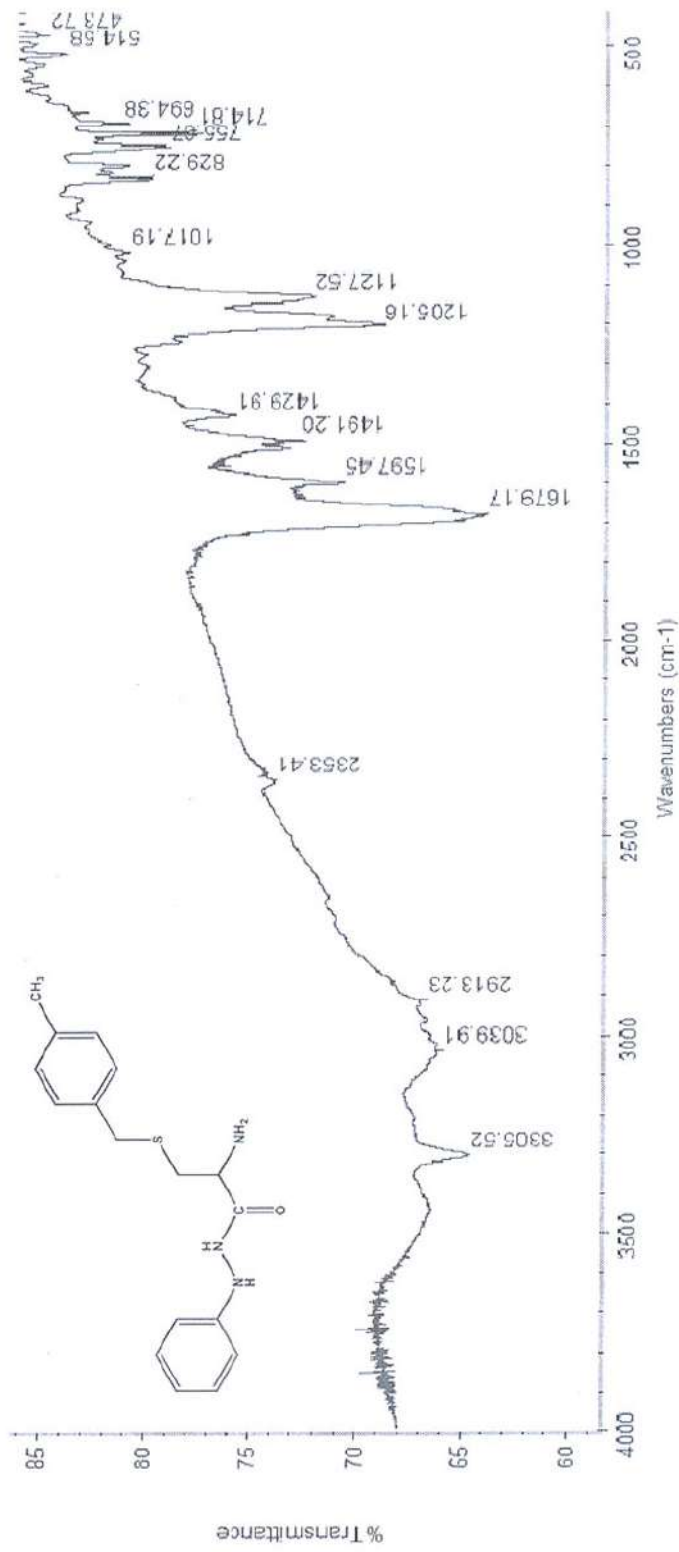
Infrared absorption spectrum of compound [20] as a potassium bromide pellet
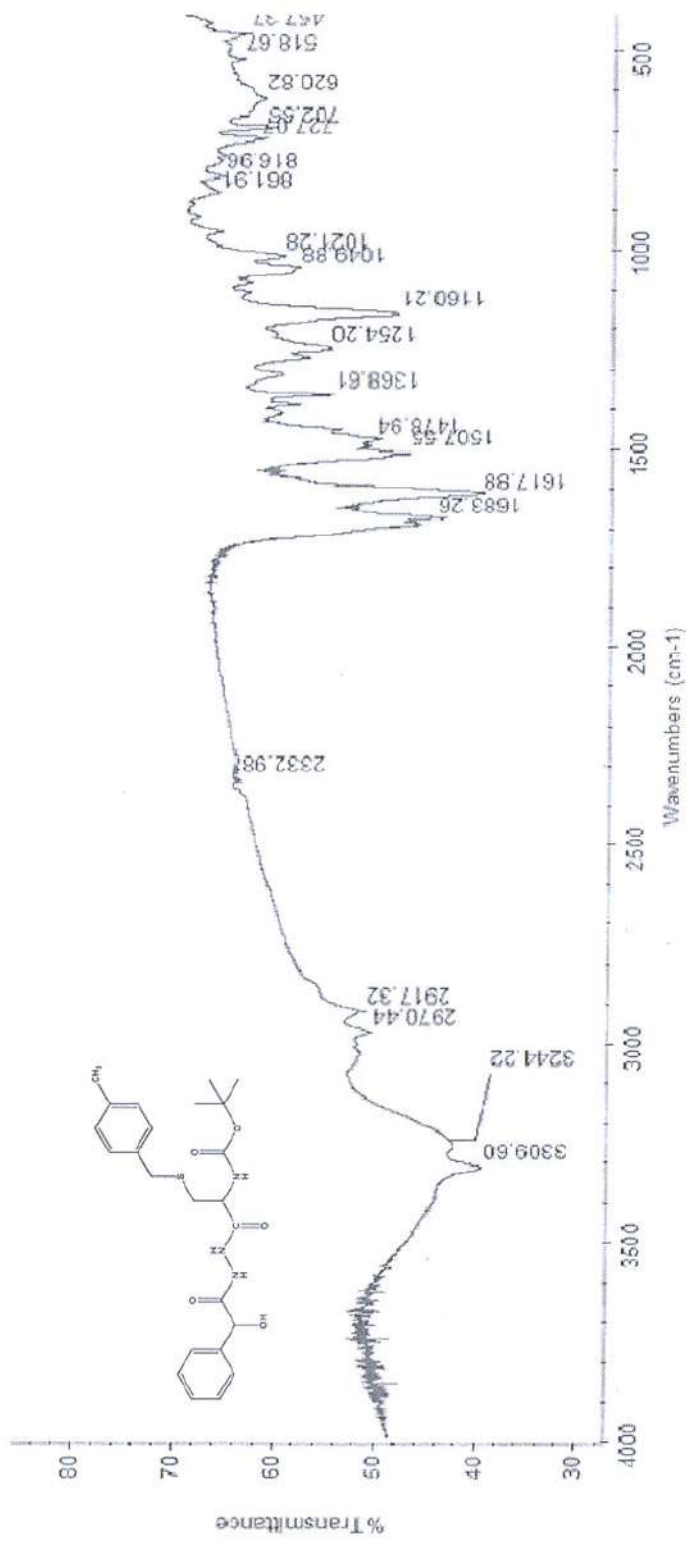
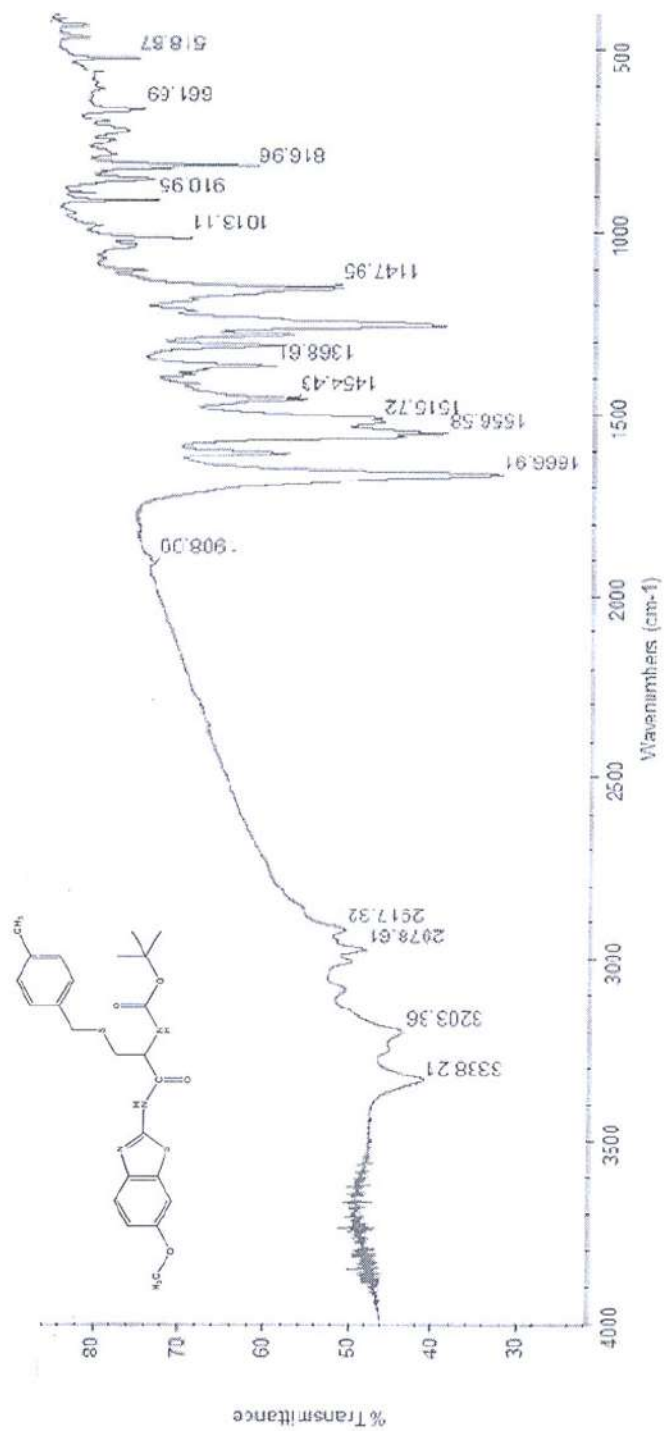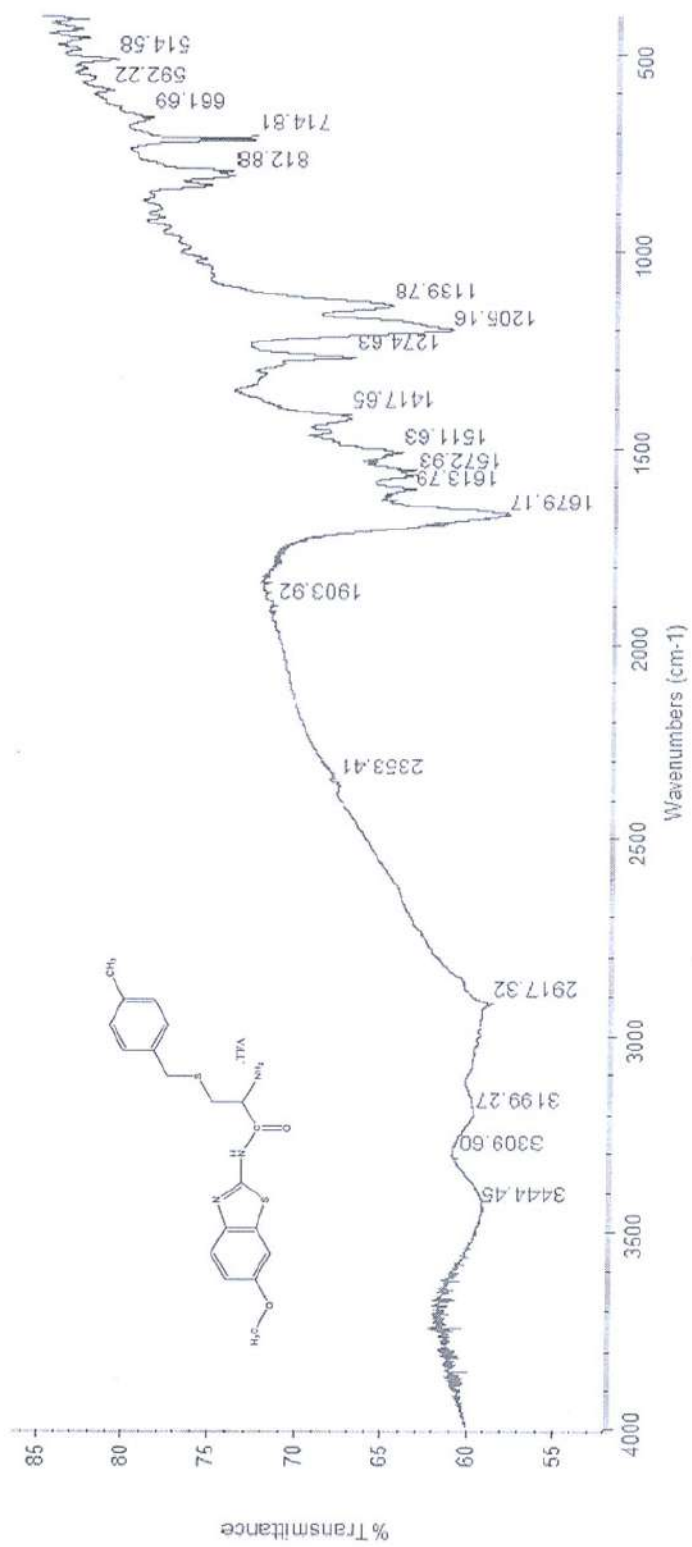Infrared absorption spectrum of compound [21] as a potassium bromide pellet
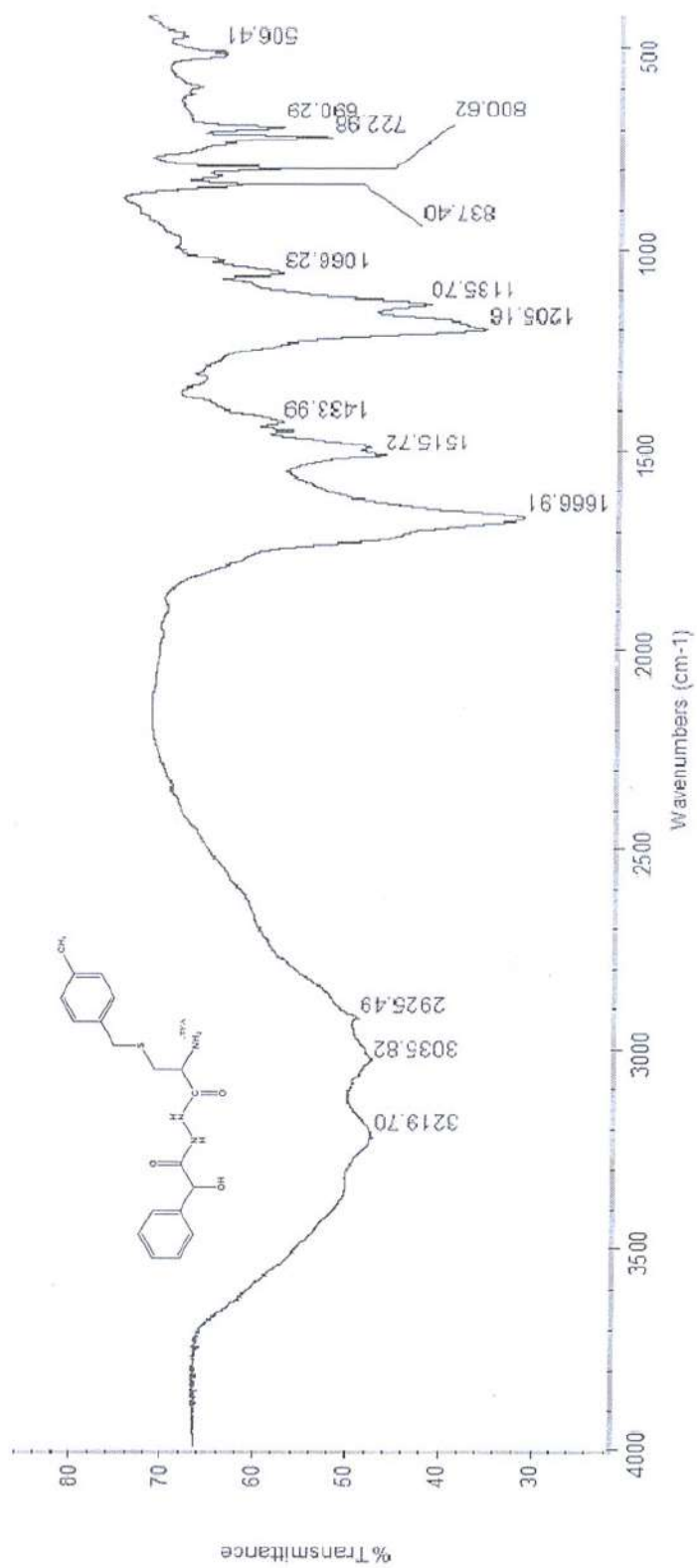
Infrared absorption spectrum of compound [22] as a potassium bromide pellet
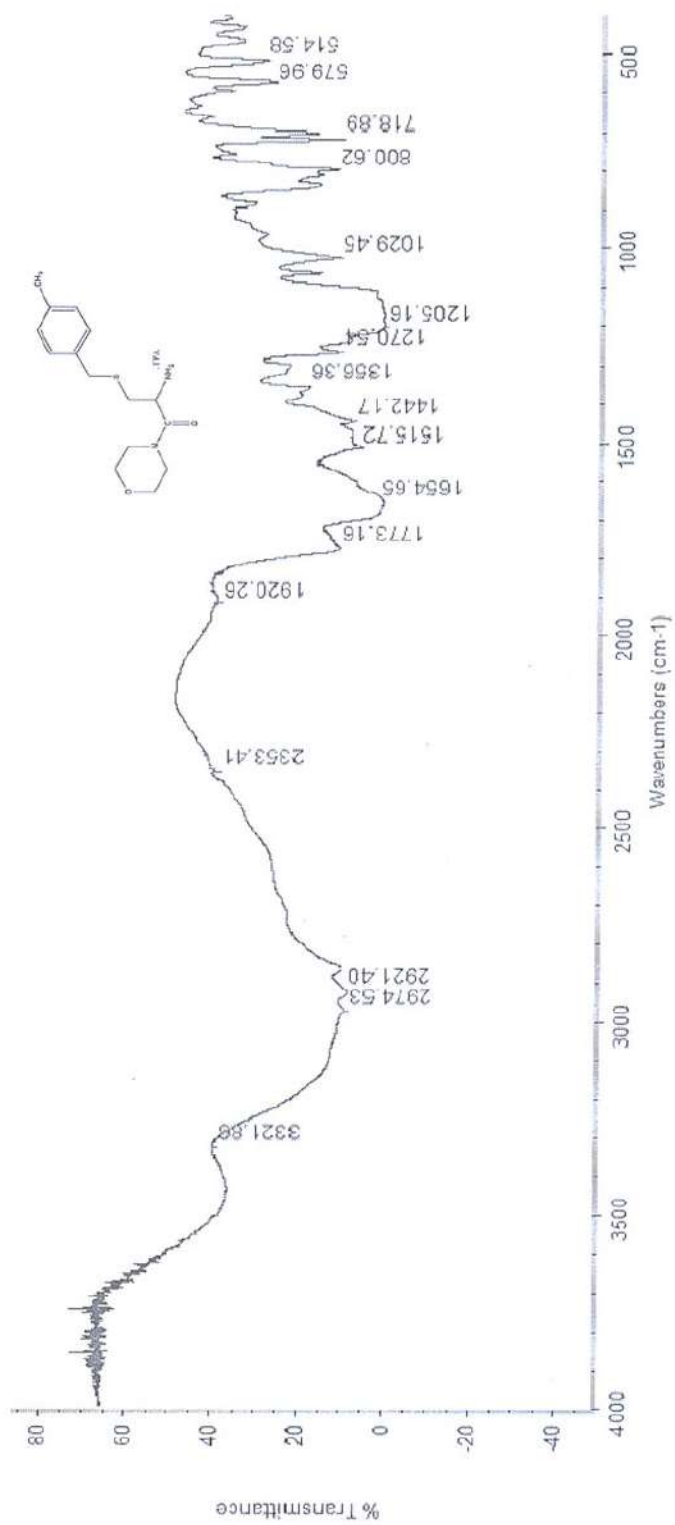
Infrared absorption spectrum of compound [24] by using ATR-ZnSe technique
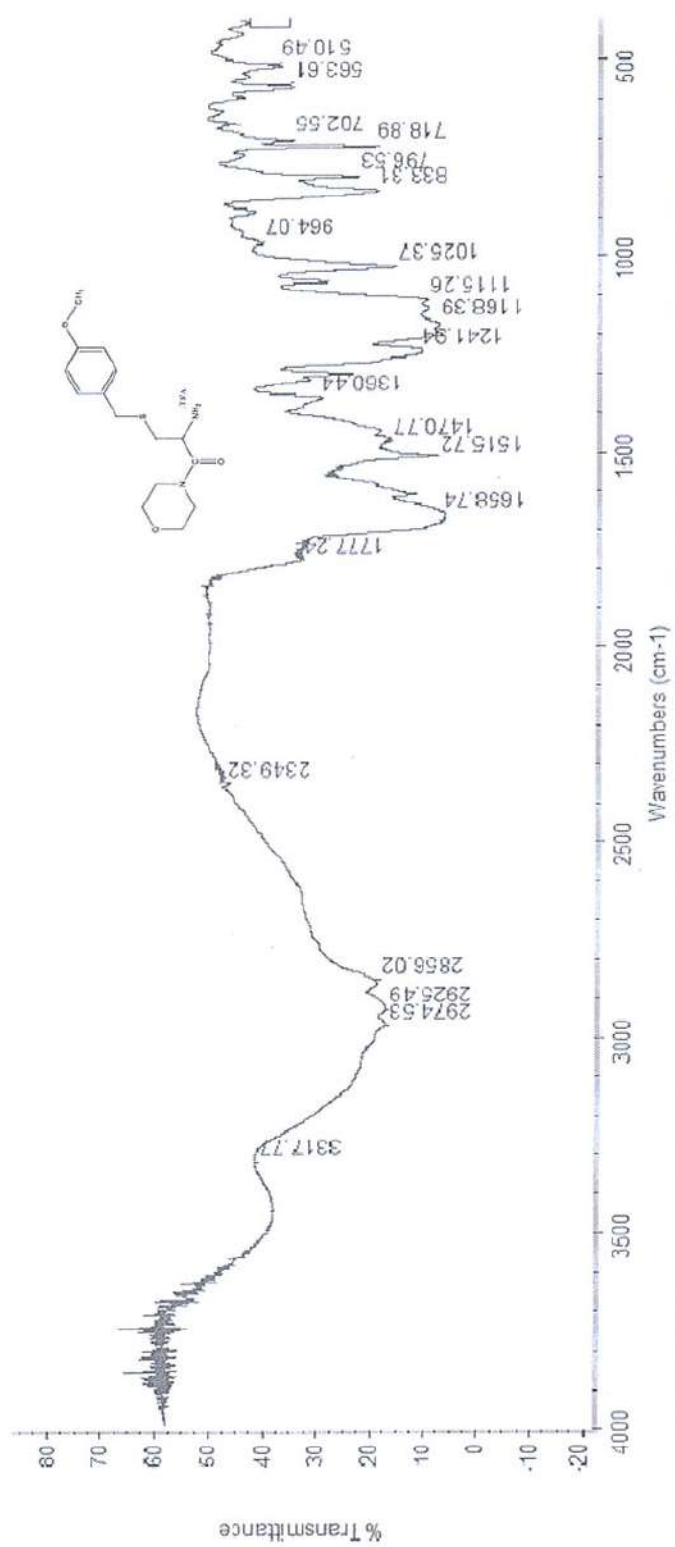
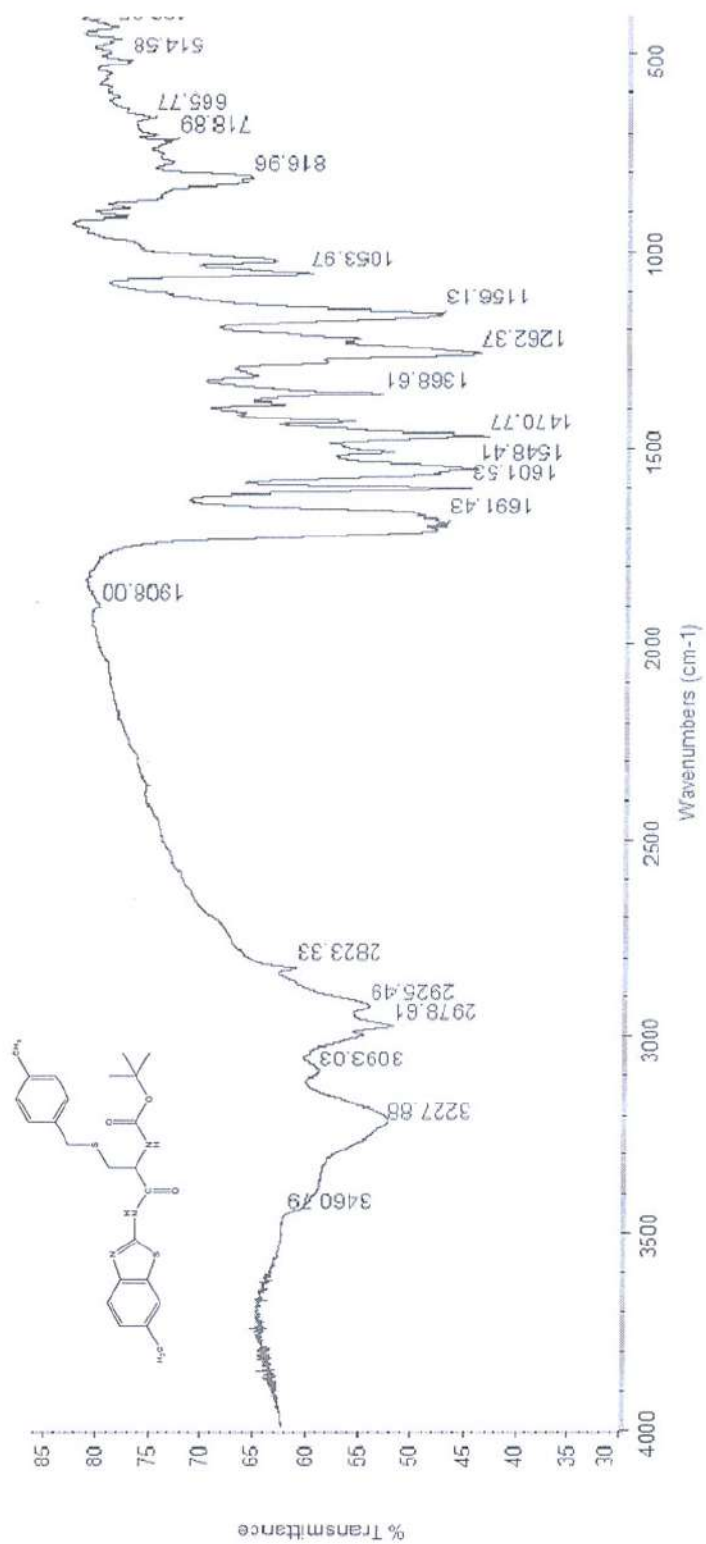Infrared absorption spectrum of compound [26] by using ATR-ZnSe technique
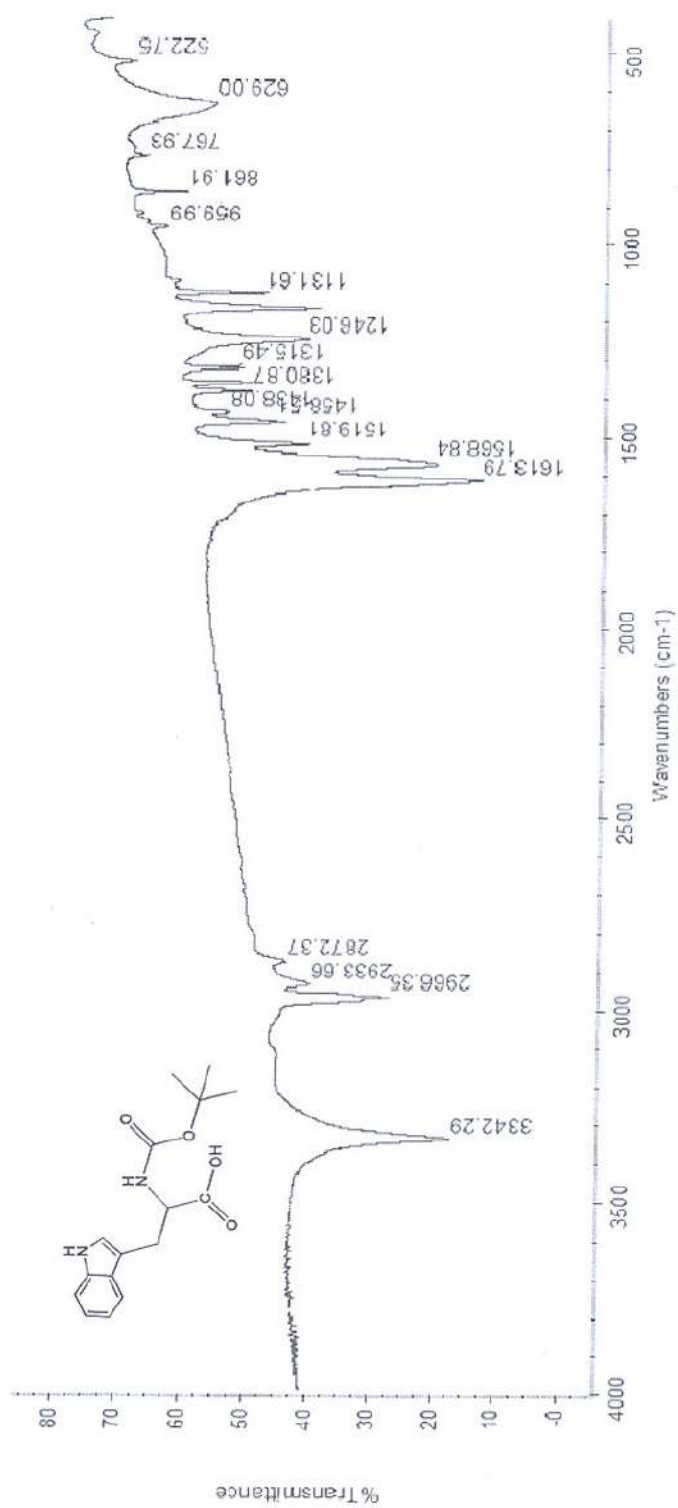
Infrared absorption spectrum of compound [27] as a potassium bromide pellet
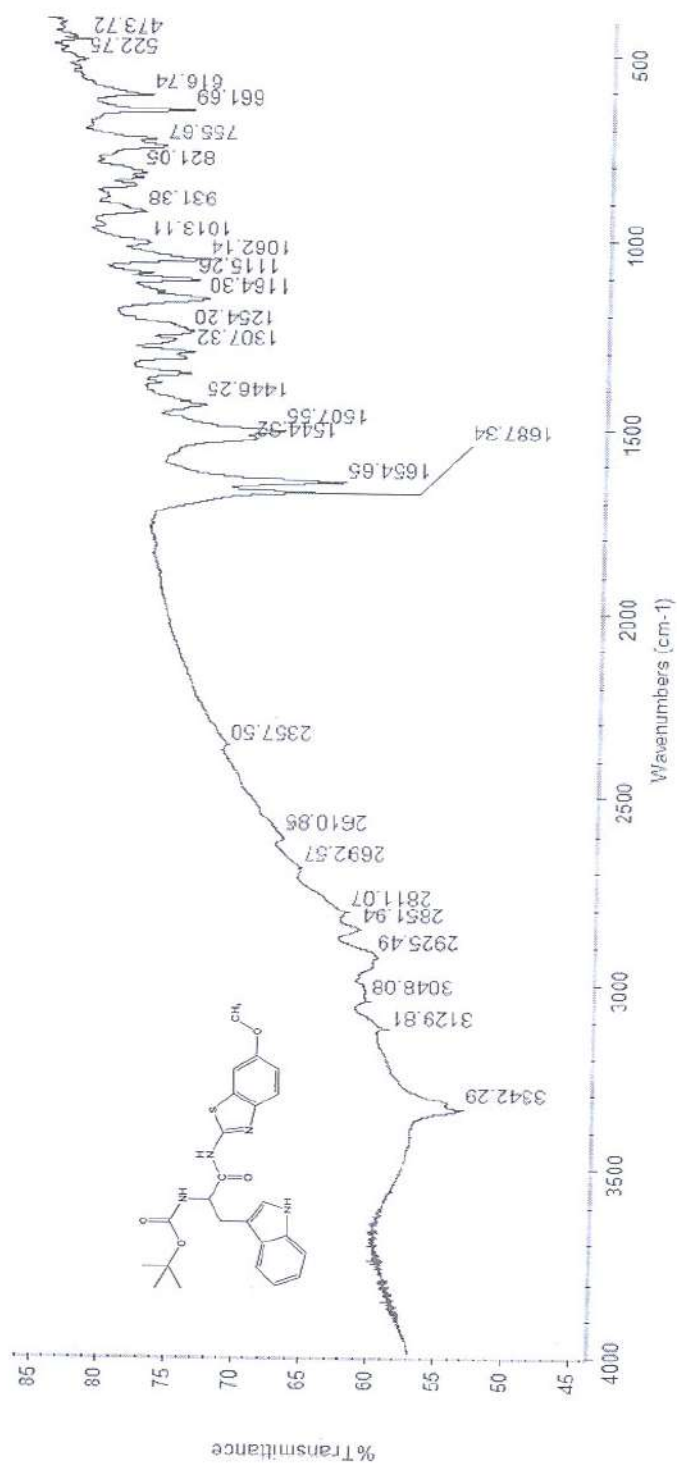
Infrared absorption spectrum of compound [28] as a potassium bromide pellet
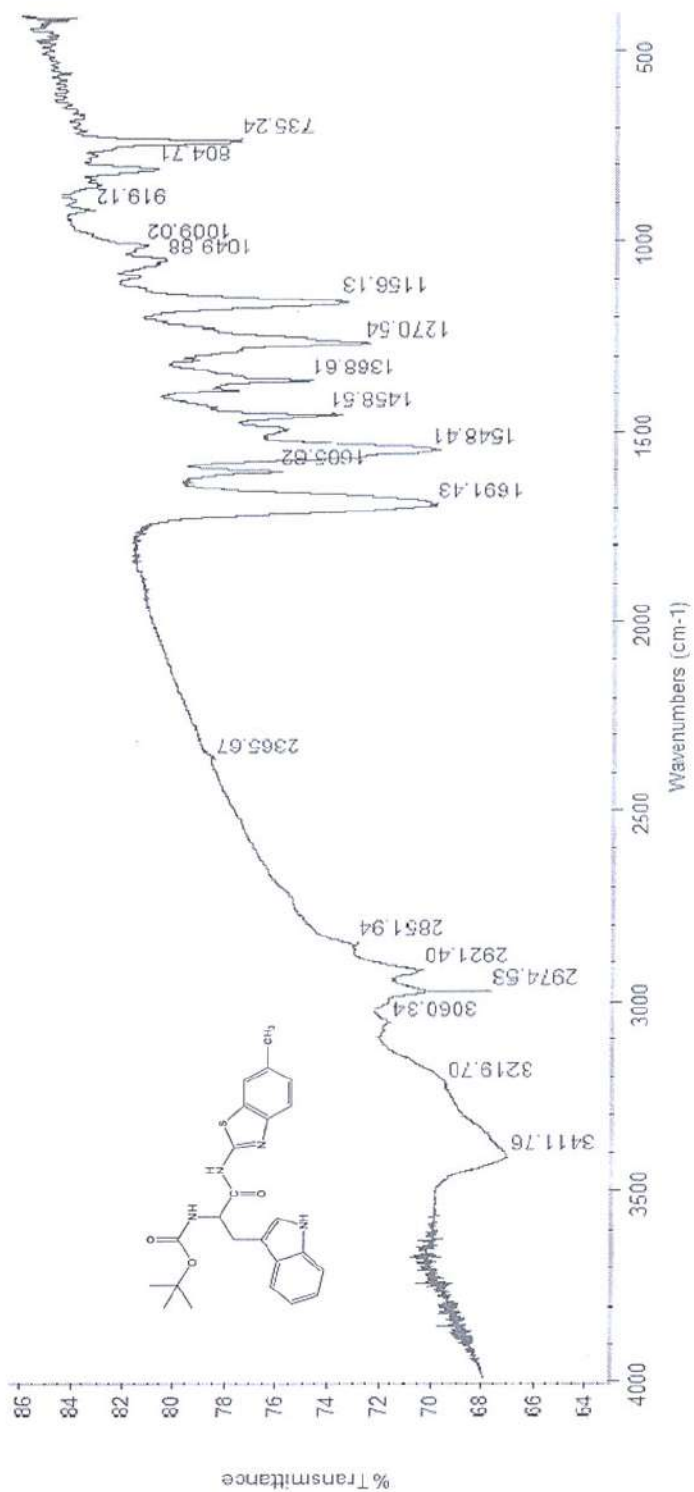
Infrared absorption spectrum of compound [29] as a potassium bromide pellet
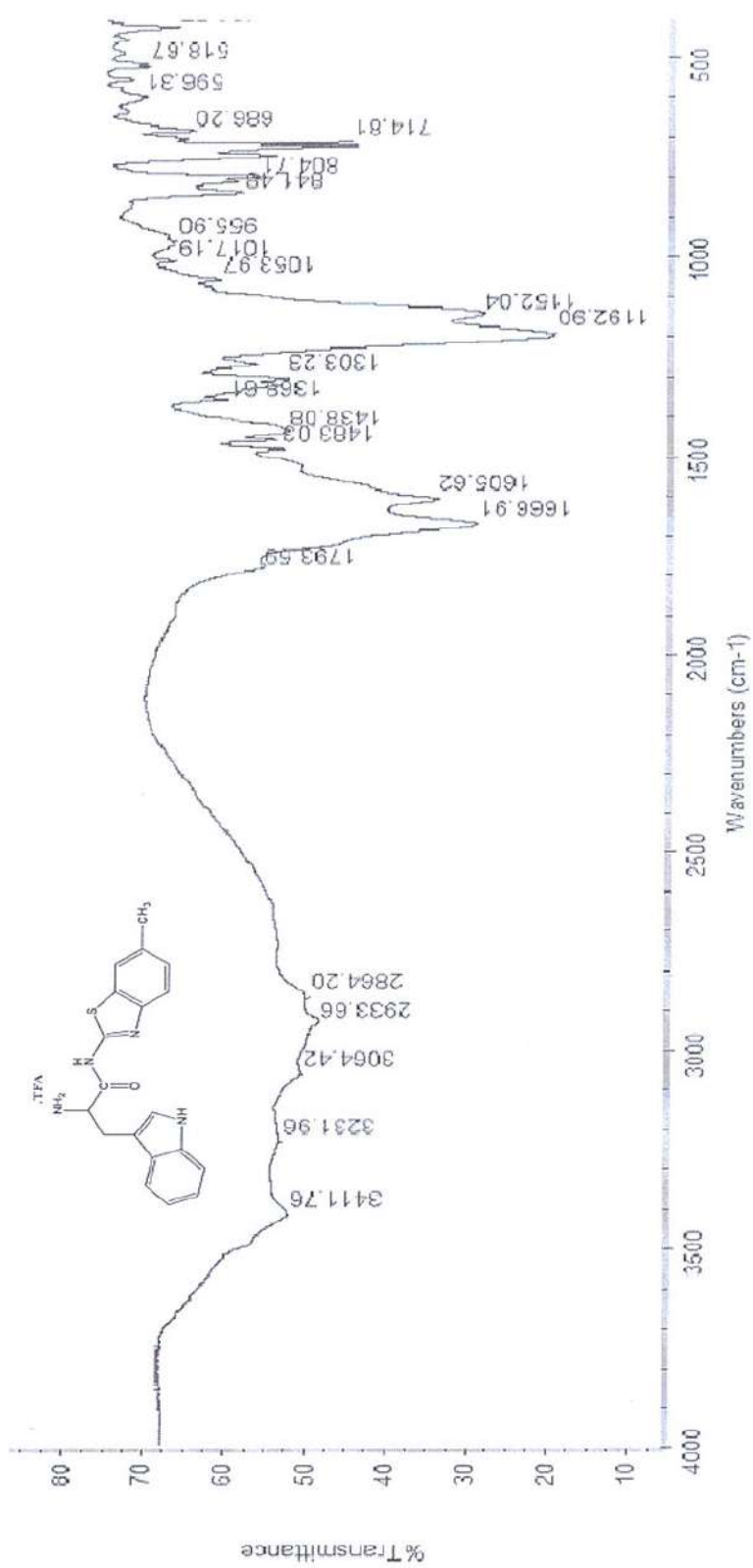
Infrared absorption spectrum of compound [30] as a potassium bromide pellet
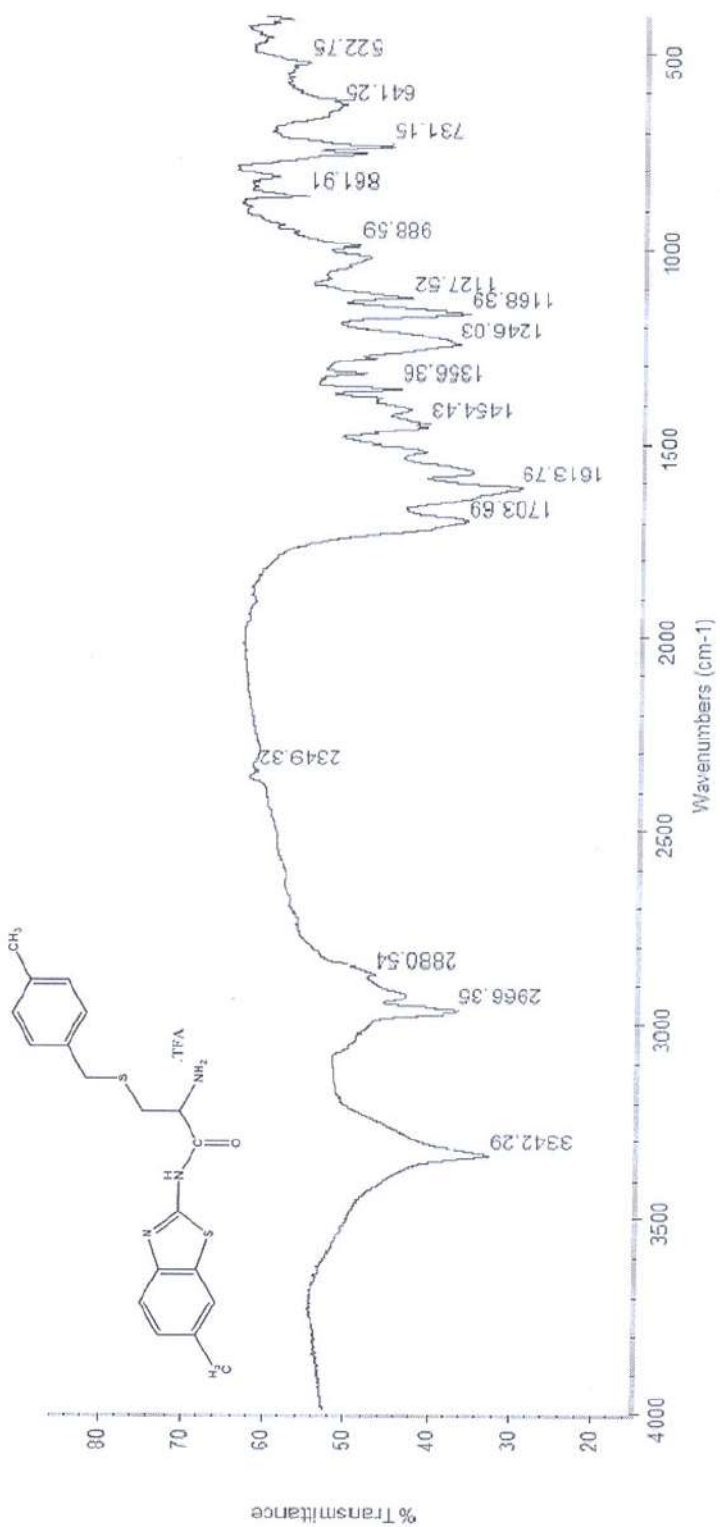
134
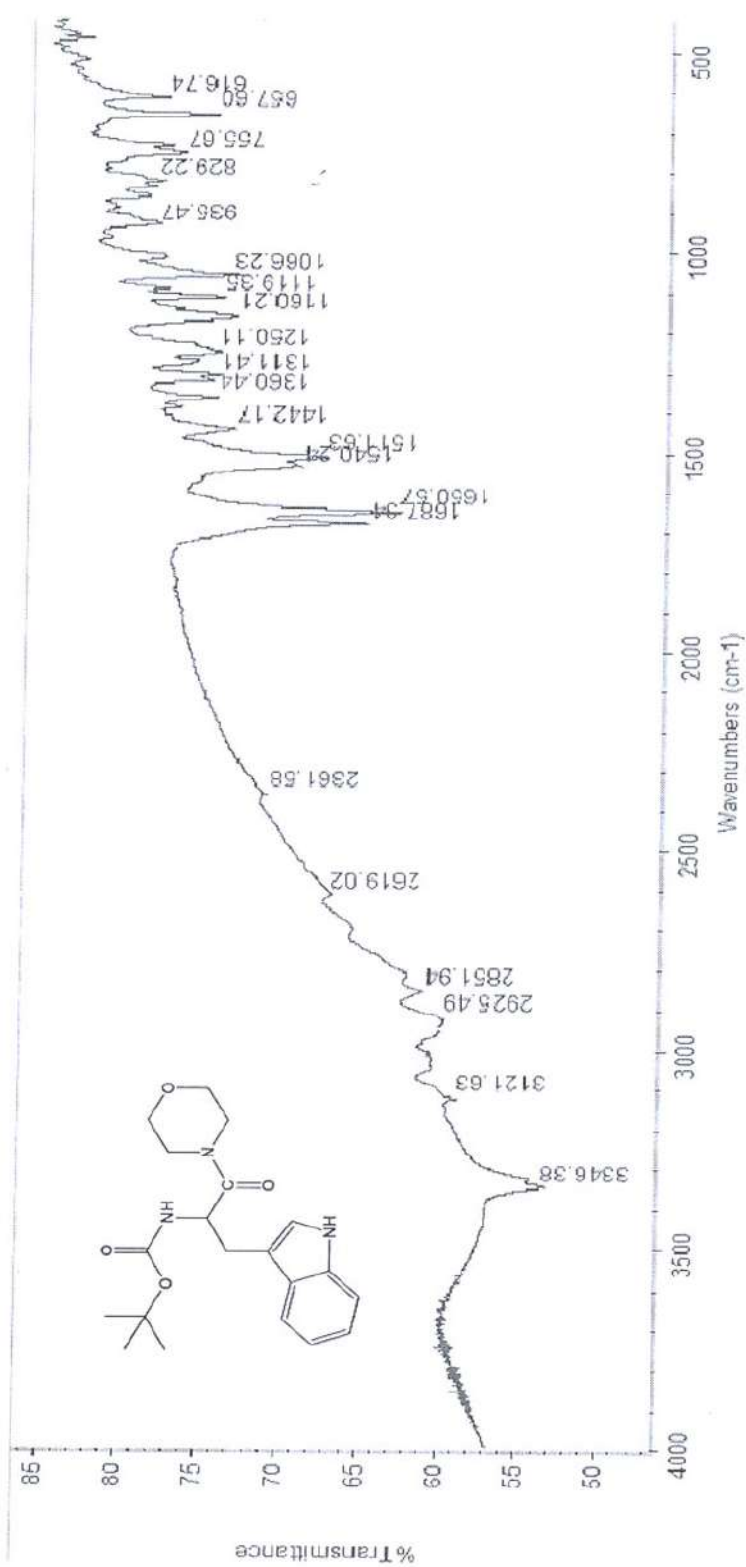
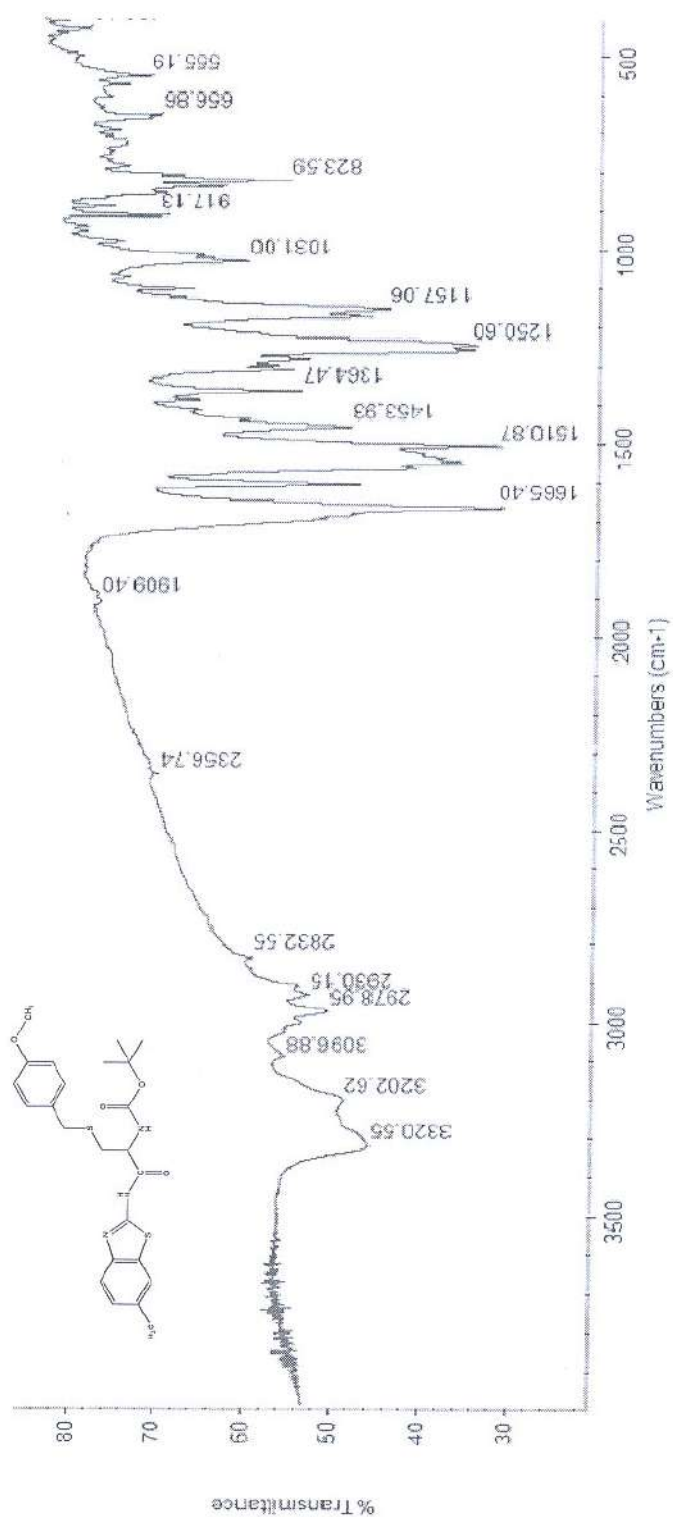Infrared absorption spectrum of compound [31] as a potassium bromide pellet
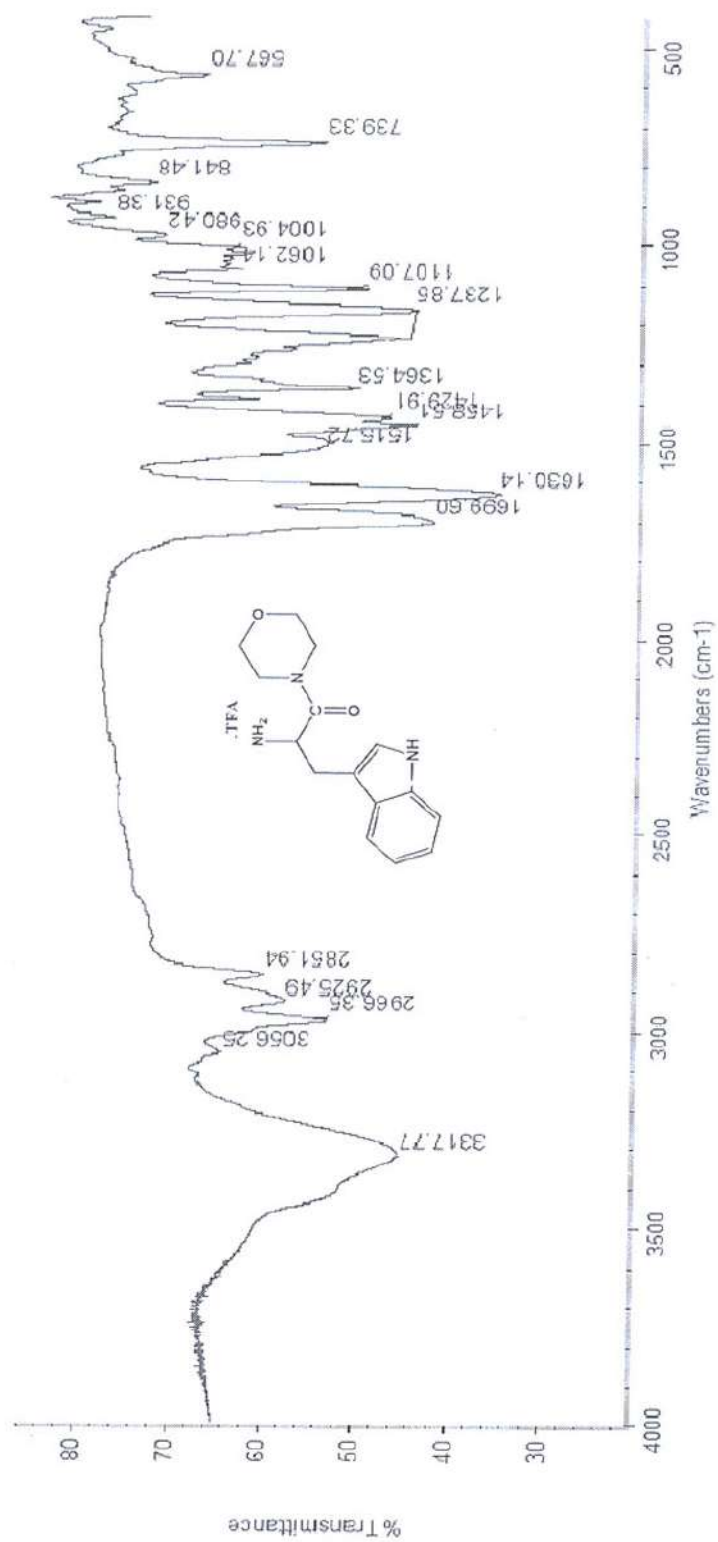
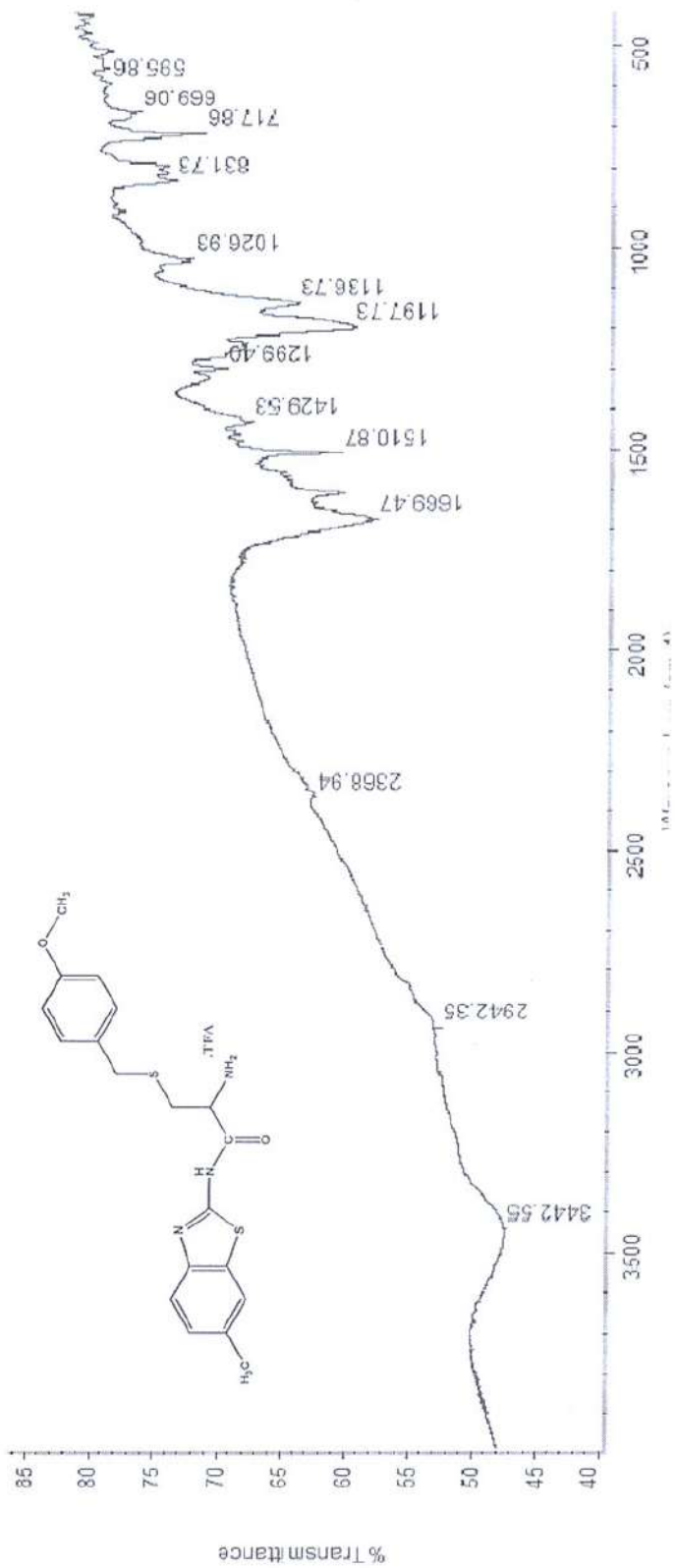Infrared absorption spectrum of compound [32] as a potassium bromide pellet

Infrared absorption spectrum of compound [33] as a potassium bromide pellet

138

^{1}H NMR spectrum (300 MHz) of compound [1] in DMSO-*d6*

^{1}H NMR spectrum (300 MHz) of compound [2] in DMSO-$d6$
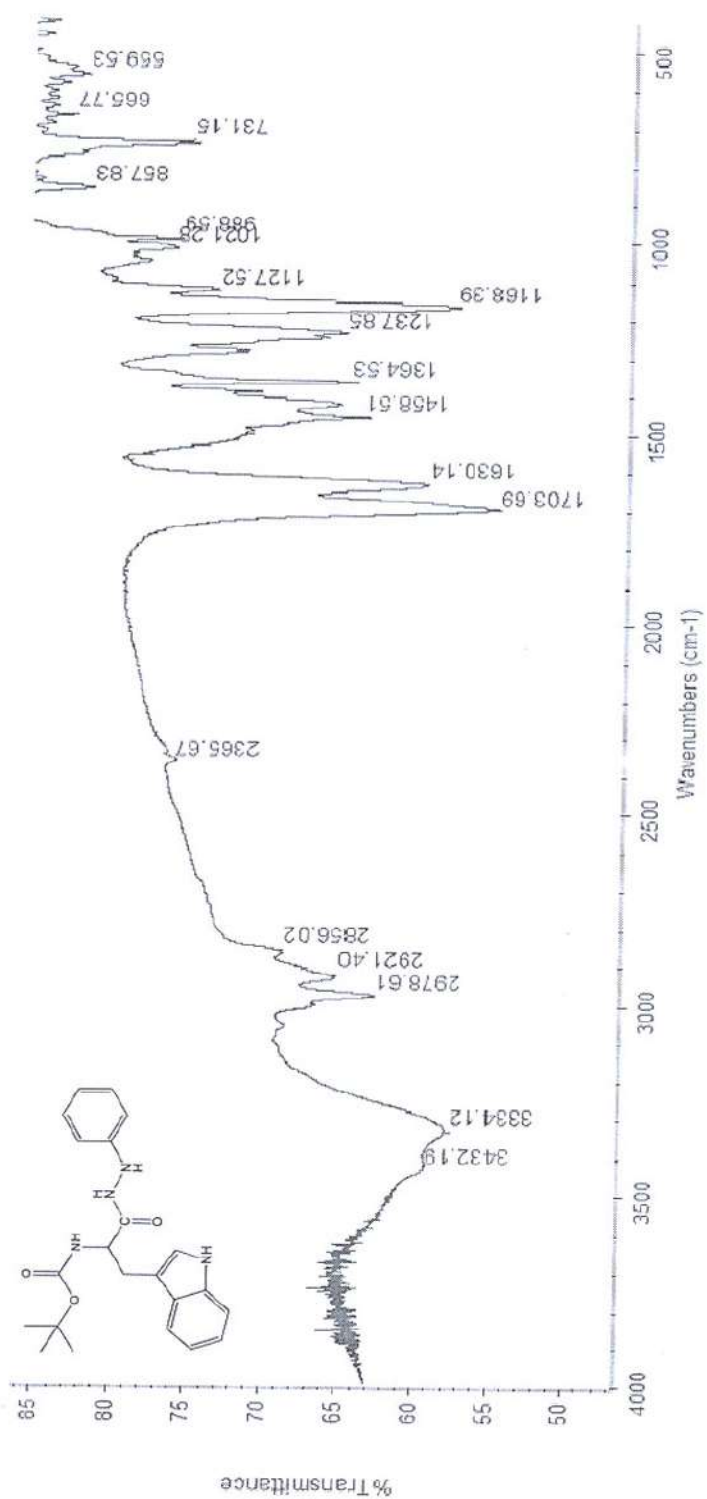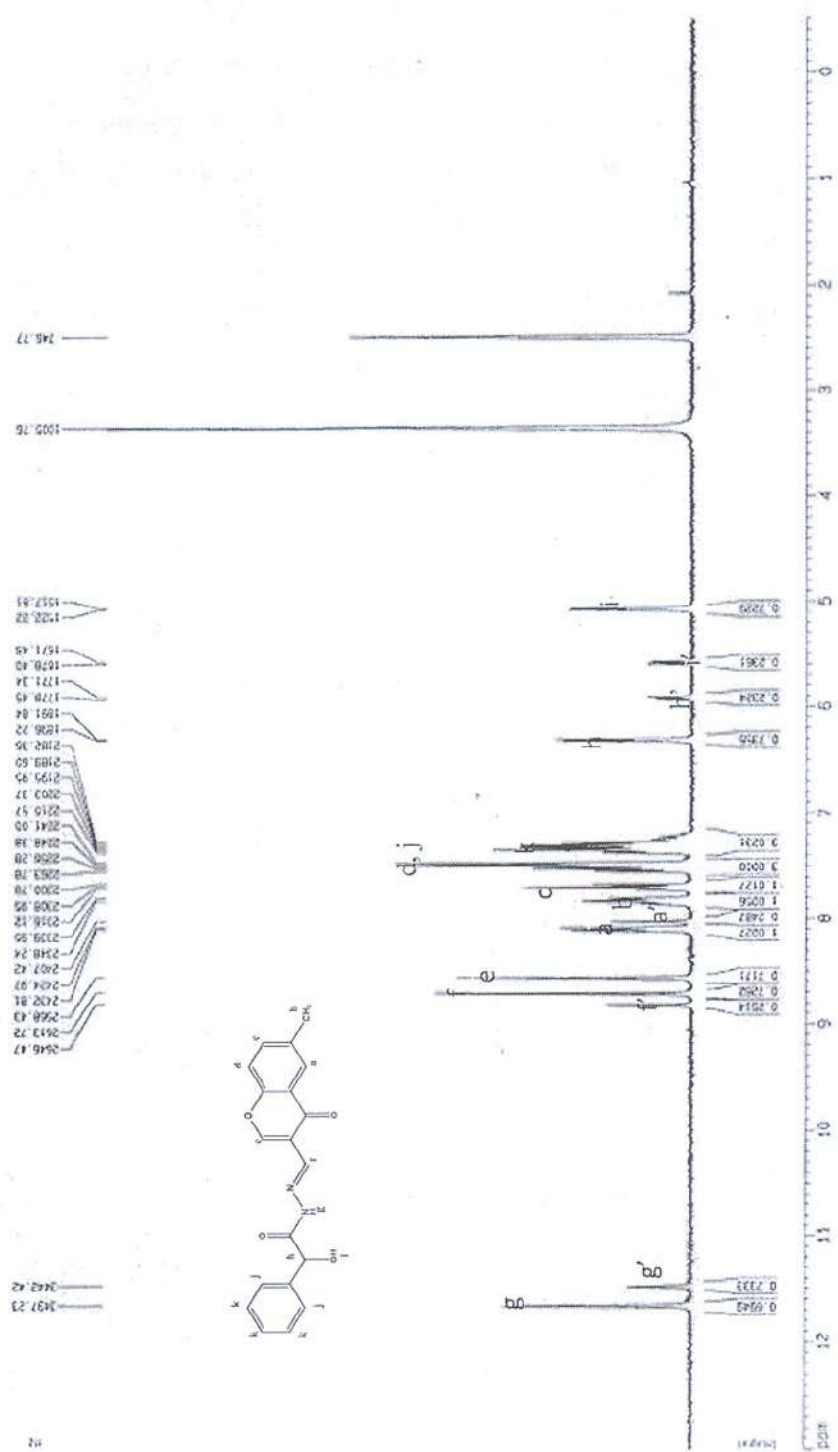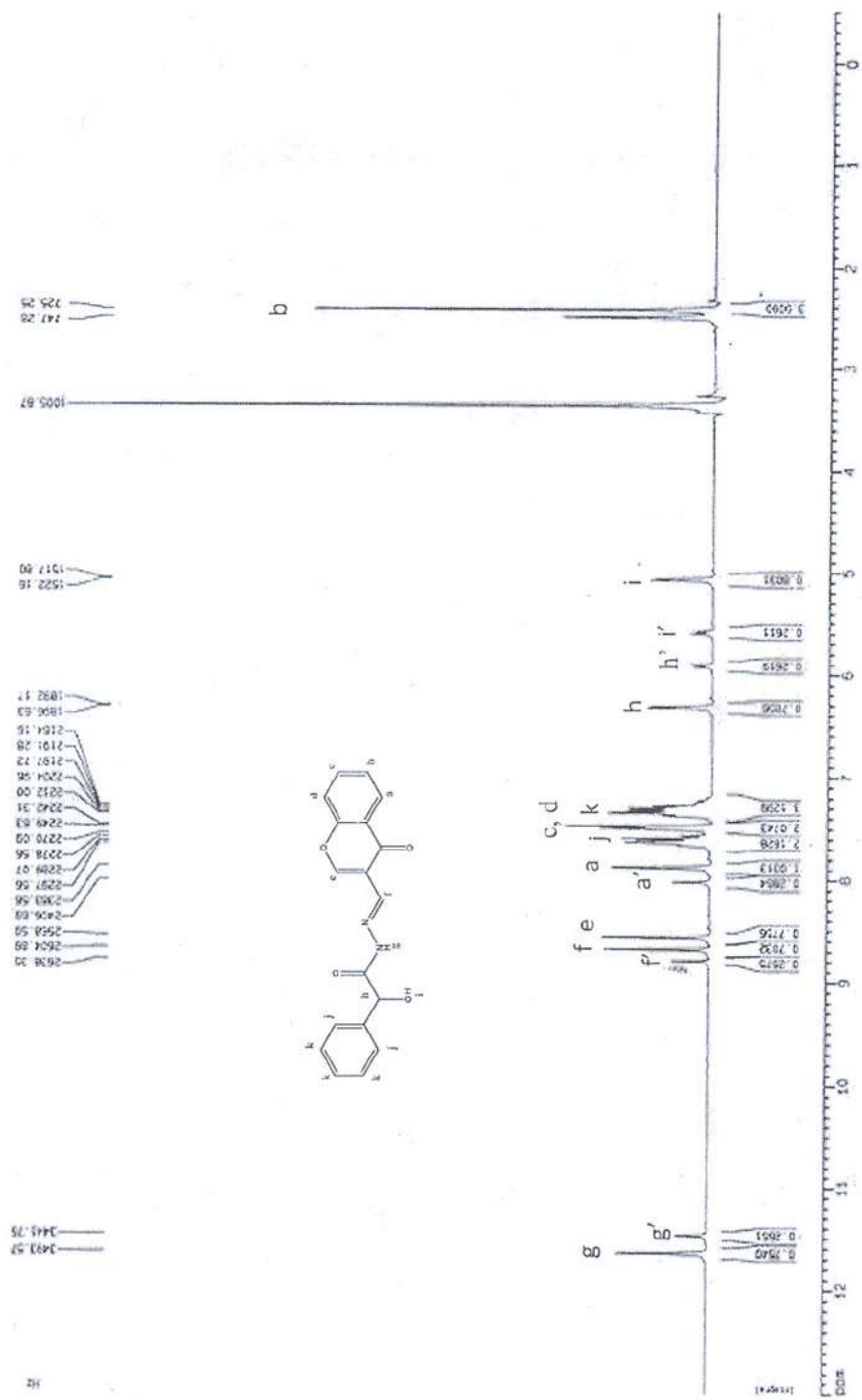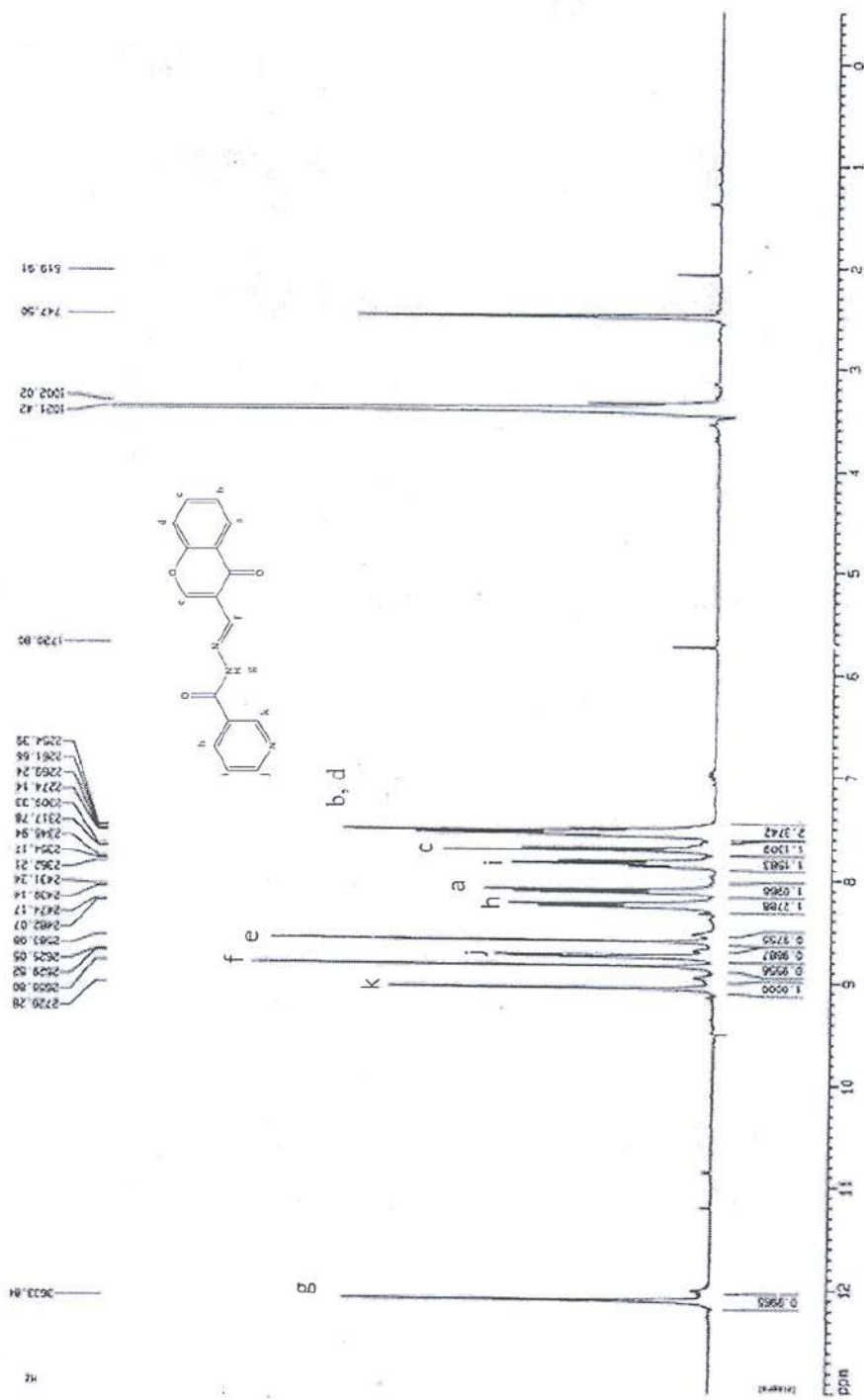
^{1}H NMR spectrum (300 MHz) of compound [3] in DMSO-*d6*
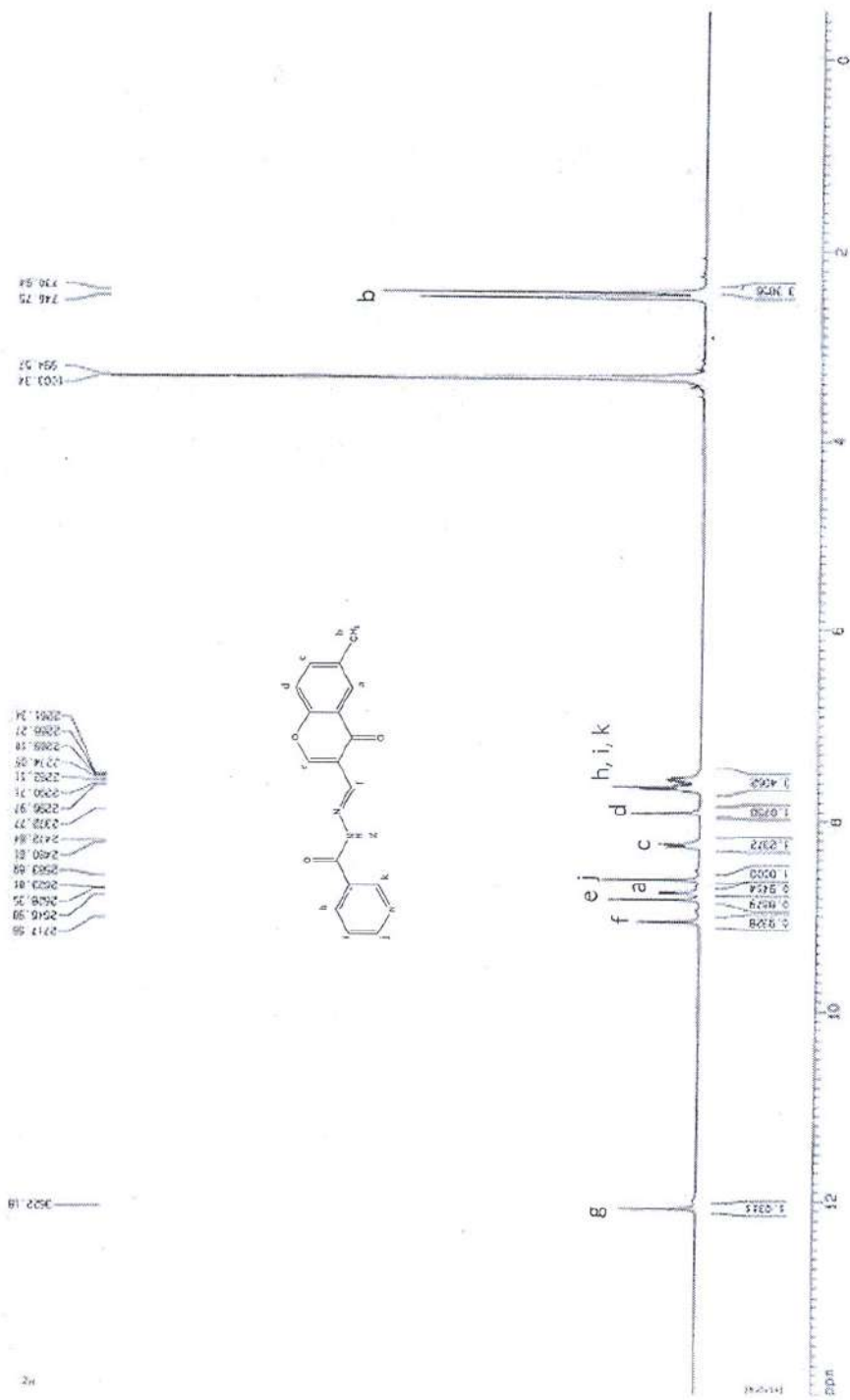
^{1}H NMR spectrum (300 MHz) of compound [4] in DMSO-$d6$

^{1}H NMR spectrum (300 MHz) of compound [5] in DMSO-$d6$
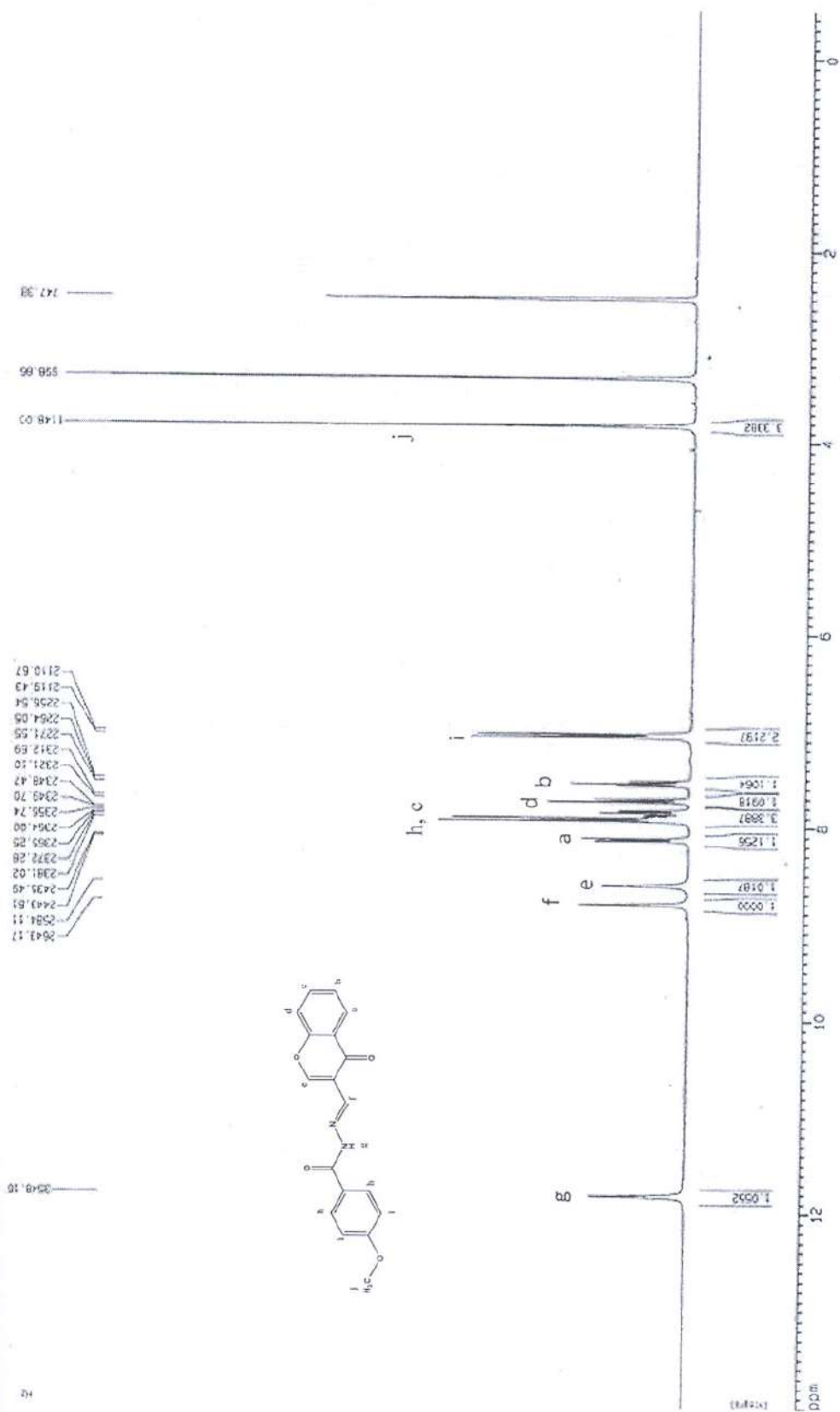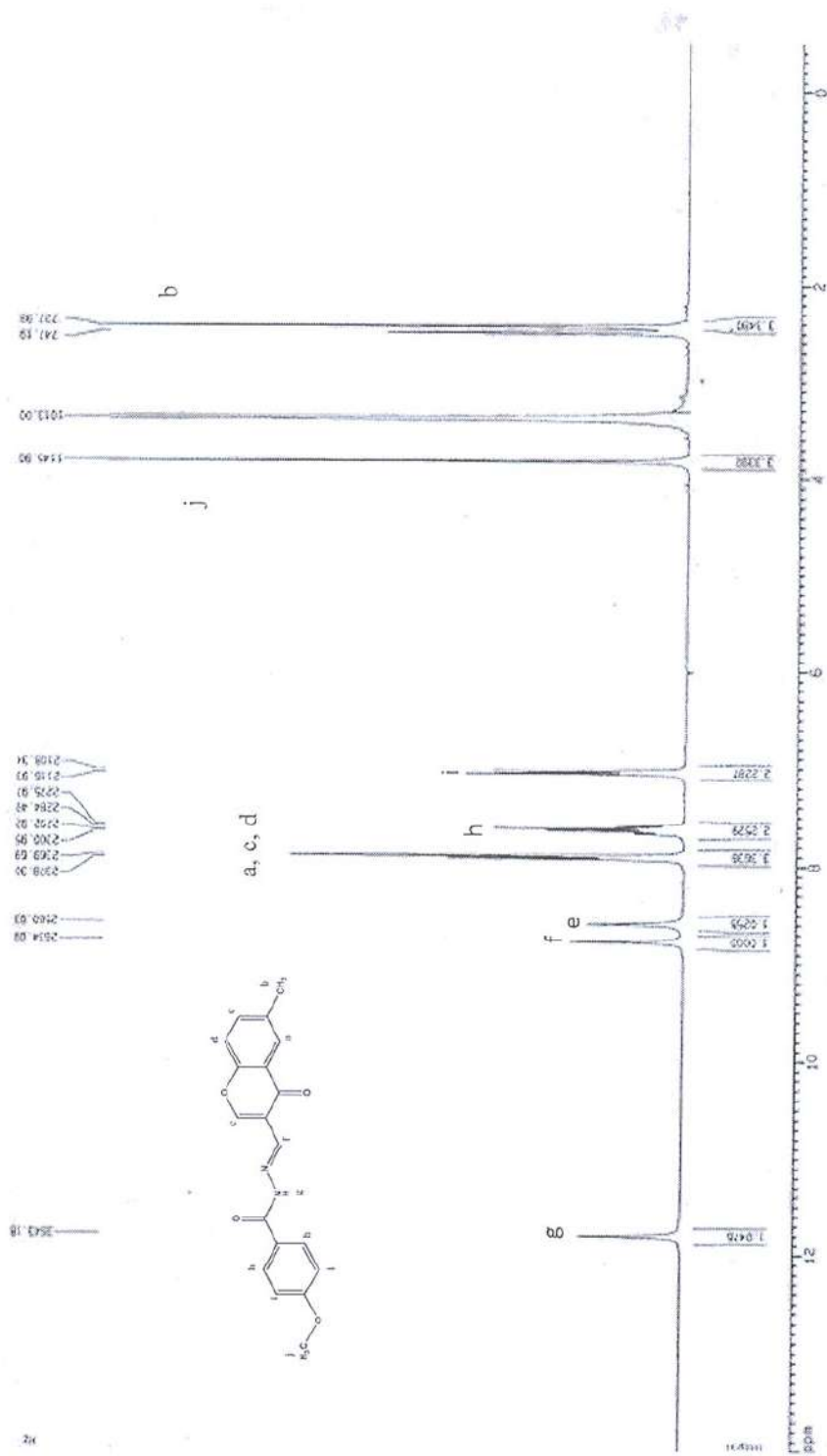
^{1}H NMR spectrum (300 MHz) of compound [6] in DMSO-*d6*

144
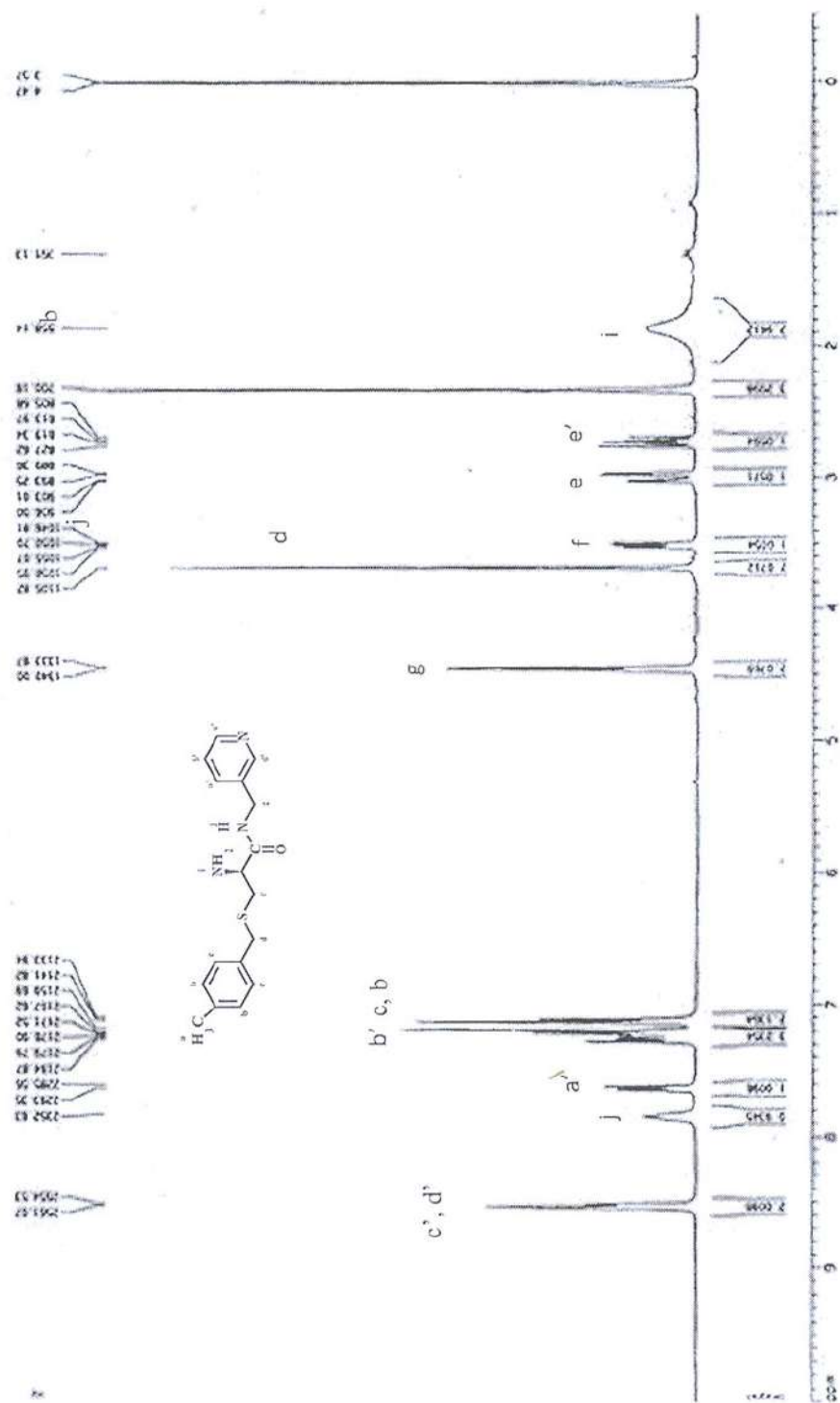
^{1}H NMR spectrum (300 MHz) of compound [8] in chloroform-*d*
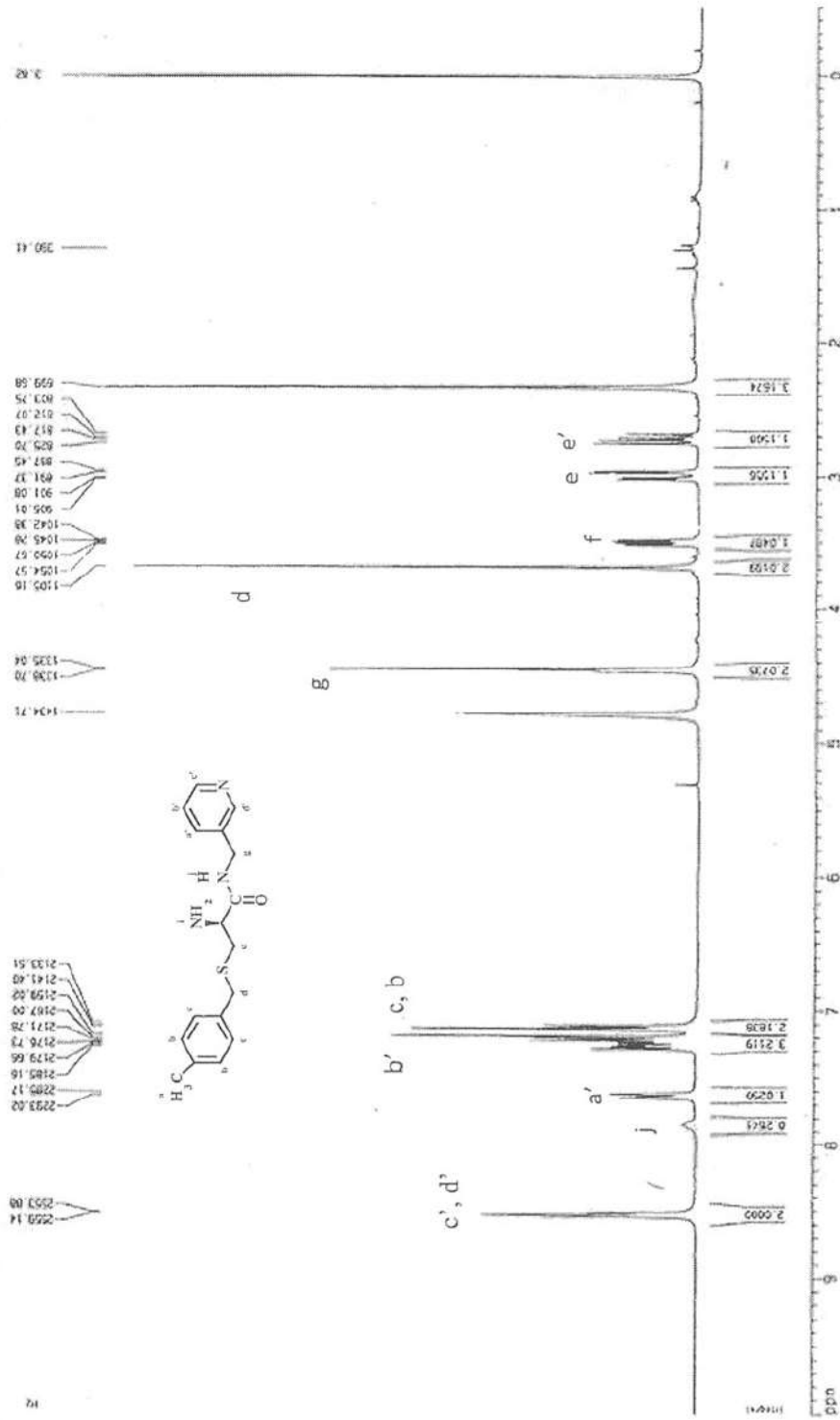
^{1}H NMR spectrum (300 MHz) of compound [8] in chloroform-*d* exchangeable with D_2O

^{1}H NMR spectrum (300 MHz) of compound [10] in DMSO-*d6*
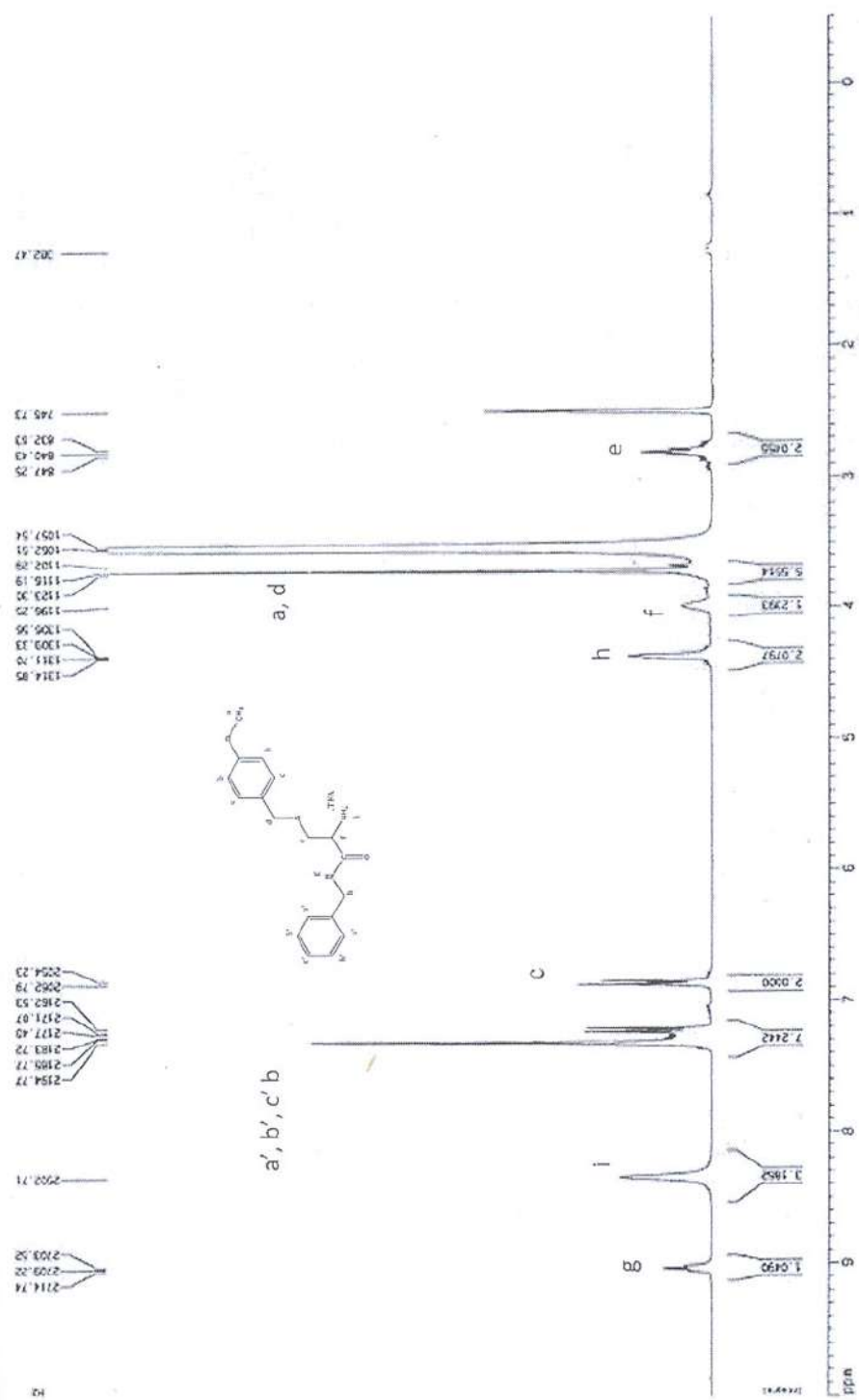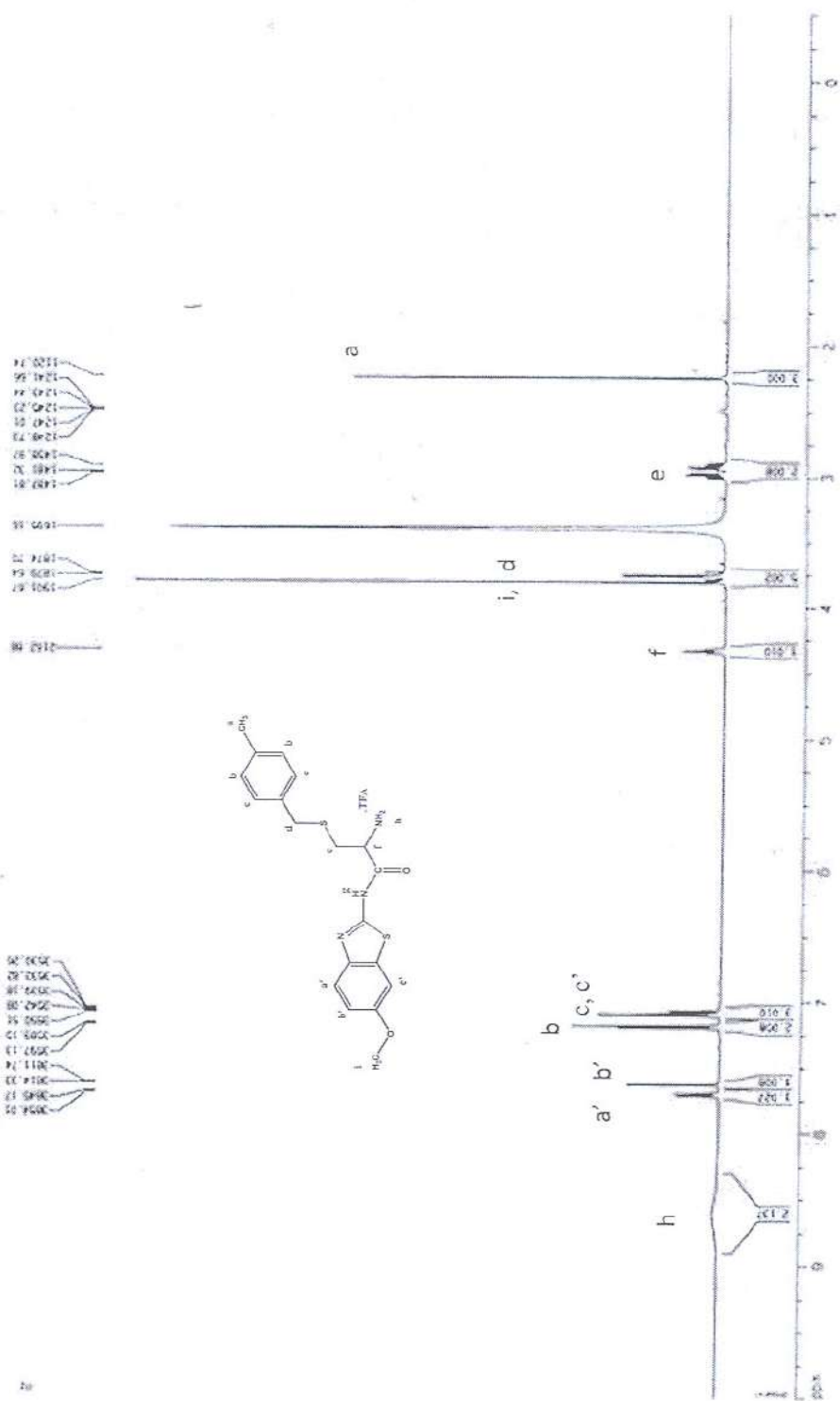
^{1}H NMR spectrum (300 MHz) of compound [12] in DMSO-*d6*

148
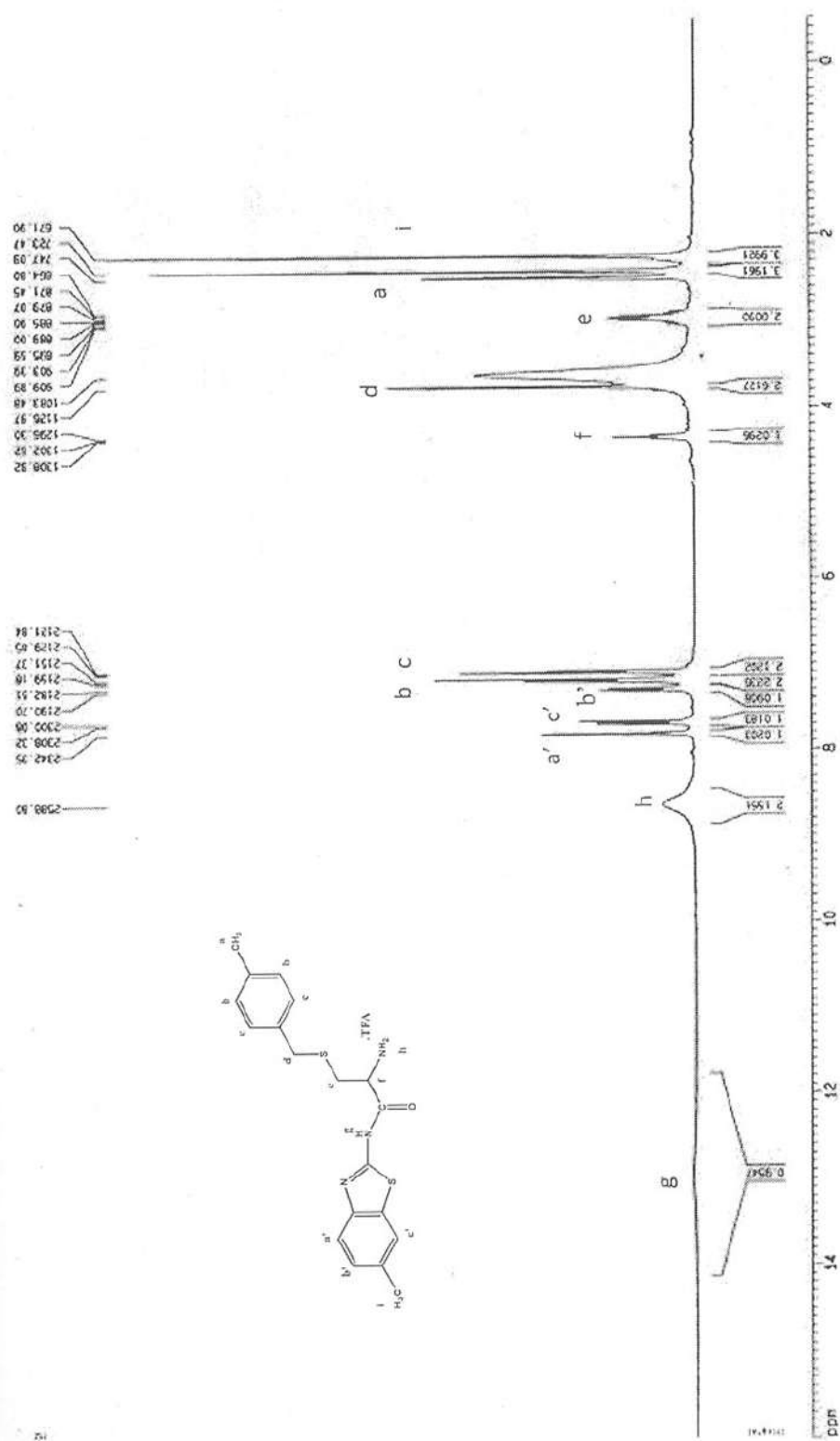
^{1}H NMR spectrum (300 MHz) of compound [14] in DMSO-$d6$
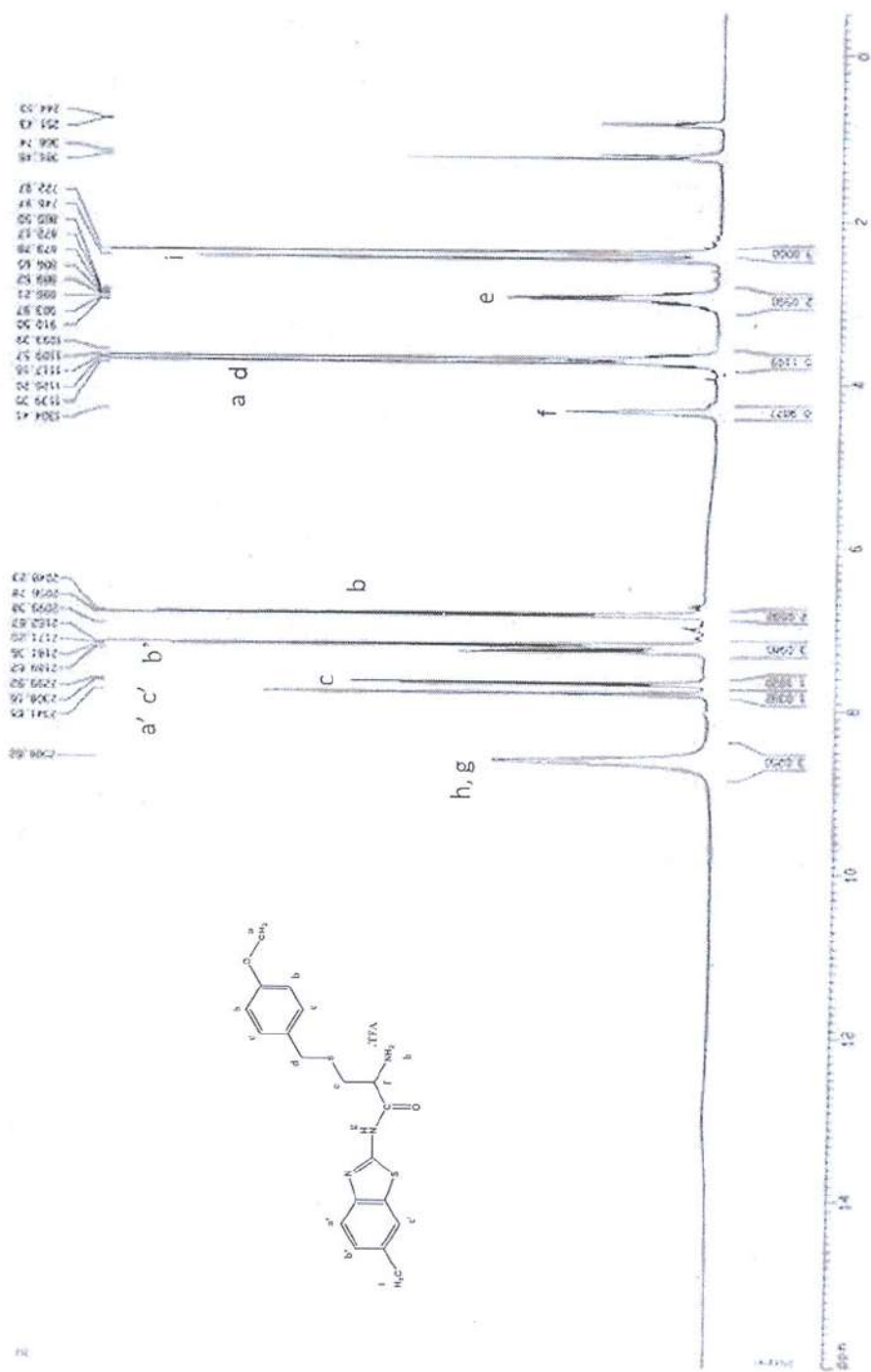
^{1}H NMR spectrum (300 MHz) of compound [16] in DMSO-*d6*
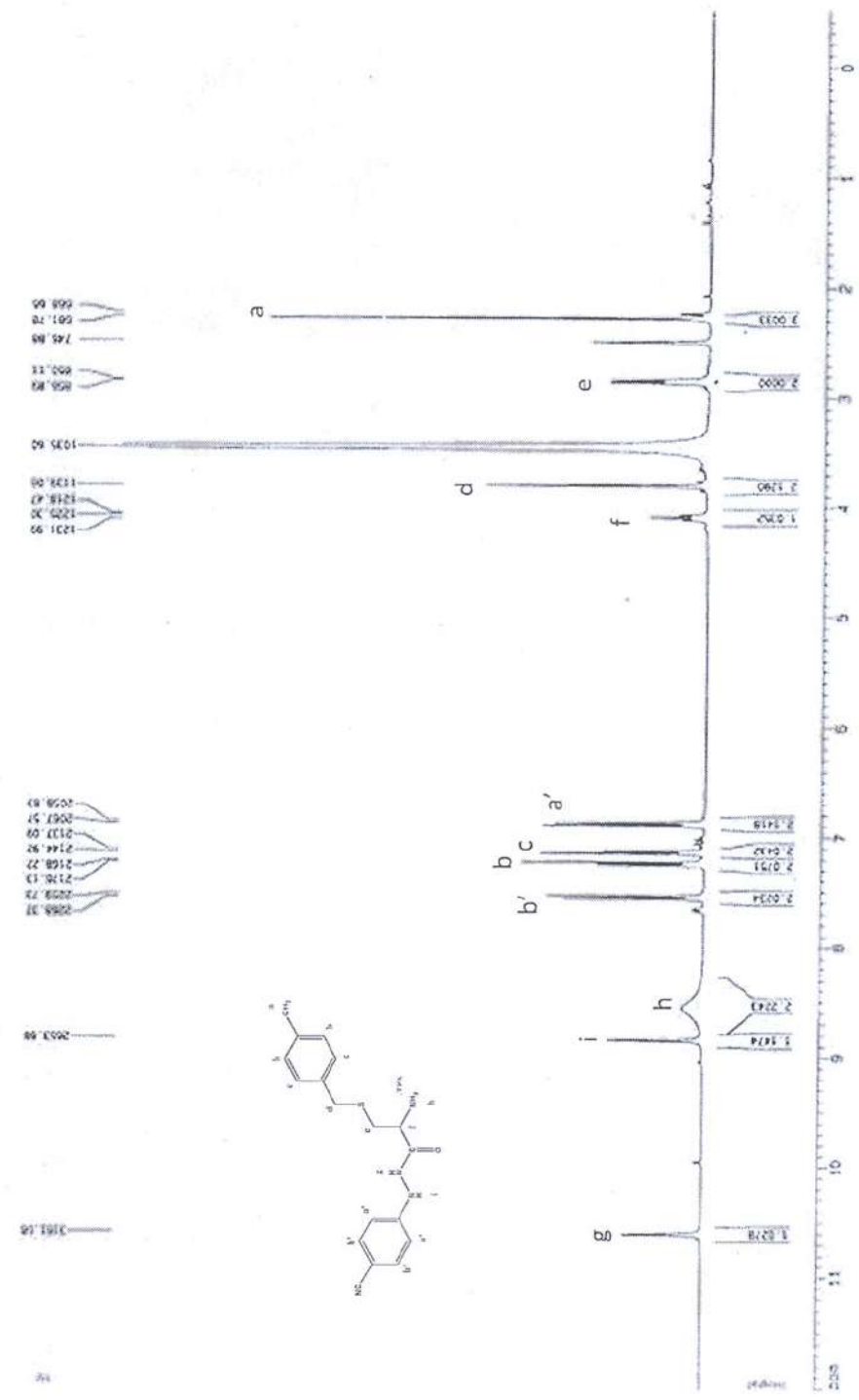
^{1}H NMR spectrum (300 MHz) of compound [18] in DMSO-*d6*

151
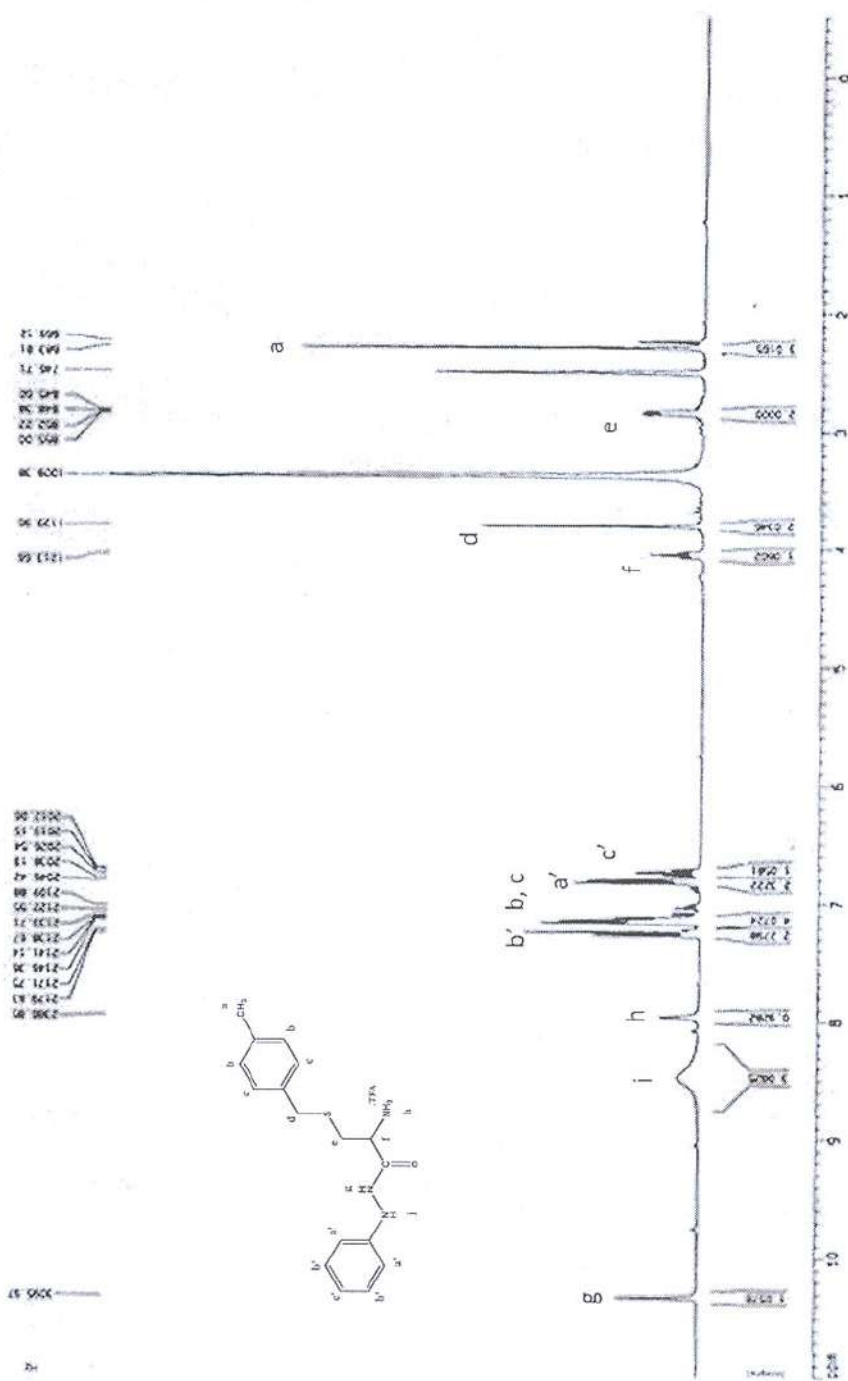
^{1}H NMR spectrum (300 MHz) of compound [20] in DMSO-*d6*

^{1}H NMR spectrum (300 MHz) of compound [22] in DMSO-*d6*
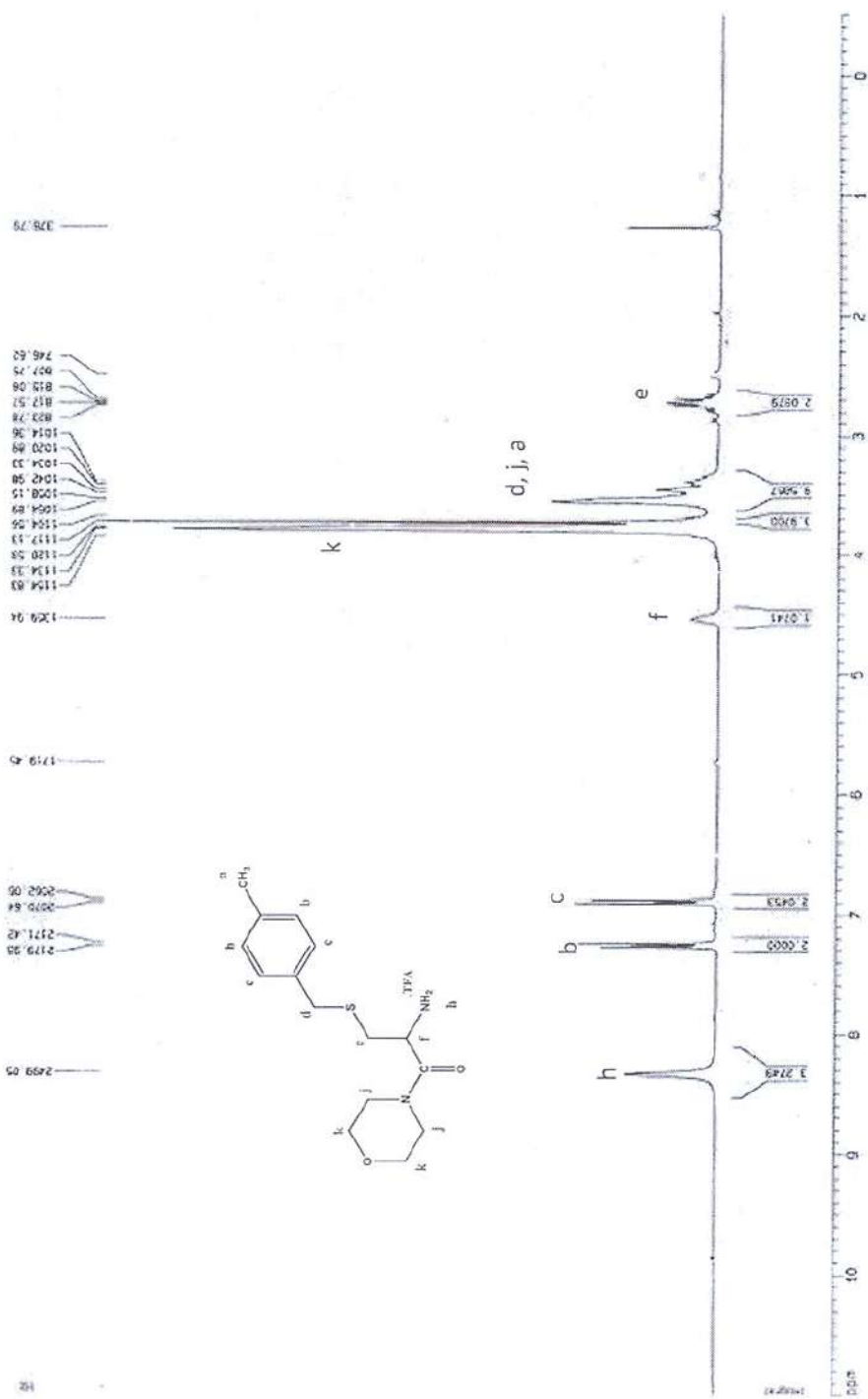
^{1}H NMR spectrum (300 MHz) of compound [24] in DMSO-*d6*
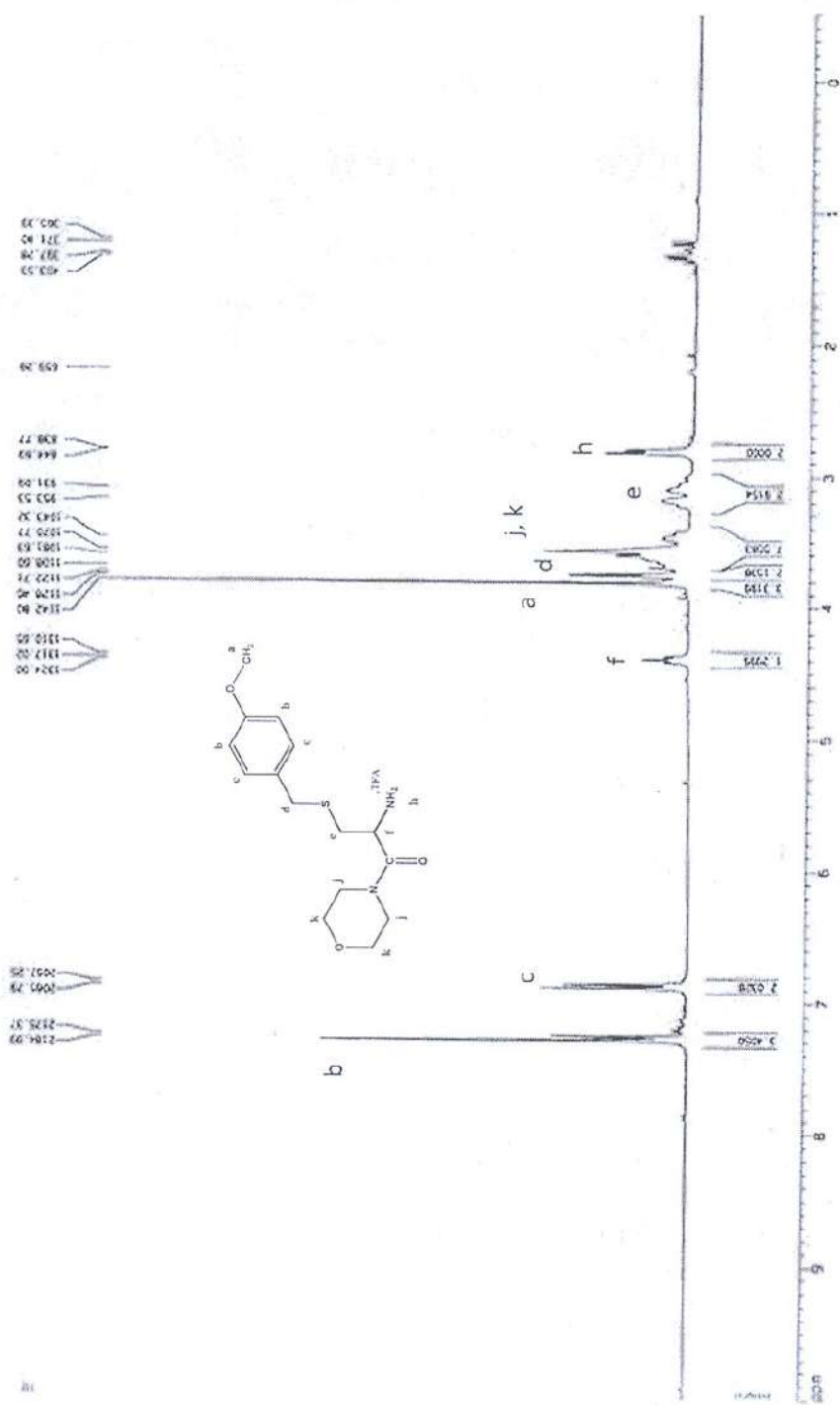
^{1}H NMR spectrum (300 MHz) of compound [26] in chloroform-*d*
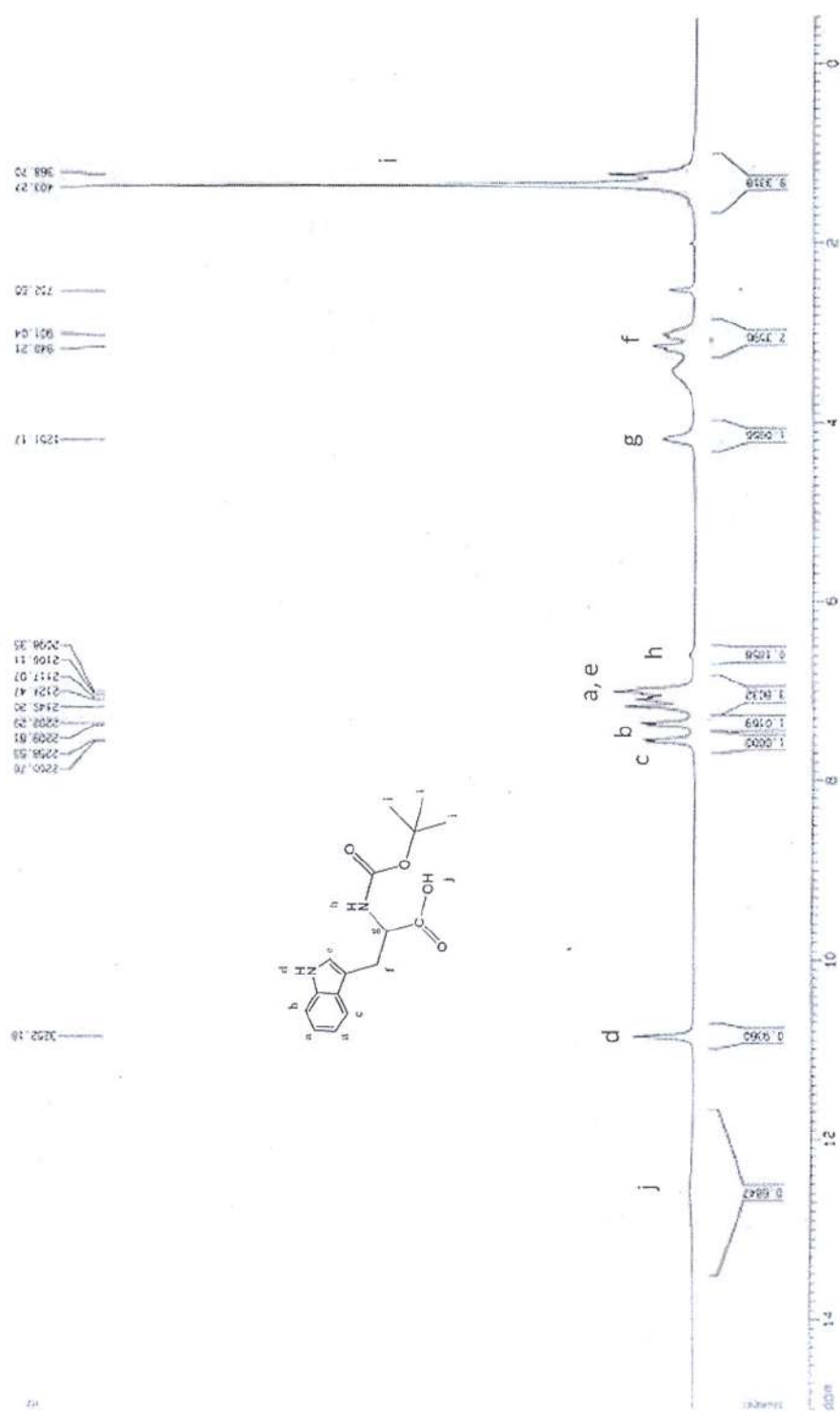
^{1}H NMR spectrum (300 MHz) of compound [27] in DMSO-$d6$
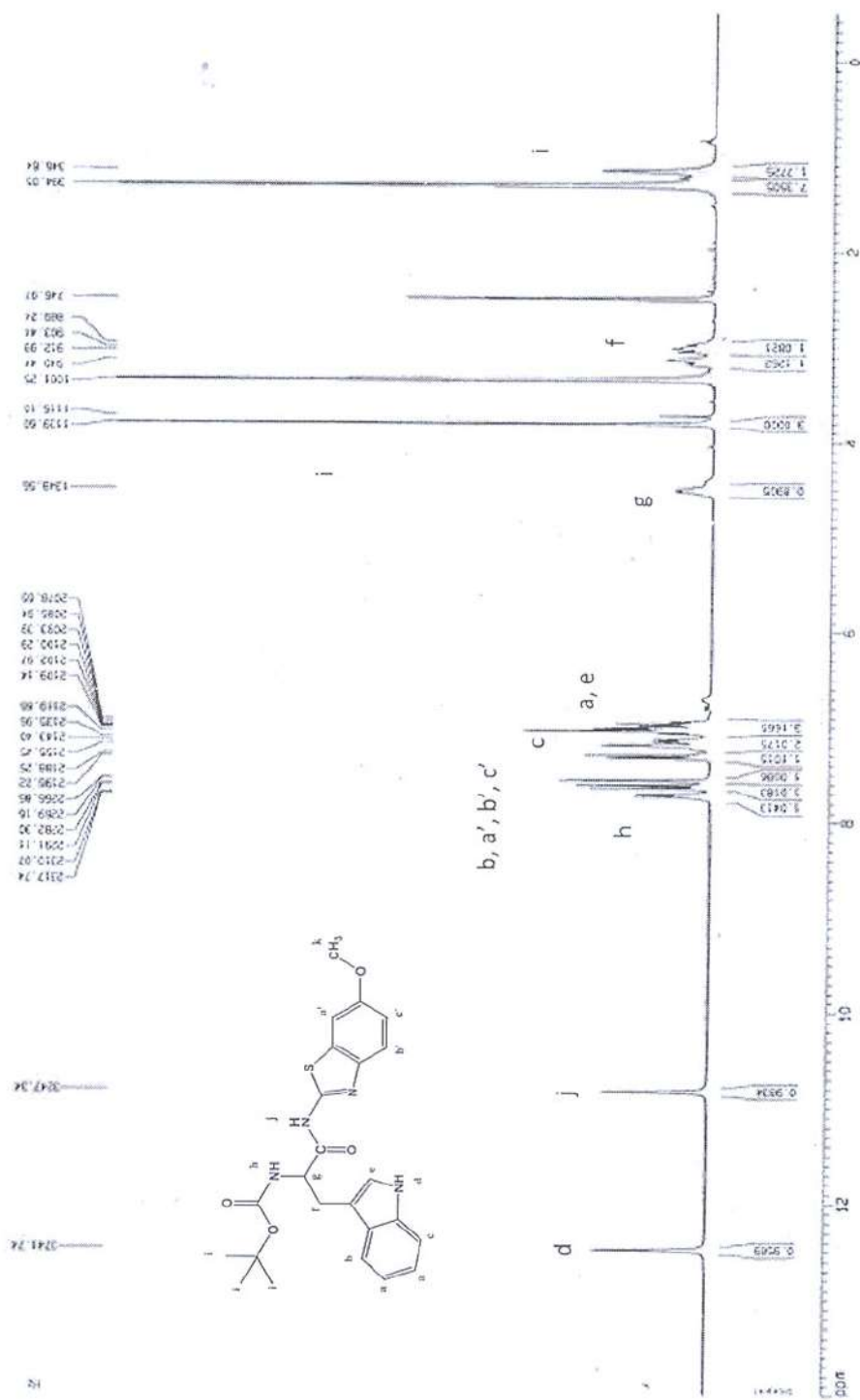
^{1}H NMR spectrum (300 MHz) of compound [28] in DMSO-*d6*
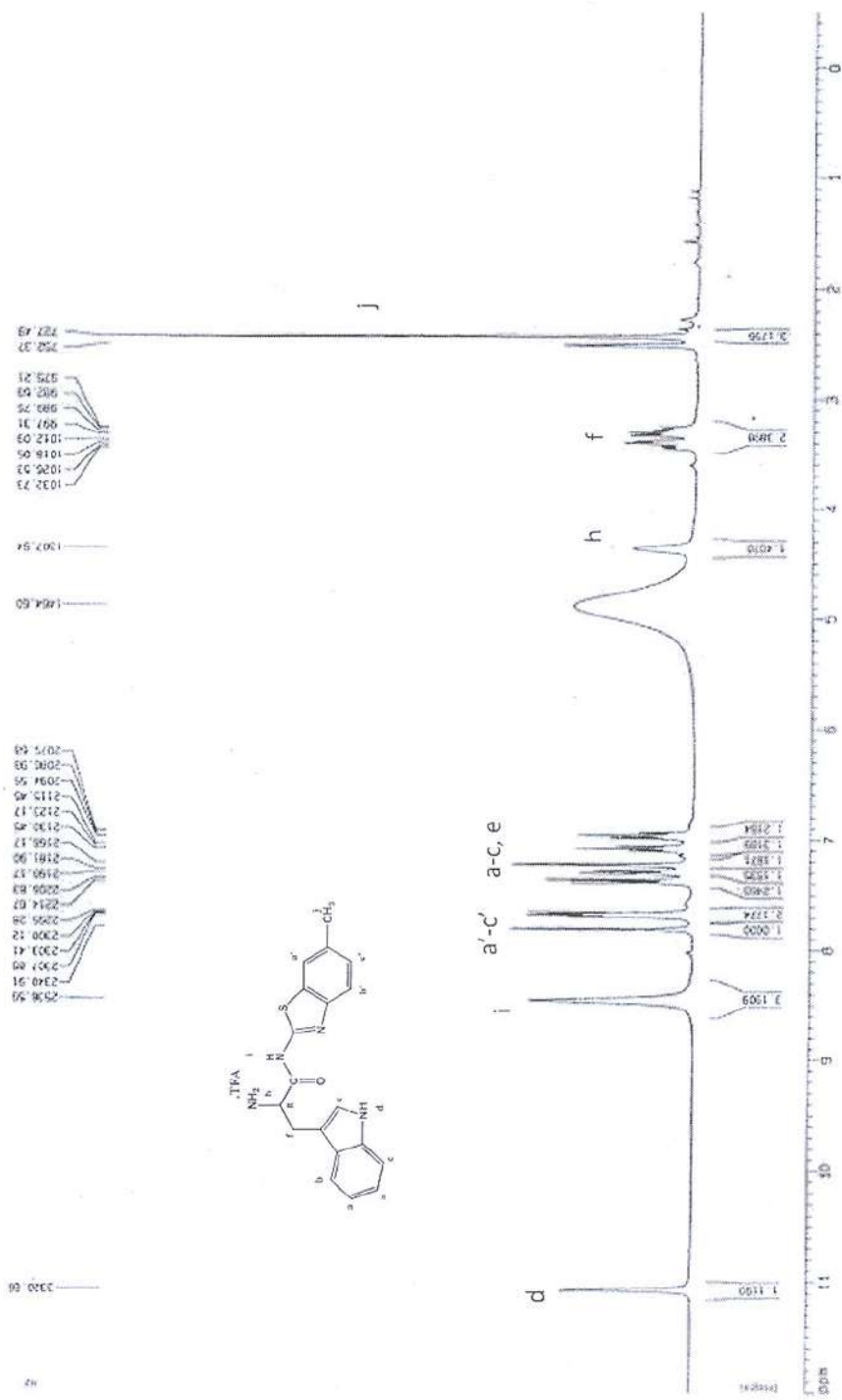
^{1}H NMR spectrum (300 MHz) of compound [30] in DMSO-*d6*
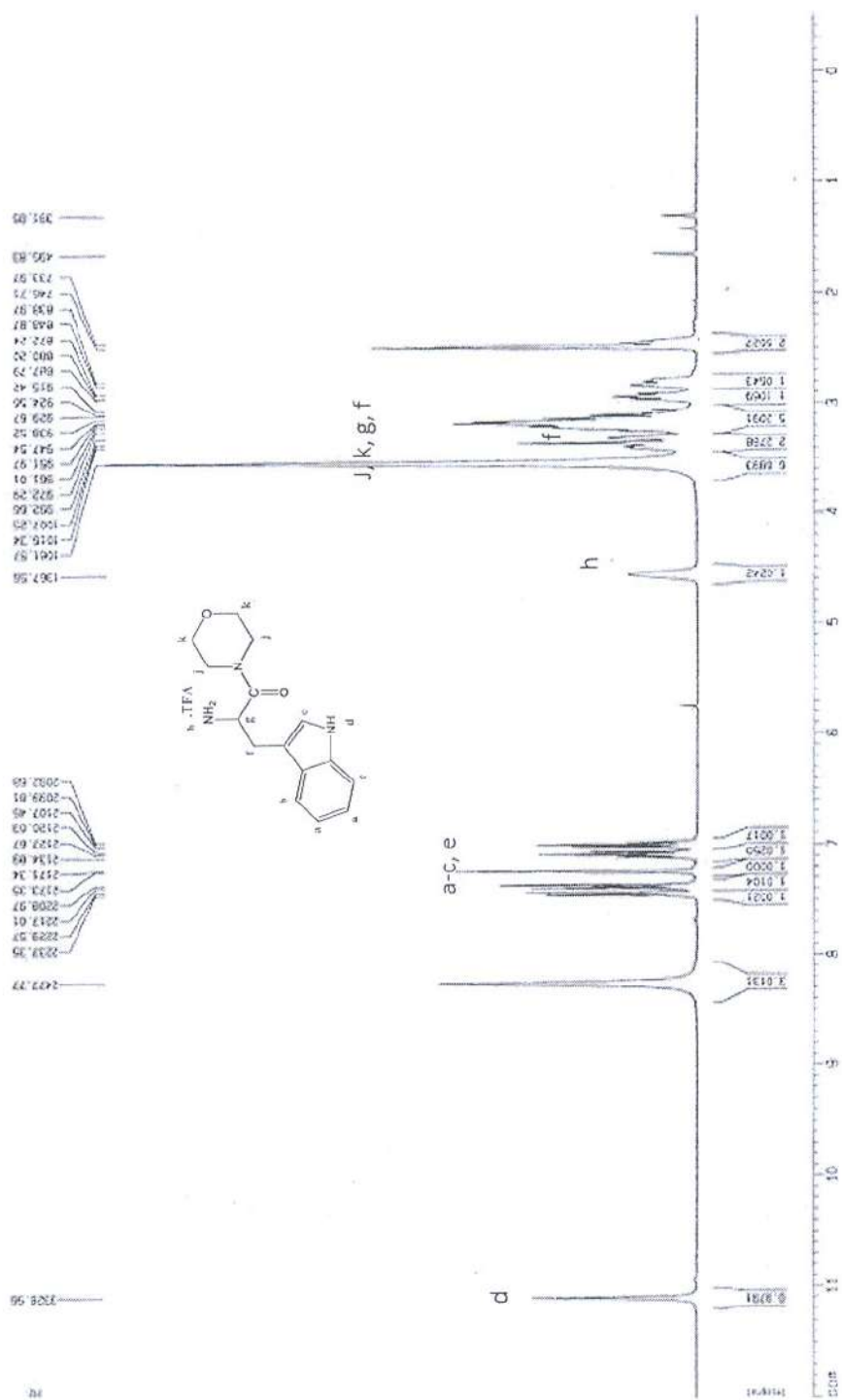
^{1}H NMR spectrum (300 MHz) of compound [32] in DMSO-*d6*
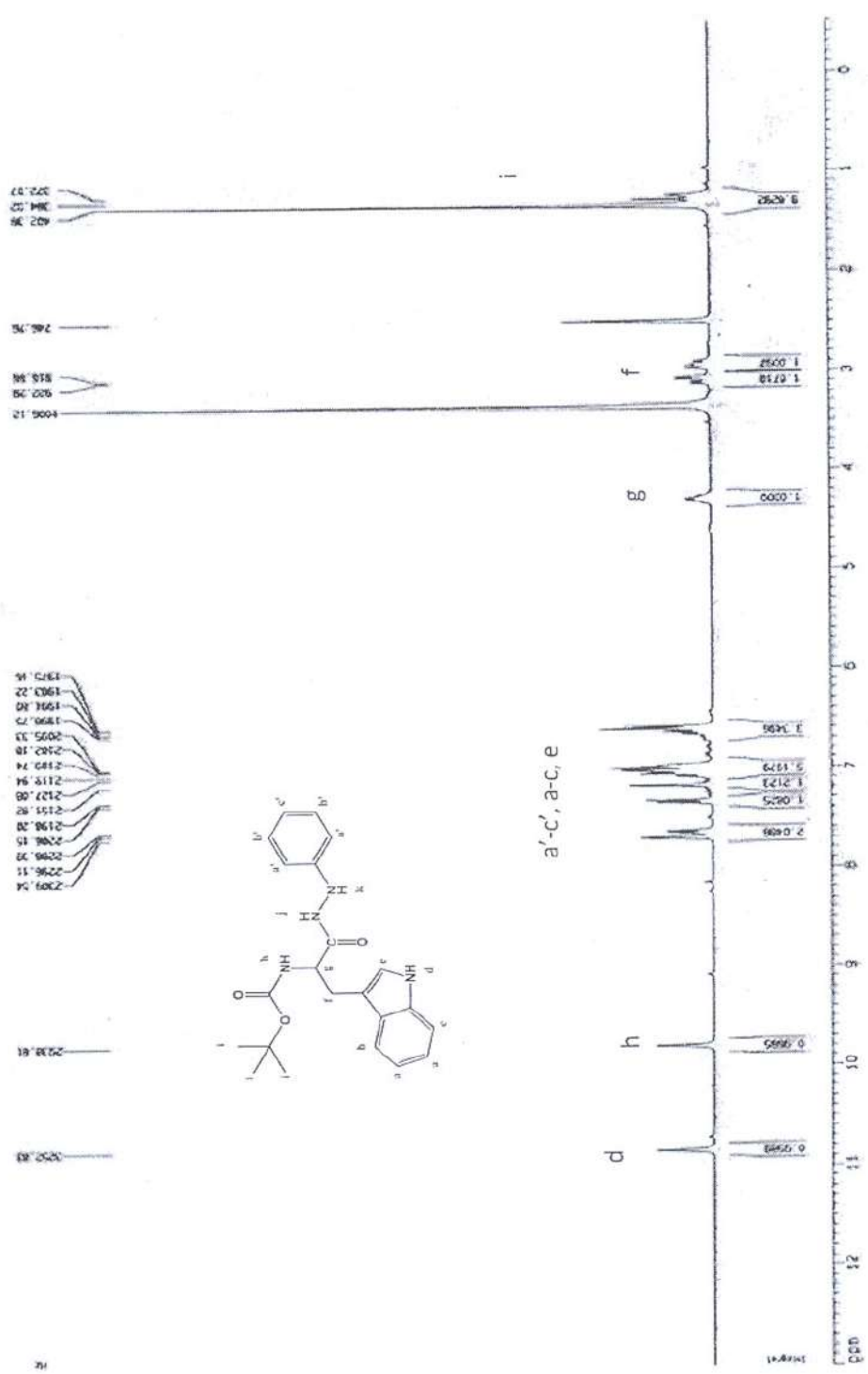
¹H NMR spectrum (300 MHz) of compound [33] in DMSO-d6

APPENDIX B

Docking results of 356 strutures.

Cpds	Structure	ΔG (kcal/mol)	%Member in highest cluster	Cpds	Structure	ΔG (kcal/mol)	%Member in highest cluster	Cpds	Structure	ΔG (kcal/mol)	%Member in highest cluster
1		-7.93	83	7		-8.62	69	13		-7.46	67
2		-9.01	80	8		-6.79	40	14		-7.62	79
3		-7.73	60	9		-8.10	51	15		-10.51	51
4		-7.30	69	10		-7.85	70	16		-10.61	47
5		-7.49	69	11		-7.18	85	17		-7.5	53
6		-8.20	53	12		-8.11	73	18		-7.87	64

Cpds	Structure	ΔG (kcal/mol)	%Member in highest cluster	Cpds	Structure	ΔG (kcal/mol)	%Member in highest cluster	Cpds	Structure	ΔG (kcal/mol)	%Member in highest cluster
19	(structure)	-7.87	64	26	(structure)	-8.02	53	33	(structure)	-10.74	46
20	(structure)	-8.34	46	27	(structure)	-8.77	99	34	(structure)	8.02	53
21	(structure)	-7.98	44	28	(structure)	-8.04	43	35	(structure)	-9.39	95
22	(structure)	-7.64	74	29	(structure)	-7.05	54	36	(structure)	-8.51	96
23	(structure)	-2.79	82	30	(structure)	-7.39	64	37	(structure)	-8.53	92
24	(structure)	-7.80	73	31	(structure)	-8.99	89	38	(structure)	-9.15	73
25	(structure)	-8.58	47	32	(structure)	-9.61	51	39	(structure)	-8.38	100

Cpds	Structure	ΔG (kcal/mol)	%Member in highest cluster
40		-8.35	42
41		-8.98	62
42		-8.06	51
43		-9.20	47
44		-7.85	56
45		-7.74	78
46		-7.14	65
47		-7.12	50
48		-760	48
49		-7.60	48
50		-7.80	96
51		-6.78	54
52		-6.65	52
53		-6.23	58
54		-8.92	69
55		-9.04	86
56		-6.91	81
57		-6.72	51
58		-7.74	94
59		-6.81	49
60		-7.45	96

Structure	Cpds	ΔG (kcal/mol)	%Member in highest cluster
		-7.56	68
		-7.23	46
		-8.97	59
		-8.0	40
		-7.14	43
		-6.69	49
		-6.12	32

Structure	Cpds	ΔG (kcal/mol)	%Member in highest cluster
	89	-8.10	72
	90	-8.04	82
	91	-8.42	46
	92	-7.32	41
	93	-7.36	52
	94	-8.12	64
	95	-6.54	25

Structure	Cpds	ΔG (kcal/mol)	%Member in highest cluster
	96	-7.55	52
	97	-8.28	85
	98	-6.99	76
	99	-7.20	43
	100	-6.66	47
	101	-8.20	66
	102	-7.86	23

Cpds	Structure	ΔG (kcal/mol)	%Member in highest cluster
103	(structure)	-6.89	30
104	(structure)	-6.72	8
105	(structure)	-6.69	53
106	(structure)	-7.63	46
107	(structure)	-6.83	52
108	(structure)	-7.69	35
109	(structure)	-6.23	72
110	(structure)	-6.50	12
111	(structure)	-5.65	14
112	(structure)	-6.76	25
113	(structure)	-7.36	62
114	(structure)	-6.72	38
115	(structure)	-7.43	42
116	(structure)	-6.12	28
117	(structure)	-7.16	60
118	(structure)	-6.10	16
119	(structure)	-6.58	20
120	(structure)	-7.32	54
121	(structure)	-6.35	32
123	(structure)	-5.61	65
124	(structure)	-5.72	31

Cpds	Structure	%Member in highest cluster	ΔG (kcal/mol)	Cpds	Structure	%Member in highest cluster	ΔG (kcal/mol)	Cpds	Structure	ΔG (kcal/mol)	%Member in highest cluster
125		35	-5.63	132		25	-5.69	140		-6.74	56
126		45	-7.65	133		38	-6.23	141		-6.23	65
127		46	-7.63	134		36	-6.48	142		-6.38	41
128		48	-6.52	135		45	-6.29	143		-6.79	52
129		42	-6.38	136		51	-6.49	144		-6.56	53
130		52	-6.96	137		50	-6.35	145		-6.89	40
131		53	-6.78	138		59	-6.31	146		-7.10	39

Cpds	Structure	ΔG (kcal/mol)	%Member in highest cluster
147		-7.01	35
148		-5.89	38
149		-6.35	41
150		-6.85	42
151		-6.75	56
152		-6.84	18
153		-6.81	26
154		-5.75	30
155		-5.62	26
156		-6.26	45
157		-7.23	32
158		-7.89	56
159		-6.69	65
160		-6.12	28
161		-8.99	56
162		-8.56	42
163		-7.85	73
164		-8.23	29
165		-7.12	65
166		-8.06	80
167		-7.05	54

167

Cpds	Structure	ΔG (kcal/mol)	%Member in highest cluster
68		-7.20	57
69		-7.23	62
70		-7.15	68
71		-7.02	54
72		-7.05	42
73		-7.26	48
74		-7.38	41

Cpds	Structure	ΔG (kcal/mol)	%Member in highest cluster
175		-8.20	54
176		-8.12	57
177		-8.75	65
178		-7.56	62
179		-7.57	60
180		-7.26	48
181		-7.89	66

Cpds	Structure	ΔG (kcal/mol)	%Member in highest cluster
182		-7.89	85
183		-7.23	53
184		-7.01	54
185		-7.86	67
186		-7.36	70
187		-7.18	79
188		-7.56	47

Cpds	Structure	ΔG (kcal/mol)	%Member in highest cluster
189	(structure)	-8.52	56
190	(structure)	-9.05	48
191	(structure)	-6.75	74
192	(structure)	-7.26	53
193	(structure)	-6.95	52
194	(structure)	-8.42	49
195	(structure)	-8.32	35
196	(structure)	-8.01	36
197	(structure)	-7.12	58
198	(structure)	-8.56	54
199	(structure)	-7.58	68
200	(structure)	-6.85	76
201	(structure)	-7.23	84
202	(structure)	-8.32	59
203	(structure)	-5.89	45
204	(structure)	-7.32	65
205	(structure)	-7.10	67
206	(structure)	-7.25	42
207	(structure)	-8.63	58
208	(structure)	-9.02	71
209	(structure)	-5.90	28

169

Cpds	Structure	ΔG (kcal/mol)	%Member in highest cluster
210	(structure)	-7.54	45
211	(structure)	-8.25	56
212	(structure)	-9.30	694
213	(structure)	-7.47	28
214	(structure)	-6.89	75
215	(structure)	-7.85	71
216	(structure)	-8.56	86
217	(structure)	-7.14	46
218	(structure)	-8.05	32
219	(structure)	-9.10	58
220	(structure)	-7.86	72
221	(structure)	-7.46	70
222	(structure)	-7.12	68
223	(structure)	-8.54	56
224	(structure)	-7.53	38
225	(structure)	-6.98	42
226	(structure)	-6.58	18
227	(structure)	-8.23	65
228	(structure)	9.12	13
229	(structure)	-7.85	56
230	(structure)	-7.68	54

Cpds	Structure	ΔG (kcal/mol)	%Member in highest cluster	Cpds	Structure	ΔG (kcal/mol)	%Member in highest cluster	Cpds	Structure	ΔG (kcal/mol)	%Member in highest cluster
231		-7.06	70	239		-6.72	68	246		-7.38	56
232		-8.15	62	240		-9.03	54	247		-8.36	45
234		-6.58	56	241		-7.55	50	248		-8.08	47
235		-6.98	50	242		-8.13	78	249		-7.98	80
236		-9.01	38	243		-8.56	65	250		-6.23	72
237		-7.85	78	244		-7.23	48	251		-5.98	73
238		-7.06	64	245		-8.96	49	252		-7.84	68

Cpds	Structure	ΔG (kcal/mol)	%Member in highest cluster	Cpds	Structure	ΔG (kcal/mol)	%Member in highest cluster	Cpds	Structure	ΔG (kcal/mol)	%Member in highest cluster
253		-7.10	40	260		-7.55	71	267		-8.65	75
254		-8.21	50	261		-8.23	54	268		-7.46	84
255		-6.32	72	262		-7.23	45	269		-6.99	80
256		-7.56	56	263		-7.15	43	270		-7.40	65
257		-8.02	52	264		-8.14	62	271		-6.88	38
258		-6.89	48	265		-6.97	63	272		-7.54	41
259		-6.76	60	266		-8.41	58	273		-7.42	40

Cpds	Structure	ΔG (kcal/mol)	%Member in highest cluster	Cpds	Structure	ΔG (kcal/mol)	%Member in highest cluster	Cpds	Structure	ΔG (kcal/mol)	%Member in highest cluster
274		-7.20	45	282		-7.08	58	290		-6.14	58
275		-6.47	75	283		-6.52	46	291		-7.82	54
276		-7.54	70	284		-8.53	40	292		-7.48	65
278		-8.04	65	285		-7.09	71	293		-8.88	28
279		-9.05	32	286		-8.83	33	294		-8.35	34
280		-9.01	27	287		-10.0	46	295		-8.56	27
281		-9.25	32	289		-12.67	77	296		-9.14	28

Cpds	Structure	ΔG (kcal/mol)	%Member in highest cluster
297	(structure)	-10.12	32
298	(structure)	-9.65	24
299	(structure)	-10.1	70
300	(structure)	-9.56	21
301	(structure)	-10.21	41
302	(structure)	-11.83	30
303	(structure)	-11.95	55
304	(structure)	-9.15	25
305	(structure)	-10.12	32
306	(structure)	-10.03	75
307	(structure)	-11.32	56
308	(structure)	-11.72	93
309	(structure)	-11.25	40
310	(structure)	-10.73	42
311	(structure)	-9.56	18
312	(structure)	-9.13	26
313	(structure)	-10.02	32
314	(structure)	-11.71	31
315	(structure)	-11.67	52
316	(structure)	-12.67	77
317	(structure)	-10.06	41

Cpds	Structure	ΔG (kcal/mol)	%Member in highest cluster	Cpds	Structure	ΔG (kcal/mol)	%Member in highest cluster	Cpds	Structure	ΔG (kcal/mol)	%Member in highest cluster
318		-11.63	31	325		-12.05	67	332		-11.98	75
319		-12.84	81	326		-11.98	75	333		-11.25	26
320		-11.20	32	327		-10.02	38	334		-9.23	36
321		-11.08	22	328		-10.00	39	335		-9.56	32
322		-12.03	25	329		-9.13	28	336		-10.19	35
323		-11.10	34	330		-10.47	23	337		-10.56	30
324		-10.87	25	331		-10.10	23	338		-10.27	24

Cpds	Structure	ΔG (kcal/mol)	%Member in highest cluster
339	(structure)	-10.12	38
340	(structure)	-8.56	24
341	(structure)	-8.97	23
342	(structure)	-10.18	18
343	(structure)	-10.23	25
344	(structure)	-9.56	21
345	(structure)	-9.97	31
346	(structure)	-9.97	32
347	(structure)	-8.98	30
348	(structure)	-10.20	28
349	(structure)	-11.53	29
350	(structure)	-8.96	26
351	(structure)	-10.61	26
352	(structure)	-10.55	22
353	(structure)	-11.58	29
354	(structure)	-9.36	35
355	(structure)	-10.23	23
356	(structure)	-9.36	37

BIOGRAPHY

NAME	Mr. ChaiyunTaomali
DATE OF BIRTH	May 3, 1986
PLACE OF BIRTH	SakonNakhon, Thailand
INSTITUTIONS ATTENDED	BansomdejchaoprayaRajabhat University, 2006-2009: Bachelor of Science in industrial chemistry BansomdejchaoprayaRajabhat University, 2009-2014: Bachelor of Science in chemistry
POSITION & OFFICE	Student Program of chemistry, and Center of Excellence for Innovation in chemistry, faculty of Science and Technology, Isaraphab 15, Bangkok 10600, Thailand Tel. 0-2473-7000 ext. 1810
FUND	Thesis scholarship from the Commission of Higher Education Thailand (CHE-RES-RG 2008) , mahidol University and Center for Innovation in chemistry: postgraduate education and research program in chemistry (PERCH-CIC)